Mode of Flow of Saskatchewan Glacier Alberta, Canada

GEOLOGICAL SURVEY PROFESSIONAL PAPER 351

Mode of Flow of Saskatchewan Glacier Alberta, Canada

By MARK F. MEIER

GEOLOGICAL SURVEY PROFESSIONAL PAPER 351

Measurement and analysis of ice movement, deformation, and structural features of a typical valley glacier

UNITED STATES GOVERNMENT PRINTING OFFICE, WASHINGTON: 1960

UNITED STATES DEPARTMENT OF THE INTERIOR

FRED A. SEATON, *Secretary*

GEOLOGICAL SURVEY

Thomas B. Nolan, *Director*

The U.S. Geological Survey Library has catalogued this publication as follows:

Meier, Mark Frederick, 1925—
Mode of flow of Saskatchewan Glacier, Alberta, Canada. Washington, U.S. Govt. Print. Off., 1959.
ix, 70 p. illus. (1 col.) maps, diagrs., profiles, tables. 30 cm. (U.S. Geological Survey. Professional paper 351)
Part of illustrative matter folded in pocket.
Measurement and analysis of ice movement, deformation, and structural features of a typical valley glacier.
Bibliography: p. 67-68.
1. Glaciers — Alberta. 2. Saskatchewan Glacier, Canada. I. Title. (Series)

For sale by the Superintendent of Documents, U. S. Government Printing Office
Washington 25, D. C.

PREFACE

This report deals with principles of glacier flow that are applicable to the many glaciers in Alaska and other parts of the United States. Permission to work in Canada was extended by the Canadian Department for External Affairs, and access to the National Park was arranged by Mr. J. R. B. Coleman, then supervisor of Banff National Park. Saskatchewan Glacier was chosen for study because it is readily accessible and affords an unusually good opportunity to obtain data and develop principles that have a direct bearing on studies being made in the United States. The work started in the summer of 1952 and was supported by a grant from an Arctic Institute of North America project of the Office of Naval Research. Equipment was supplied by the California Institute of Technology under a contract with the Office of Naval Research. The work in 1953–54 was supported solely by the Office of Naval Research. The final phases of computation and manuscript preparation were supported by the U.S. Geological Survey. The author's work in the Geological Survey was under the general supervision of C. C. McDonald, chief, Branch of General Hydrology.

The success of this project in its conception, field program and preparation of this final report is due in large measure to the direction and the assistance given by Robert P. Sharp, B. Gunnar Bergmann, James E. Conel, Donald O. Emerson, Jean A. Hoerni, Benjamin F. Jones, William B. Lindley, Lee R. Magnolia, Jack Rocchio, Gordon Seele, Jack B. Shepard and George Wallerstein assisted in the field without compensation, and this assistance was of greatest value. Clarence R. Allen sacrificed his own research time to conduct seismic studies on the glacier which provided essential data on the thickness of ice and configuration of the bedrock channel. Kermit Jacobson, purchasing agent of the California Institute of Technology, took time from his regular duties to expedite the shipment of material and equipment to Canada. William Black, formerly warden of the Saskatchewan District, Banff National Park, and Peter Withers of Jasper National Park assisted the project in many ways beyond their official duties. Permission to use the Saskatchewan Hut was kindly extended by the Alpine Club of Canada, R. C. Hind, hut chairman. A Parsons Drill Hole Inclinometer was generously loaned by the Parsons Survey Co., South Gate, Calif. Thanks are also due to the Defence Research Board of Canada for the loan of magnesium sleds, and the California Institute of Technology for the acquisition and loan of special surveying equipment. The critical comments of C. R. Allen, W. B. Ray and W. D. Simons have been most helpful in the preparation of the manuscript.

GLOSSARY

Ablation. Wastage of ice and snow by melting, evaporation, erosion, calving, and other minor processes. On Saskatchewan Glacier wastage occurs mostly as surface melting.

Accumulation. Deposition of snow, hail, hoarfrost, rime and ice on a glacier. Most of this deposition takes place as snowfall on the glacier surface on Saskatchewan Glacier.

Accumulation area. That part of the glacier surface where accumulation exceeds ablation for a 1-year period.

Compressing flow. Flow in which the velocity decreases in the downglacier direction.

Extending flow. Flow in which the velocity increases in the downglacier direction.

Firn. Material in transition from snow to glacier ice. It consists of coarse granules, is compact but permeable, and ranges in density from about 0.4 to about 0.84 gram per cubic centimeter.

Firn limit. Line separating the accumulation area from the ablation area.

Flow centerline. An imaginary line on the surface of the glacier that is everywhere parallel to the projection on the surface of the velocity vectors and which passes as closely as possible through points of maximum surface velocity in transverse profiles.

Flow law. Steady-state creep rate as a function of the applied stress for a given material.

Foliation. A compact, layered structure or planar anisotropy caused by flow, as defined in this report. It is expressed mainly by differences in grain size or bubble content of the ice.

Octahedral shear stress (or strain rate). A value expressing the intensity of shearing stress (or strain rate) in a body equal to the stress (or strain rate) acting on planes of an octahedron oriented with its corners on the axes of principal stress (or strain rate).

Plastic flow. Flow in which the strain rate is not linearly proportional to the applied shear stress.

Principal axes of stress (or strain rate). In a general state of stress (or strain rate) there are three mutually perpendicular planes on which the shear stresses (shear strain rates) vanish. The three principal axes are normal to these three planes.

Principal stresses (or strain rates). The normal (strain rates) in the direction of the principal axes of stress (strain rate).

Strain rate. Velocity of deformation, usually restricted to the velocity of shearing deformation in this report.

Temporary snowline. Line delineating the snow-covered area at any instant.

Viscous flow. Flow in which the strain rate is linearly proportional to the applied shear stress.

SYMBOLS

A area of a cross section

$C = \frac{R}{d}\gamma \sin \alpha$

d depth

$f( )$ a function of ( )

i,j,k $= x$, y, or z

k,k_1,k_2 arbitrary, empirical constants

n empirical constant

p iced perimeter, analogous to the wetted perimeter as used in hydraulics, except that p is measured in a cross section perpendicular to the glacier surface

$R = \frac{A}{p}$, the hydraulic radius (measured in a plane perpendicular to the surface of the glacier)

s standard deviation

S, δS, δS surfaces (defined on p. 25)

u displacement

V the velocity vector

V the absolute magnitude of V

V_d the surfaceward flow (defined on p. 20)

V_i, V_j velocity component parallel to a coordinate axis i or j ($i,j = x, y,$ or z)

V_x, V_y, V_z velocity components parallel to the x, y, z-axes

V_x', V_y' velocity components parallel to the x', y'-axes

w width

x,y,z rectangular coordinate axes (defined on p. 10)

$x'y'$ curvilinear "natural" coordinate axes (defined on p. 11)

x_i, x_j coordinate axes ($i, j = x, y,$ or z)

α surface slope, measured from the horizontal in the direction of the x'-axis

β bed slope, measured from the horizontal in the direction of the x'-axis

γ specific weight of ice (generally assumed to be 56.1 pounds per cubic foot)

δ_{ij} Kronicker delta or idem factor ($\delta = 0$ when $i = j$, $= 1$ when $i \neq j$)

$\dot{\epsilon}_{ij}$ strain rate

$\dot{\epsilon}_{xx}$ normal strain rate in the direction of the x-axis, extending strain rates are considered positive

$\dot{\epsilon}_{xy}$ shearing strain rate on a plane perpendicular to the x axis, in the direction of the y axis

$\dot{\epsilon}_1$ greatest (most extending) principal strain rate

$\dot{\epsilon}_2$ least (most compressing) principal strain rate

$\dot{\epsilon}'_{ij}$ deviator of strain rate (defined on p. 38)

$\dot{\epsilon}_0, \dot{\epsilon}_0'$ octahedral strain rate (defined on p. 38, 41)

θ horizontal angle between x' axis and ϵ_1 (table 4)

ξ inclination of streamline from the horizontal

ρ density of ice

σ_{ij} stress

σ hydrostatic (mean) stress

σ_{xx} normal stress in the direction of the x axis, tensile stresses are considered positive

σ_{xy} shearing stress on a plane perpendicular to the x axis, in the direction of the y axis

$\sigma_1, \sigma_2, \sigma_3$ principal stresses

σ_{ij}' deviator of stress (defined on p. 38)

σ_0, σ_0' octahedral shear stress (defined on p. 38, 41)

ϕ horizontal angle between x' axis and V (fig. 17)

$\dot{\omega}$ rotation rate (table 4)

		Page
FIGURE 1.	Map of the eastern part of the Columbia Icefield, Alberta-British Columbia, Canada	4
2.	Area-altitude graph of Saskatchewan Glacier and firn	5
3.	Castleguard sector in 1952–54	7
4.	Average surface lowering, 1948–54, in feet per year	8
5.	Bedrock topography	9
6.	Cross sections in Castleguard sector	10
7.	Daily ablation rate, positions of the temporary snowline, and average yearly ablation expressed as a function of elevation along the central part of Saskatchewan Glacier	11
8.	Total ablation and positions of temporary snowlines	12
9.	Nomenclature of velocity stakes, transit points, and coordinate systems	13
10.	Dates of survey of velocity stakes	14
11.	Relative difference between summer and yearly velocity as a funtion of longitudinal position	16
12.	Velocity variations in 1952	16
13.	Short-interval velocity variations in 1953	17
14.	Velocity deviations and meteorological observations, 1953	18
15.	Relation of deviation of velocity to temperature	19
16.	Velocity dispersion spectrum at stake 6–4	19
17.	Definition sketch of velocity components	20
18.	Distribution of V_x' and V_d on Saskatchewan Glacier	20
19.	Distribution of V_x, and horizontal projection of velocity vectors in Castleguard sector	21
20.	Distribution of V_y' in Castleguard sector	23
21.	Distribution of V_z in Castleguard sector	23
22.	Distribution of V_d in Castleguard sector	24
23.	Downglacier, surfaceward, and vertical velocities and surface slope along the flow centerline	25
24.	Downglacier velocity along four transverse profiles in Castleguard sector	26
25.	Ratio of downglacier velocity (V_x) to centerline downglacier velocity (V_{xcl}) as a function of relative distance from the centerline for four transverse profiles	26
26.	Ablation velocity (V_a) compared with difference between surface lowering velocity (V_s) and surfaceward flow velocity (V_d)	26
27.	Velocity vectors projected onto a transverse plane perpendicular to the glacier surface at $x' = 10{,}000$, viewed upglacier	27
28.	Simplified sketch of hotpoint	29
29.	Configurations of borehole number 1 in 1952 and 1954	30
30.	Deformation of vertical borehole parallel to the centerline of flow. Circles indicate measurement points, short horizontal lines indicate approximate limits of measurement error	31
31.	Measured velocity gradients in Castleguard sector	32
32.	Mohr's circle constructions showing changes in strain rate along a transverse profile at $x' = 10{,}000$	33
33.	Orientations and magnitudes of principal strain rates in Castleguard sector	33
34.	Principal strain-rate trajectories in Castleguard sector	34
35.	Trajectories of greatest shear-strain rate in Castleguard sector	34
36.	Normal strain rates parallel to the x'- and y'-axes in Castleguard sector	36
37.	Definition sketch for analysis of stress and deformation in a vertical profile	39
38.	Vertical gradient of horizontal velocity along vertical borehole. Circles indicate measurement points, short horizontal lines indicate approximate limits of measurement error	39
39.	Strain rate as a function of shear stress in Saskatchewan Glacier	40
40.	Strain rate as a function of shear stress, data from many sources	43
41.	Difference between velocity at the surface and velocity at depth as a function of depth	47
42.	Distribution of velocity in transverse section at $x' = 5{,}000$	48
43.	Diagrammatic longitudinal section of a glacier showing sedimentary layering	52
44.	Crevasses in Castleguard sector	56
45.	Orientation of structural features in Castleguard sector	58
46.	Crevasse and open-crack orientations as a function of transverse location	61
47.	Phantom view of part of Saskatchewan Glacier showing possible fracture planes leading to formation of en echelon crevasses at the surface	63
48.	Error distribution for 50 measurements of a fixed angle	65

TABLES

			Page
TABLE	1.	Measured summer and annual velocity components, in feet per year	15
	2.	Standard deviation of velocity	16
	3.	Velocity components, slope, ablation, and surface lowering at velocity stakes	22
	4.	Strain-rate components	35
	5.	Stress and strain-rate data from vertical borehole	41
	6.	Stress and strain-rate data from transverse surface profile	42
	7.	Mass-budget data for the south half of the tongue of Saskatchewan Glacier	46
	8.	Criteria for distinguishing foliation from stratification	54
	9.	Characteristics of orientation maxima	59
	10.	Coordinates of velocity stakes	66
	11.	Inclination data for boreholes	67

MODE OF FLOW OF SASKATCHEWAN GLACIER, ALBERTA, CANADA

By Mark F. Meier

ABSTRACT

Research in 1952–54 on Saskatchewan Glacier was directed toward the measurement of velocity on the surface and at depth, the surface and bedrock topography, ablation, and structures produced by flow. These field data are used to test current theories of flow and to derive new conclusions about the flow of a valley glacier.

Positions in space of 51 velocity stations fixed in the ice were computed from triangulation surveys. Summer velocities are generally greater than yearly velocities. Short-interval (½–1 day) observations recorded great velocity fluctuations and intermittent backward movements. Some of these fluctuations represent domains not more than 100 feet in extent. Dispersion values indicate that jerkey motion is probably due to irregular shearing and is not predominantly perpendicular to crevasses. Dispersion of velocity decreases with increasing time intervals of measurement. Maximum surface velocity of 383 fpy (feet per year) occurs at the firn limit; velocity decreases unevenly along the midglacier line to 12 fpy at the terminus. Velocity vectors plunge below the surface along the centerline from above the firn limit to 1.3 miles below. Further downglacier the vectors rise out from the surface and the angular divergence increases both downglacier and toward the margins. The flow of ice toward the surface is constant at 10 fpy in the lower 3 miles. Rates of surface lowering computed from these data and ablation data agree approximately with independently measured thinning.

Velocity gradients in an area of detailed study are analyzed to determine the surface strain-rate field. Deformation is largely caused by the transverse gradient of the longitudinal velocity. Longitudinal and transverse extensions and compressions were measured. One principal strain-rate trajectory lies along the flow centerline; a trajectory of maximum shearing strain rate parallels the valley wall at the margin.

Velocity to a depth of 140 feet decreases exponentially. The flow law of ice is determined by an analysis of this short vertical profile and a transverse velocity profile on the surface. The two sets of data give consistent results which agree with results from other glaciers, and suggest that the flow law is unaffected by either hydrostatic pressure or extending or compressing flow. The strain rate cannot be expressed as a simple power function of the stress. A viscouslike flow seems to predominate at low stresses. Above a shear stress of 0.7 bar the flow velocity changes much more rapidly with slight changes in stress.

The derived flow law is used to compute velocity as a function of depth and the mass-budget. These results show that the ice currently being supplied to the surface is not as great as the surface ablation but is just sufficient to keep the glacier thinning at an unchanged rate in time. Computed streamlines parallel the bedrock channel closely.

Three main classes of features in the ice are distinguished: (1) primary sedimentary layering, (2) secondary flow foliation and (3) secondary cracks and crevasses. Primary stratification is flatlying in general but wrinkled longitudinally in detail. Foliation generally dips steeply, strikes longitudinally, and shears other structures. However, some foliation attitudes do not relate to measured directions of maximum shearing strain rate at the point of observation or at any conceivable point of origin. The orientation of the most prominent set of cracks agrees approximately with measured trajectories of principal compressing strain rate. Other minor sets of cracks are related to trajectories of maximum shearing strain rate.

INTRODUCTION

"One of the difficulties in the past has been that theories of glacier flow have often had to start from arbitrary assumptions about the mechanical properties of ice, which had never been adequately investigated, and to proceed to predictions about velocity distributions in glaciers which could not be verified by experiment." (Gerrard, Perutz, and Roch, 1952, p. 547)

The flow of glaciers has long been a subject of controversy, and many completely different theories of flow have been propounded. Rigorous checking by field measurement, however, has lagged far behind the development of theoretical concepts. The complete velocity field on the surface or at depth of a glacier has never been satisfactorily measured. This information is basic to the framing and testing of theories of flow.

The objective of the study on Saskatchewan Glacier was to gather these basic data, together with essential supplementary information such as the variation of the velocity field with time, the shape of the glacier and its bed, and the structures produced by flow. An ultimate goal was to relate these field data to known mechanical properties of ice and modern theories of glacier flow. Saskatchewan Glacier is favorably situated for this study because it is easily accessible, facilitating fieldwork, and is of simple geometrical shape, simplifying the mathe-

matical treatment. The detailed mechanism of flow (the process by which individual crystals yield to stress) is not a matter of principal concern here, and the glacier is assumed to be a continuous, homogenous body. Some work has been done on the mechanism of flow of Saskatchewan Glacier by G. P. Rigsby.[1]

The organization of this report is as follows: Data bearing on the general characteristics of the glacier, its physical setting, surface topography, channel configuration and surface ablation are presented first. This basic information is the background material for analysis of the flow.

Results of measurement of the surface velocity field are then described. Velocity at fixed points varied from day to day and from season to season, but changed little from year to year. Short-interval (12-hr) fluctuations in velocity are greater and offer some insight into the mechanism of flow. These fluctuations limit the accuracy with which the time-averaged velocity field can be measured. After the time variations in velocity are described, attention is given to the time-averaged configuration of the surface velocity field. This is a vector field and the vectors do not parallel the surface, so it is necessary to measure three components of velocity in space. Values of the horizontal component directed down-glacier, the horizontal transverse component, and the vertical component relative to a fixed coordinate system are discussed. A vertical component measured relative to the instantaneous ice surface, which represents the surfaceward flow, is then presented. Finally, results of measurement of velocity at depth are given.

The mentioned sections which present basic data are followed by interpretive discussions. The surface strain rate field is computed from measured velocity gradients, providing information on the deformation of ice at the surface. An analysis of the geometry of flow is made involving: (1) The total discharge of the glacier as compared with the surfaceward flow and ablation on the surface; (2) a computation of the streamlines of flow at depth; and (3) some statements about the equilibrium and quasiequilibrium longitudinal profiles of this glacier. The data from Saskatchewan Glacier offer some insight into the flow law (strain rate as a function of stress) of ice, and these results are presented and analyzed.

Structural features in the ice offer additional insight into the mode of flow and are discussed in the final section. A prominent flow foliation is apparently a shear phenomenon but cannot be related precisely to measured planes of greatest shearing distortion. Cracks form in close correspondence to the principal elongations and are used as indicators of strain rate and stress conditions on parts of the glacier where the flow was not measured.

Fieldwork on Saskatchewan Glacier was done from June 23 to September 2, 1952; June 19 to September 8, 1953; and from July 8 to August 13, 1954. Camps were maintained at the Alpine Club of Canada's Saskatchewan Hut (1.7 miles below the glacier terminus) and outside the south lateral moraine near Castleguard Pass (fig. 1). A road extends to within 2,000 feet of the present terminus of the ice, making the glacier easily accessible. Most of the movement of equipment and supplies on the glacier was by backpack, but some material was hauled upglacier by truck and packhorses. Uncertain weather, unpredictable operation of specially designed equipment, necessity for precautions against the hazards of glacier travel, as well as time spent on logistical matters, severely restricted the amount of scientific work that could be done in a field season, even on this easily accessible glacier.

PHYSICAL SETTING OF SASKATCHEWAN GLACIER

Saskatchewan Glacier, at the head of North Saskatchewan River in Banff National Park, is the largest of the six principal outlet tongues[2] of the Columbia Icefield (fig. 1). This icefield lies astride the Alberta-British Columbia line in the Canadian Rockies (lat 52°08′, long 117°12′). The part of the firn region of the Columbia Icefield that feeds Saskatchewan Glacier is entirely in Alberta and covers an area of about 9 square miles and ranges in altitudes from 8,000 to 11,300 feet. Almost half of this area lies between altitudes 8,500 and 9,000 feet (fig. 2). About 2 square miles of firn is split off the main part of the icefield by a high mountain ridge, and the only medial moraine on Saskatchewan Glacier is formed where this ice joins the flow from the main icefield. Two former tributaries approach the trunk glacier on each side about 2 miles above the terminus, but do not join at present. The usual firn limit lies almost at the juncture between icefield and tongue and ranges in altitude from 8,000 to slightly more than 8,300 feet. The tongue is 5.5 miles long and descends to an altitude of 5,900 feet (pl. 6). It is about 1 mile wide in the upper 2.5 miles

[1] Rigsby, G. P., 1953, Studies of crystal fabrics and structures in glaciers, Ph.D. thesis, California Inst. Technology, 51 p. *See also* Meier, Rigsby and Sharp (1954, p. 21–24).

[2] In this report, the term "Saskatchewan Glacier" refers to the tongue only and does not include the firn area within the Columbia Icefield. The glacier according to this definition lies entirely below the firn limit.

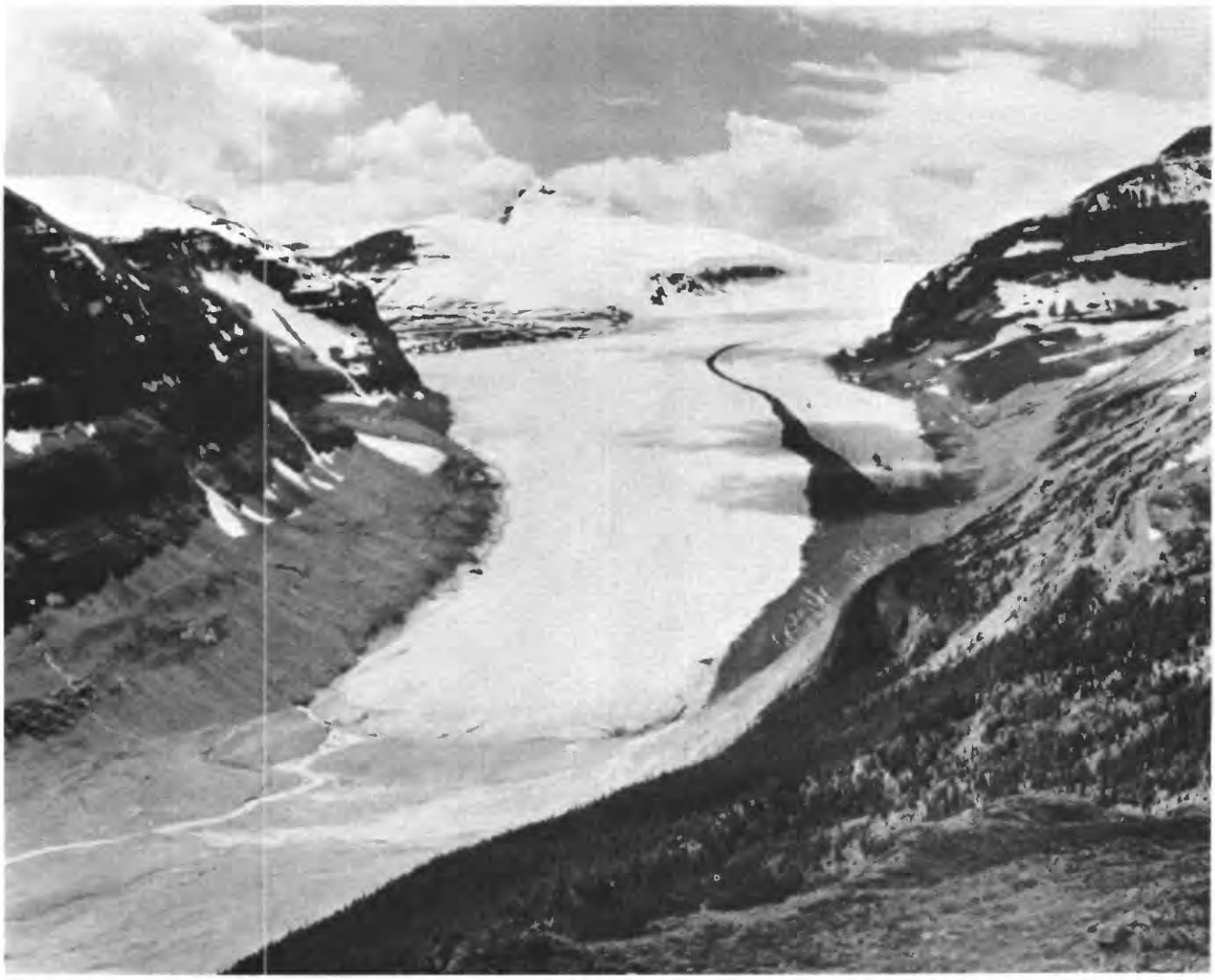

SASKATCHEWAN GLACIER VIEWED FROM PARKER RIDGE, JULY 11, 1952

509755 O - 60 - 2

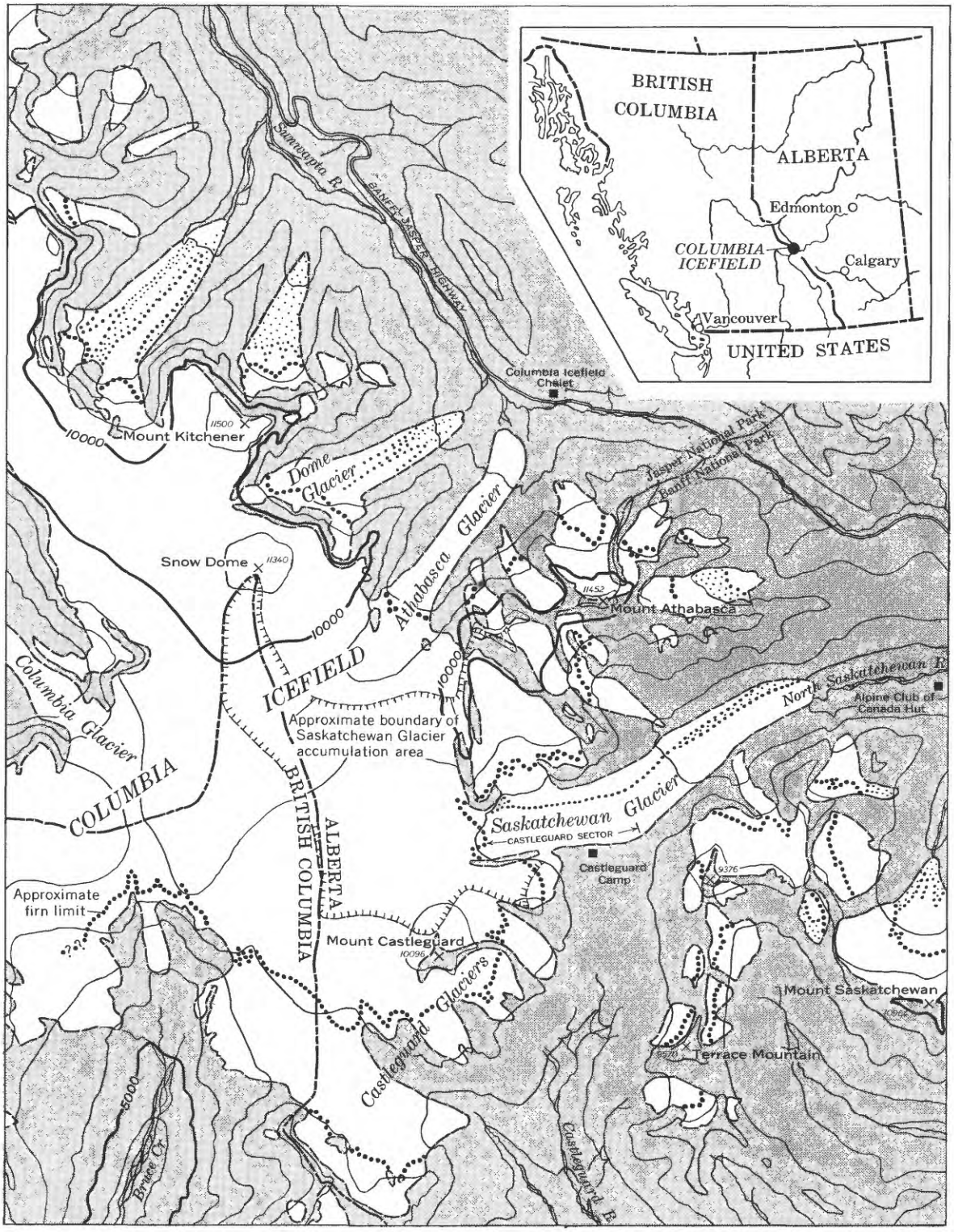

Map modified from Banff and Jasper National Parks maps (1:190,080) and Interprovincial Boundary Commission maps (1:62,500); glacier margins mapped by reference to 1948 aerial photographs and 1952–1954 ground observations

1 0 1 2 3 4 Miles

Contour interval 1000 feet
Datum is sea level

N

FIGURE 1.—Map of the eastern part of the Columbia Icefield, Alberta–British Columbia, Canada.

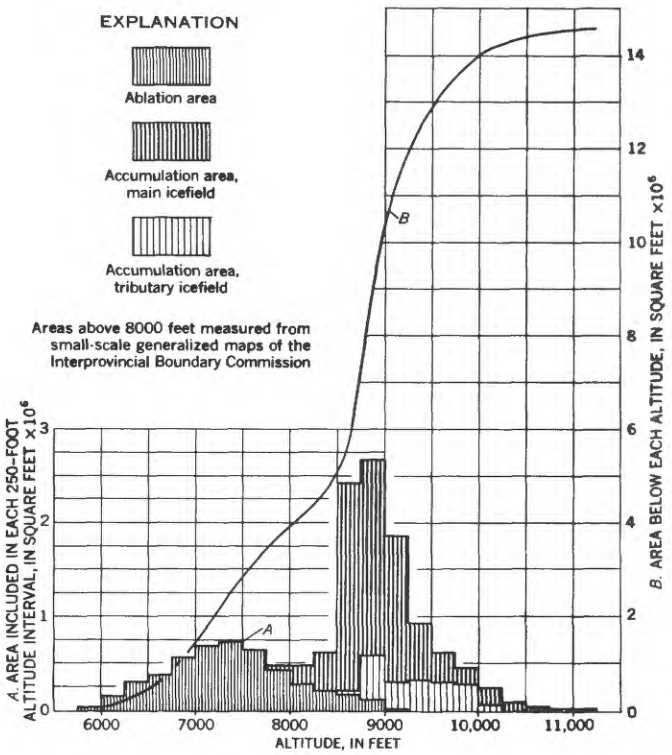

FIGURE 2.—Area-altitude graph of Saskatchewan Glacier and firn.

(the "Castleguard sector," see fig. 1) and tapers to a width of 2,000 feet near the terminus. It has only one gentle curve of about 30° 3.5 miles above the terminus.

The total area of Saskatchewan Glacier and its firn field is 14.5 square miles of which the accumulation area embraces 68 percent. The average net accumulation over this area can be computed because the amount of ice discharged into the Saskatchewan Glacier tongue is known for 1953–54. An average annual accumulation of 3.2 feet of water over the area of the firn basin would have supplied this known discharge.

GENERAL CHARACTERISTICS OF THE GLACIER

Glaciers can be classified and compared in three ways according to Ahlmann (1948, p. 59–67): by shape (morphological), by activity (dynamic), and by thermal characteristics (geophysical). The shape of this glacier, as indicated by the area-altitude graph (fig. 2), is that of a valley glacier of the alpine type (Ahlmann, 1948, p. 62, type II). It may be termed an "outlet" glacier but not an "outflow" glacier in the sense used by Finsterwalder (1951, p. 557).

The activity—or the metabolism—of a glacier can be expressed quantitatively as the gradient of net accumulation (total yearly accumulation minus total yearly ablation) with increasing altitude at the firn limit. This parameter has been termed the "energy of glacierization" by Shumskii (1947) and it expresses the "degree of activity" as discussed by Ahlmann (1948, p. 63). The gradient on Saskatchewan Glacier is 0.013 (13 mm per meter) just below the firn limit. This indicates a high degree of activity, comparable to that of glaciers of the Alps—Rhone Glacier, 12.4 mm per meter and Hintereisferner, 15.8 mm per meter according to Shumskii (1947) and suggests some maritime quality in the local climate.

No investigations were made of the thermal regimen of Saskatchewan Glacier, but it is assumed to be thermally temperate because it lies at a relatively low latitude, and copious meltwater is produced in the summer. However, unexpected freezing conditions were found in drilling operations (p. 31). This suggests that subfreezing temperatures can exist in the crustal ice even in late summer, although the bulk of the glacier probably exists at the pressure-melting temperature.

It seems reasonable to treat Saskatchewan Glacier in its larger aspects as a homogeneous and isotropic body in spite of many small-scale inhomogeneities. Exposed ice in the ablation area shows irregular patterns of differences in grain size. Average grain sizes over areas of several feet range from about 1 millimeter to nearly 10 centimeters. Grains are largest along the margins, smallest along the centerline, and show an uneven but noticeable increase downglacier. Complex intergrowths of crystals were observed in coarse-grained ice. Except for local zones of young, partly icified firn in midglacier, all of the exposed ice seems to be of about the same compactness and hardness. The density is assumed to range between 0.85 and 0.91. Except for a foliated structure that is pronounced near the margins no consistent patterns of differences in bubble content were observed, and no crystal-shape orientation patterns were discovered. Crystal-fabric studies by Rigsby[9] and Meier, Rigsby and Sharp (1954, p. 21–24) revealed very weak crystal axes orientations except along the extreme margins and at the terminus. To a reasonable approximation, therefore, the bulk of the glacier can be described as constant in density, homogenous, and isotropic in physical characteristics. This approximation is probably not valid near the valley walls.

Saskatchewan Glacier apparently began to with-

[3] Rigsby, G. P., op. cit.

draw from its greatest recent extent in 1854 (Field and Heusser, 1954, p. 135), and the terminus has retreated subsequently about 4,000 feet. High abandoned lateral moraines indicate a concurrent thinning of more than 100 feet over most of the tongue. Recession and thinning were continuing at the time of these field studies.

SURFACE CONFIGURATION

Quantitative study of stress and flow in a glacier requires an accurate topographic map of the surface. In 1952–53, a triangulation net of 14 bench marks was established along both sides of the glacier. Nine of these bench marks were used as control for the construction of a topographic map from Royal Canadian Air Force stereoscopic aerial photographs taken in 1948. In addition, a map of the terminus (1953), 3 transverse profiles (1952) and a 5-mile longitudinal profile (1954) were compiled from stadia surveys. These data, plus 46 accurate spot elevations on the glacier surface, were used to construct maps of the glacier surface as it existed in 1954 (pl. 4, fig. 3). Longitudinal and transverse profiles are shown in plate 1.

These data show that Saskatchewan Glacier has a very uniform longitudinal slope which averages 3°23′, exceeding this markedly only at the extreme terminus (maximum of 11°9′) and near the firn limit (reaching 8°40′). The transverse profiles are flat to slightly concave near the firn limit and flat to slightly convex (sometimes with a slight concavity along the centerline) over the rest of the tongue. Marginal troughs are prominent in the Castleguard sector.

RECENT CHANGES IN SURFACE LEVEL

Comparison of a longitudinal profile drawn from the map constructed from 1948 aerial photographs with the 1954 stadia profile suggests pronounced thinning over the whole tongue (pl. 1). The elevation difference between those profiles is probably accurate to within 10 or 15 feet in the vicinity of 13 accurately surveyed velocity markers and 25 feet elsewhere. The possibility of cumulative error is discounted because both the stereoscopic model and the elevations of velocity markers were controlled by the same points on bedrock. Thinning data for the whole glacier, computed in this manner, are shown in figure 4. In figure 4 and plate 1 the five firn limit points were computed as of 1953 (they were buried under snow in the 1954 field season) and the glacier surface was assumed not to have changed in elevation at these points from 1953 to 1954.

The thinning data show that the tongue is not in equilibrium, but is wasting downward at a rate of 4 to 13 feet per year (fpy). Thinning rates oscillate between 11 fpy at the firn limit, 5 fpy 2 miles below the firn limit, 16 fpy 3.5 miles below the firn limit, 5 fpy at 5 miles below, and a maximum of 15 fpy at the extreme terminus. Thinning is more conservative along the south margin; few data are available for the north margin. Whether this apparent periodicity along the centerline represents a wavelike flow response or periodic climatic changes, or just coincidence, is not clear. However, the data are too crude for firm conclusions.

Recent abandoned lateral moraines which can be traced for more than 4 miles upglacier indicate that thinning has been going on for some time. The elevations above the ice of the two most prominent moraines are plotted in plate 1, and show that thinning has not been uniform in the past.

CHANNEL CONFIGURATION

Seismic explorations in 1952 by C. R. Allen provide information on the shape of the glacier's bedrock channel. Reliable reflections were obtained at 9 locations comprising 1 longitudinal and 2 transverse profiles, using equipment and techniques described elsewhere (Allen and Smith, 1953, p. 756). These data[4] (C. R. Allen, written communication) are plotted on figure 5 together with the approximate bedrock topography and 7 transverse cross sections. The channel shape at the firn limit is unknown, but the approximate area has been computed from flow data (p. 46) and a half-elliptical shape has been assumed.

These data show a broad, U-shaped, evenly inclined channel section. The shape of the whole glacier in its channel approximates a circular cylinder having a diameter of 5,250 feet, inclined east at an agle of 0°46′, curved slightly in a horizontal direction, and cut by a plane inclined 3°23′, in the same direction.

In Castleguard sector the southern parts of the cross sections are nearly elliptical (fig. 6). Because the sections are not quite symmetrical, most of the analytical work was concentrated on the southern part. The term "plane of symmetry" is defined by the vertical projection of the flow centerline. This flow centerline was determined from surface ve-

[4] The data from the shot point nearest the terminus are open to several interpretations: the first identifiable reflection (565 feet) may be from a contact between bedrock and moraine or outwash materials, because the plunge of surface velocity vectors in the glacier (p. 27) and geologic evidence beyond the terminus suggests that the ice is no more than 240 feet thick here. A reflection from less than 300 feet would probably have been obscured by noise from the initial explosion.

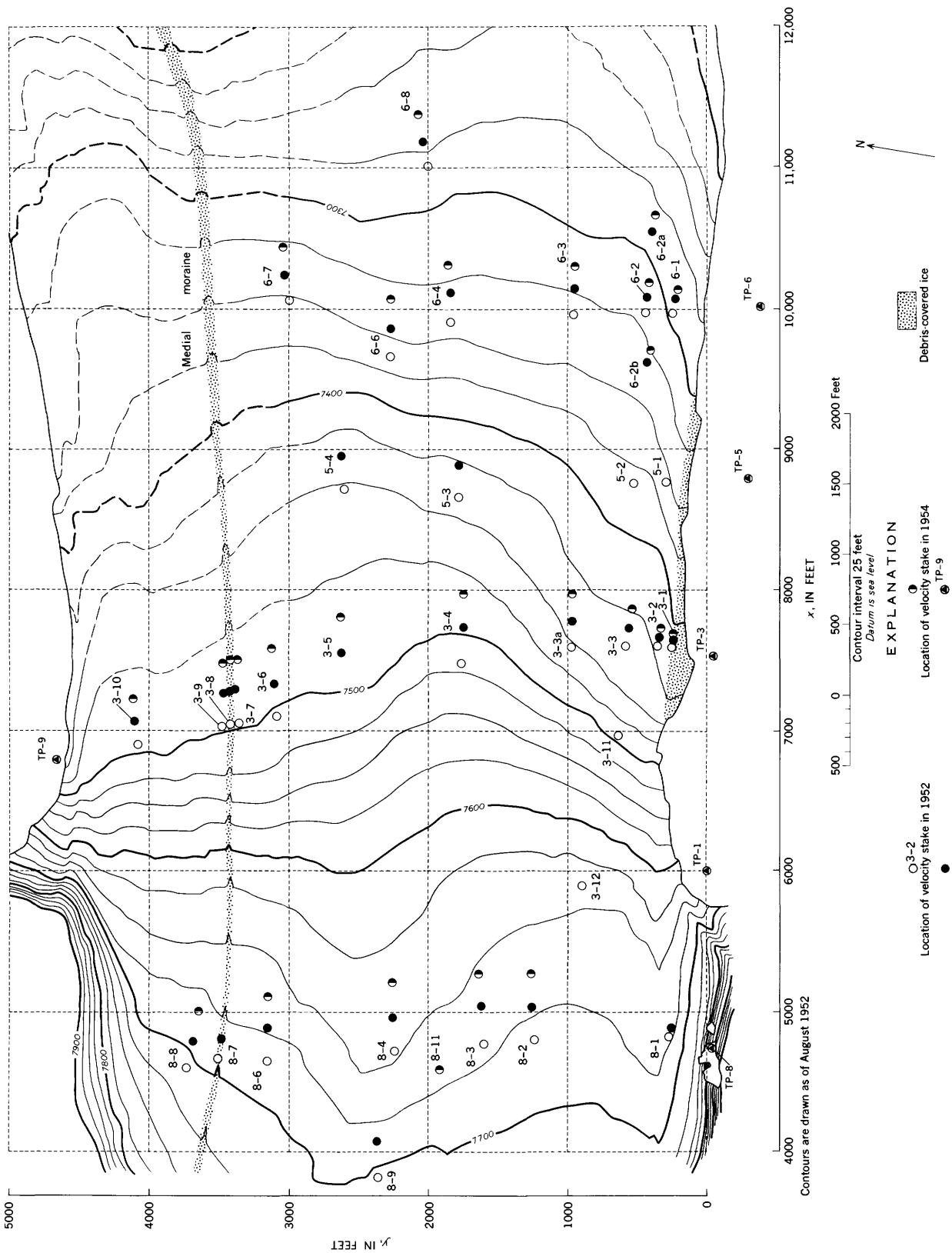

FIGURE 3.—Castleguard sector in 1952–54.

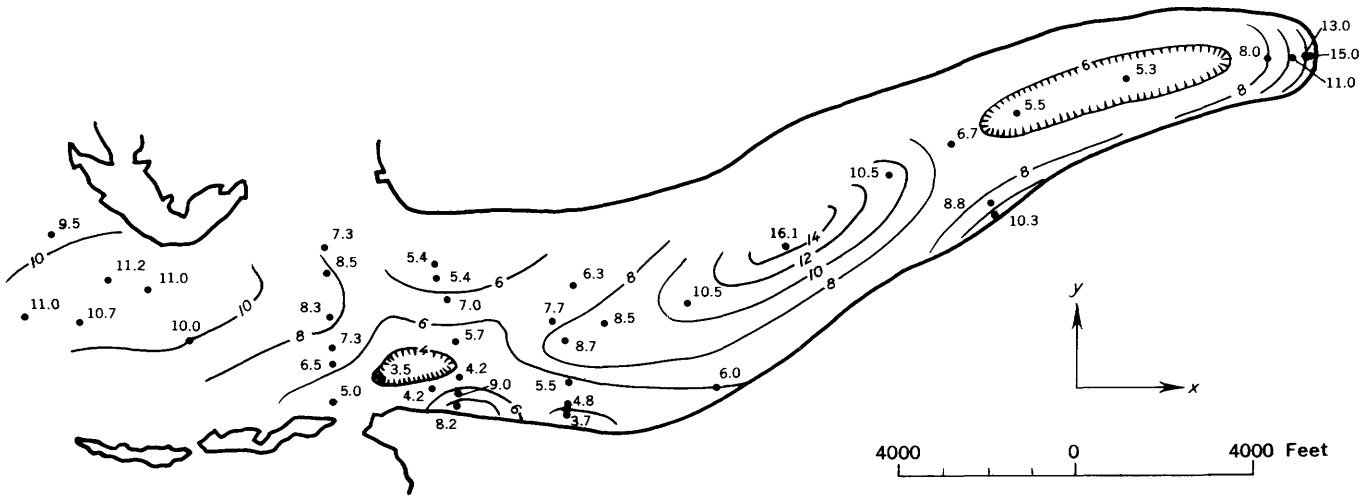

FIGURE 4.—Average surface lowering, 1948–54, in feet per year.

locity measurement (p. 10), but it conforms closely with the geometric symmetry plane of the cross sections. Data on the width, depth, area, ice perimeter and hydraulic radius[5] are given for the Castleguard sector cross sections in figure 6.

ABLATION

The regimen of Saskatchewan Glacier was not measured directly, but ablation measurements were made for comparison with surfaceward flow data. Records were kept of the lowering by melting of the ice surface at each velocity marker at irregular intervals during the 1952 field season and only as markers were reset after that. Values of ablation are reported in feet of ice melted per year. No density measurements were made. Probably the density of ice in the tongue ranges from 0.85 to 0.91, and the error due to this variance is less than the probable error of measurement.

Measured ablation rates are shown as a function of altitude in figure 7*a*. The rates reported here are average values for a period of observation of not less than a month, taken at the height of the ablation season. Points near the lateral margins are not included. These data show that ablation rate decreases slightly, but very irregularly, with increasing altitude. The noticeable scatter is presumably due to differences in ice density, roughness, exposure, and albedo at different points. The scatter is greatest in the higher altitudes where local differences in ice density and character are greatest; farther downglacier these local differences are largely eliminated by recrystallization and the scatter in ablation rates is less. Apparently ablation rates in 1953 were generally less than in 1952 and 1954.

The total ablation of ice decreases markedly from a high value at the terminus to zero at the firn limit, but the measured daily rates decrease only slightly. Therefore the total ablation at a given point must be determined largely by the length of the ice ablation season. Lengths of the actual ice ablation seasons can be estimated from data on positions of the temporary snowline; these data are shown in figures 7 and 8. The data in figure 7*b* show the progress of ablation during the seasons of 1952, 1953, and 1954. The time of the first permanent snowfall in autumn (marking the end of ablation of ice) is not known but is assumed to be about the end of September. In 1954 the season began at the lower altitudes not less than 6 weeks later than in 1952 or 1953, but the temporary snowline progressed rapidly upglacier and was about 1 month behind 1953 in the Castleguard sector (7,300 to 7,700 feet). On the basis of the measurements in 1952–54 and photographs and verbal reports from previous years, 1953 probably had the most "normal" ablation conditions of the years studied.

Velocity stakes were reset at irregular intervals during the summers so it was necessary to interpolate or extrapolate the observed ablation data to obtain equivalent values of total ablation during 1953. This required consideration of the different rates and lengths of ablation seasons in the three summers. The final 1953 equivalent ablation values may be incorrect by as much as a foot in some instances. Average yearly ablation values are presented as a function of altitude in figure 7*c* (marginal points excepted), and the variation of ablation over the

[5] The term "hydraulic radius" as commonly used in the hydraulics of rivers (area divided by wetted perimeter) is measured in a vertical plane. In this report hydraulic radius is defined similarly but is measured in a plane perpendicular to the surface.

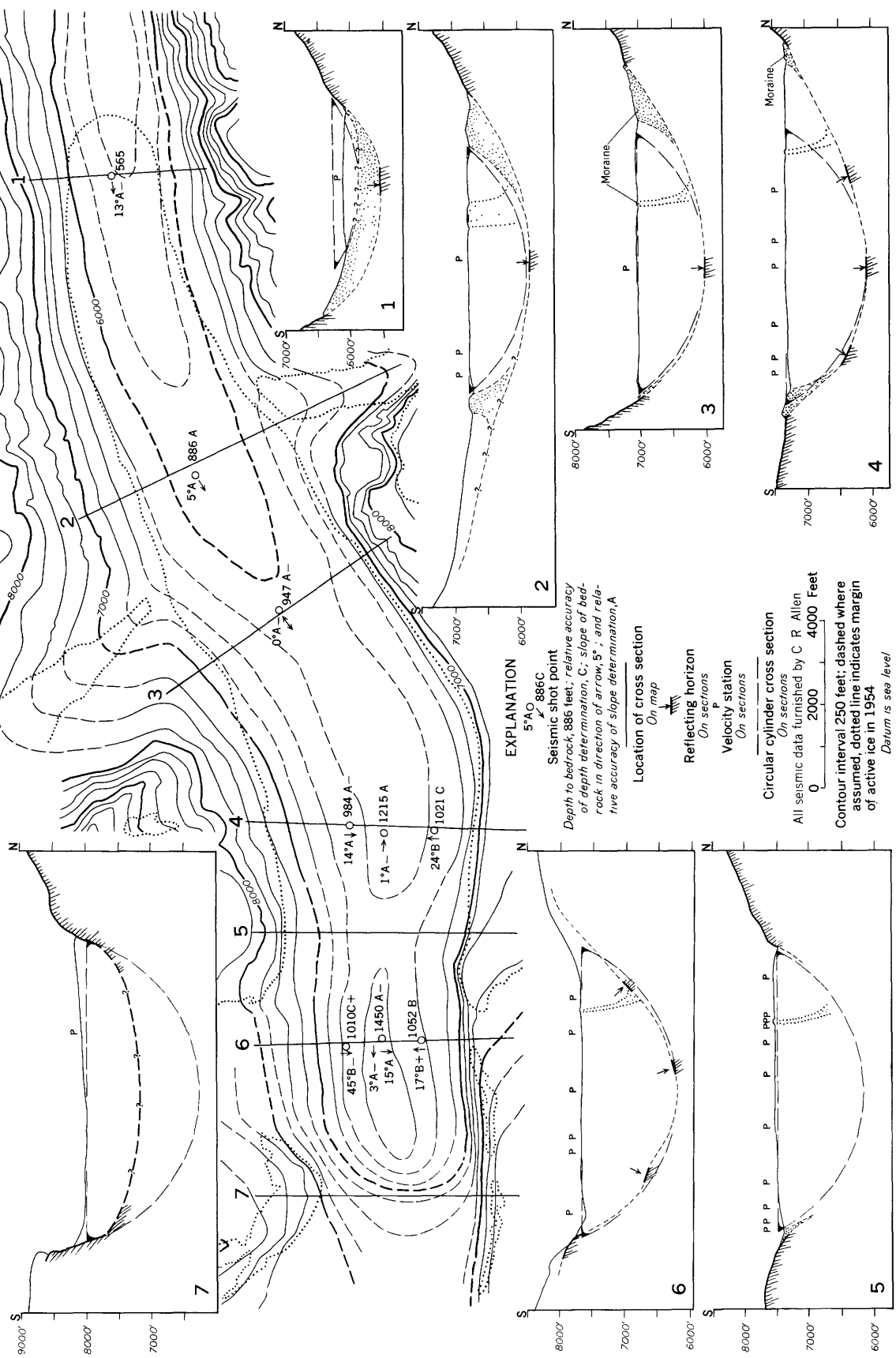

FIGURE 5.—Bedrock topography.

Coordinate distance x, feet	5000	10,000
Half width, feet	2040	2070
Maximum depth d, feet	1450	1240
Half area $A/2$, square feet	2.20×10^6	2.02×10^6
Half iced perimeter $P/2$, feet	2750	2630
Hydraulic radius $R (= A/P)$, feet	800	768
Shape factor R/d	0.552	0.620

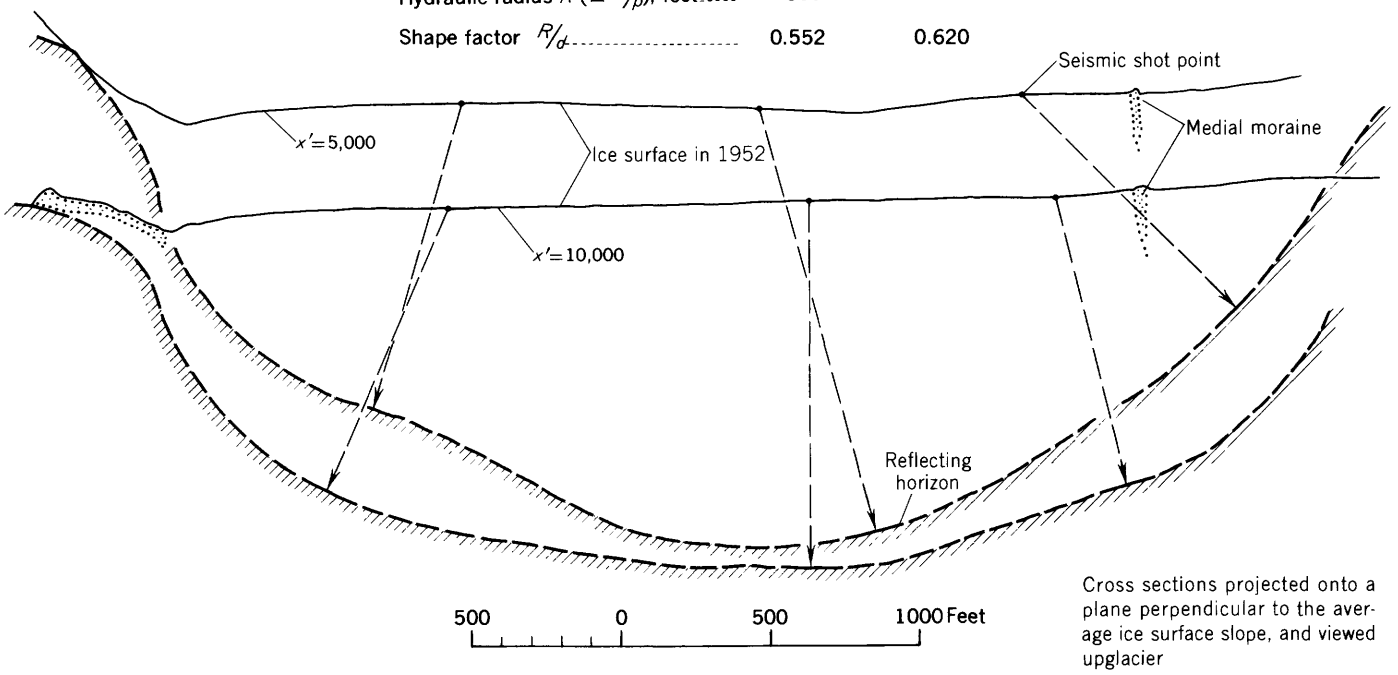

FIGURE 6.—Cross sections in Castleguard sector.

surface is mapped in figure 8. Rates of ablation and yearly ablation at each velocity stake are also given in page 22. These data show that seasonal ablation decreases smoothly, almost linearly, from terminus to firn limit. Ablation is greater along the south margin than in midglacier, especially in the Castleguard sector. This is undoubtedly due to the warmer climatic environment and the dirtier marginal ice; the effect may be especially pronounced in the Castleguard sector because of a lack of protecting cliffs. Total ablation is markedly less than normal on both sides of the medial moraine because of a persistent drift of snow that delays the ablation season. The average ablation, obtained by measuring areas within the ablation contours of figure 8, was 3.2 fpy in the highest part of Castleguard sector, 8.7 fpy in Castleguard sector as a whole, and 13.2 fpy for the remainder of the tongue below Castleguard sector.

SURFACE VELOCITY OBSERVATIONS

METHOD OF MEASUREMENT

The surface movement was measured by transit or theodolite surveys of velocity stations on the ice from fixed points on bedrock or stable deposits. Positions of the 15 transit points were determined by a triangulation survey using as its base line the distance between Mount Castleguard and "point 86" (9,376-foot peak), 2 survey points of the Alberta-British Columbia Interprovincial Boundary Survey. The base line length may be slightly in error; this would introduce a constant scale-factor error of negligible magnitude (probably less than 0.1 percent) in all measured velocities. Transit points were surveyed to an internal precision of about 1 foot for horizontal locations, and vertical locations are probably more precise. Nomenclature and locations of the transit stations and the form of the triangulation net are shown in figure 9.

All transit-point and velocity-station locations are referred to an arbitrary rectangular coordinate system defined as follows: $x = 6{,}000$, $y = 0$, and $z = 7{,}741.6$ feet at TP–1, the x- and y-axes are horizontal and the z-axis is directed upwards, and the bearing of TP–9 as seen from TP–1 is assumed to be 9°30′0″ to the right of the positive y-direction. The

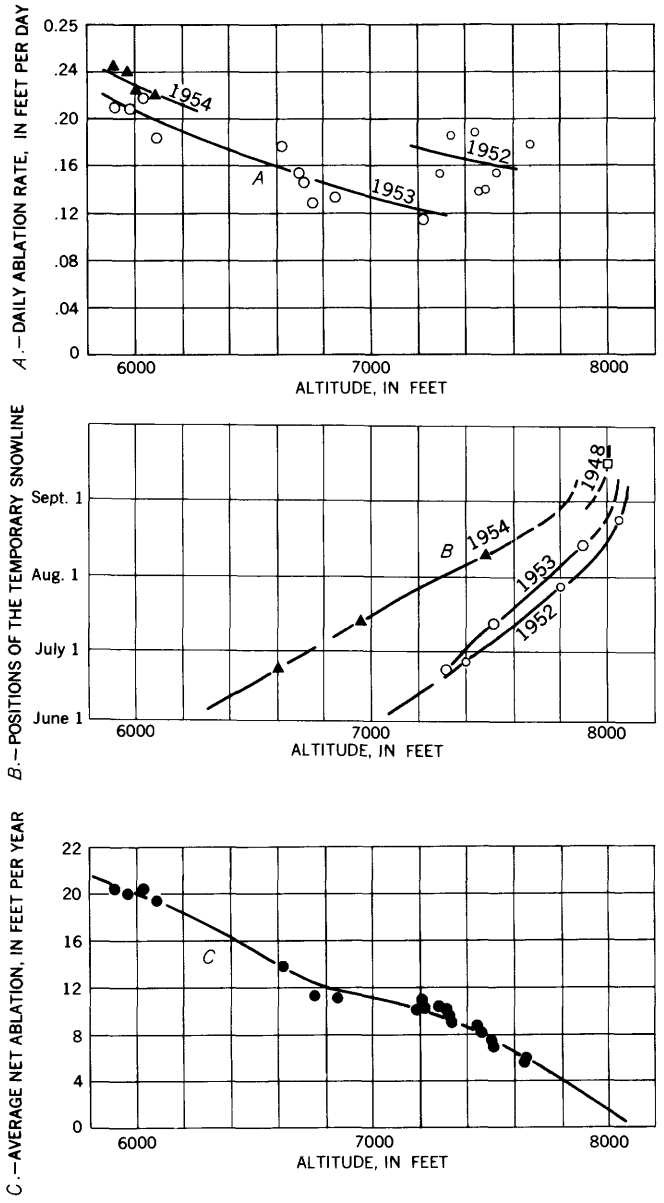

FIGURE 7.—Daily ablation rate, positions of the temporary snowline, and average yearly ablation expressed as a function of altitude along the central part of Saskatchewan Glacier.

y-axis is therefore directed approximately to 8°55′ west of true north. In addition, a 2-dimensional curvilinear coordinate system is defined as follows: $x' = y' = 0$ at $x = 0$, $y = +2{,}250$ feet; the positive x'-axis is directed along the horizontal projection of the "flow centerline"[6] in the direction of movement; the y'-axis is horizontal, perpendicular to x', and considered positive to the left when viewed down-glacier. In the Castleguard sector the x, y and x', y' coordinate systems approximately coincide except for a translation of 2,250 feet in the y-direction. The x' coordinate measures the distance below the approximate firn limit, and the y' coordinate measures the distance away from the flow centerline. These coordinate systems are shown on figure 9.

Velocity stations on the glacier surface generally consisted of 1-inch wooden dowel stakes set snugly in holes bored 8 to 9 feet into the ice. Holes were drilled with a modified "Ahlmann spoon" (Allen and Smith, 1953, p. 757). Stakes were reset periodically as ablation demanded. About a cubic foot of sand was packed around each stake on top of the ice to retard enlargement of the hole by melting; this technique was only partly successful. Sighting was done to the center of the top of each stake, which generally remained tight until more than 8 feet had been exposed by ablation; only 3 times were stakes found to be loose in the holes a day or so after setting.

Originally 53 stakes were set and surveyed but only 47 were retained for velocity determinations. In addition, 4 stations of other types (aluminum pipestem, log structures) were surveyed, but 3 of these stations provided no information on vertical motion independent of ablation. The nomenclature and mean location of each of the 51 velocity stations is shown on figure 9, and the locations of the 34 stations in Castleguard sector during each field season are shown on figure 3. These stations form a longitudinal profile from terminus to above the firn limit and 8 partial or complete transverse profiles. The main ice stream south of the medial moraine in Castleguard sector was covered in greatest detail.

Angles were measured from bench marks to the velocity stations using either a precise transit or theodolite. Coordinate locations and velocity components were computed from the triangulation information. An essential part of this project was to measure the experimental error so that the reality of many apparent fluctuations in glacier velocity can be established. The precision of the measuring procedure is discussed on page 64. In general, the probable error of measurement of yearly velocities is about 0.7 fpy for horizontal components and 1.3 fpy for vertical components. Velocities measured over an interval of less than a year are generally not as accurate.

TIME-VARIATION OF VELOCITY

Most velocity stations were surveyed twice during each of two summers and once during the third summer so that the two average summer velocities could be compared with average velocities measured over 1 or 2 years. In addition, a few stations were sur-

[6] An imaginary line on the surface of the glacier that is everywhere parallel to the projection on the surface of the velocity vectors and which passes as closely through points of maximum surface velocity in transverse profiles.

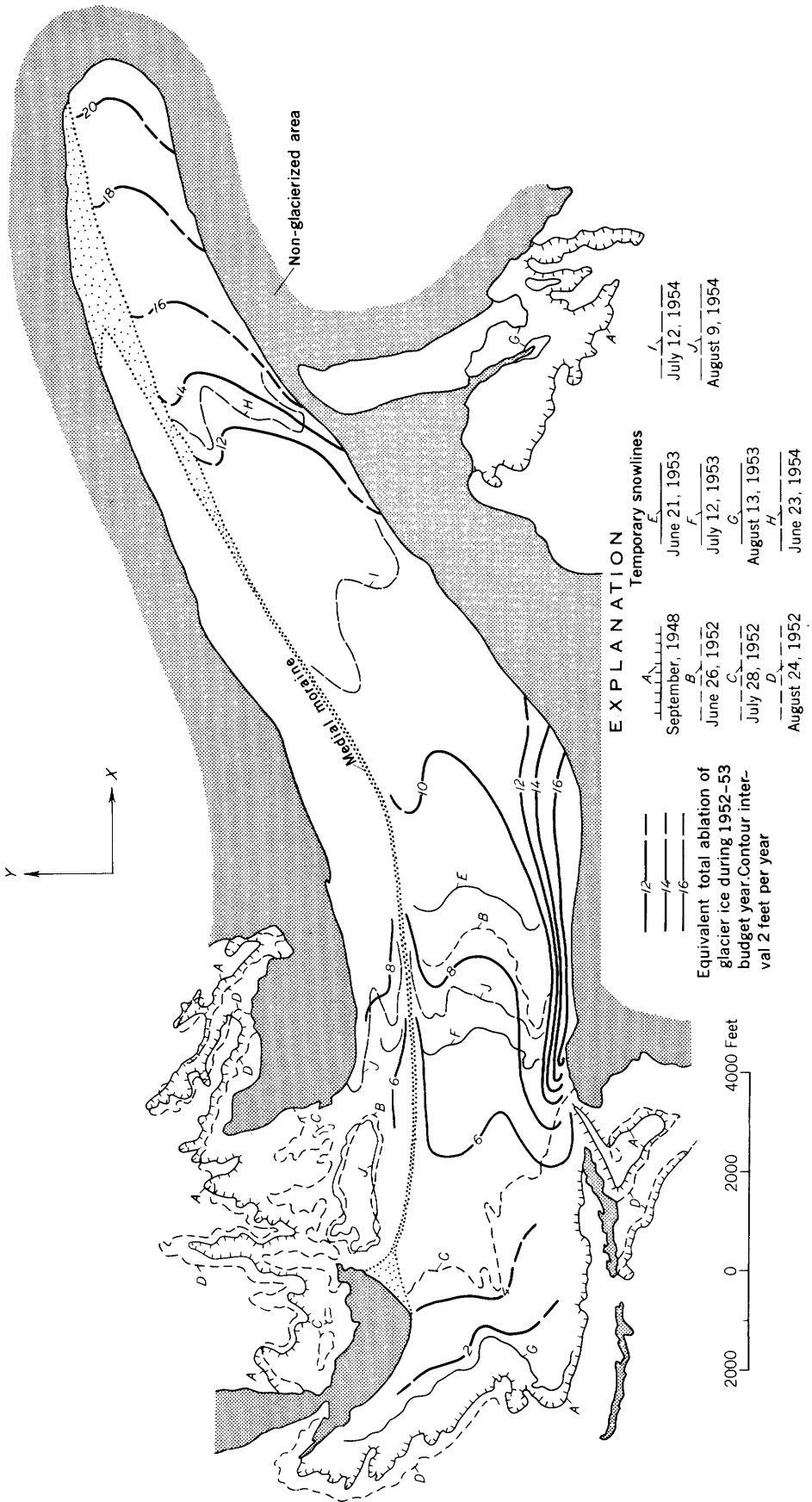

FIGURE 8.—Total ablation and positions of temporary snowlines.

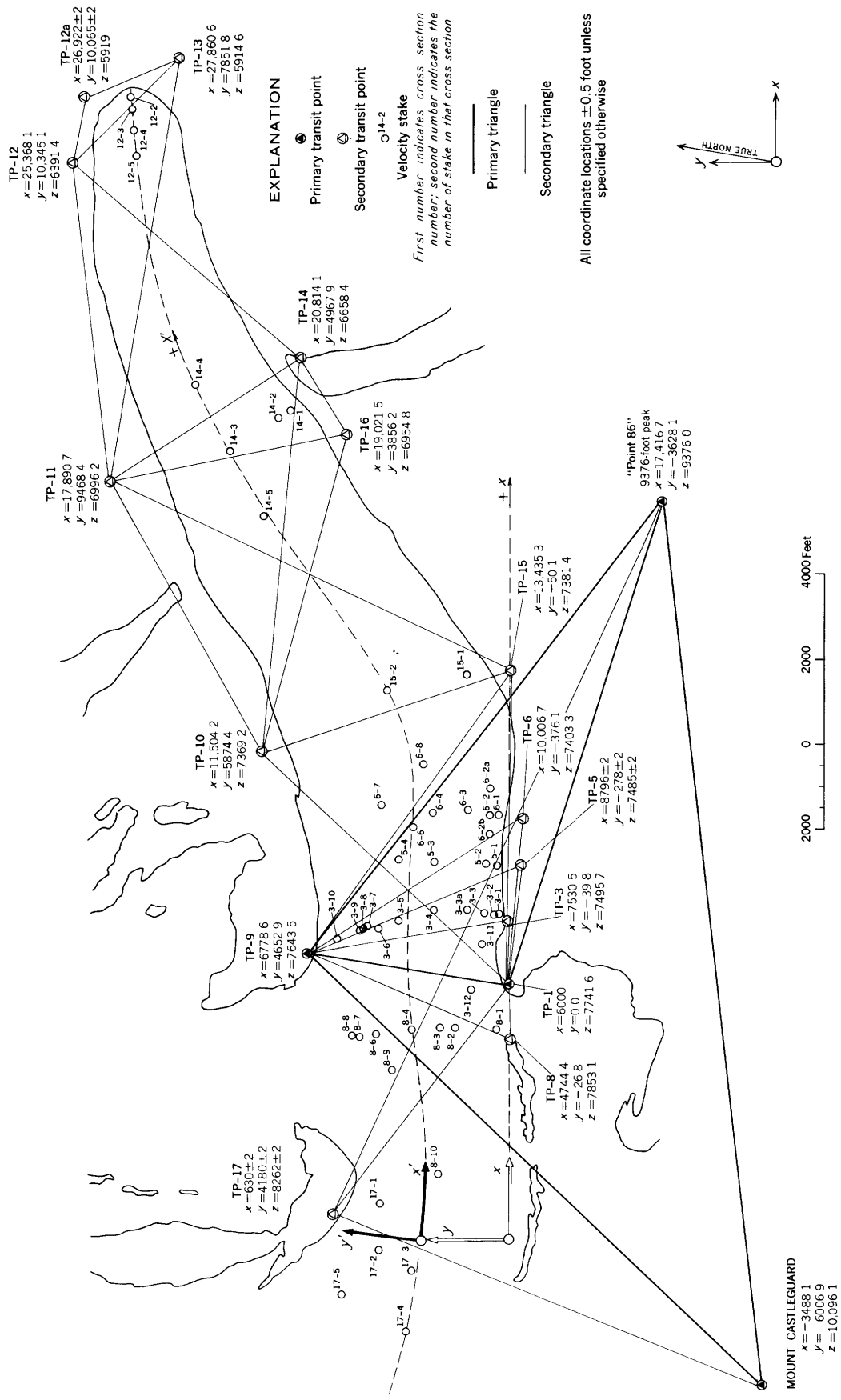

FIGURE 9.—Nomenclature of velocity stakes, transit points, and coordinate systems.

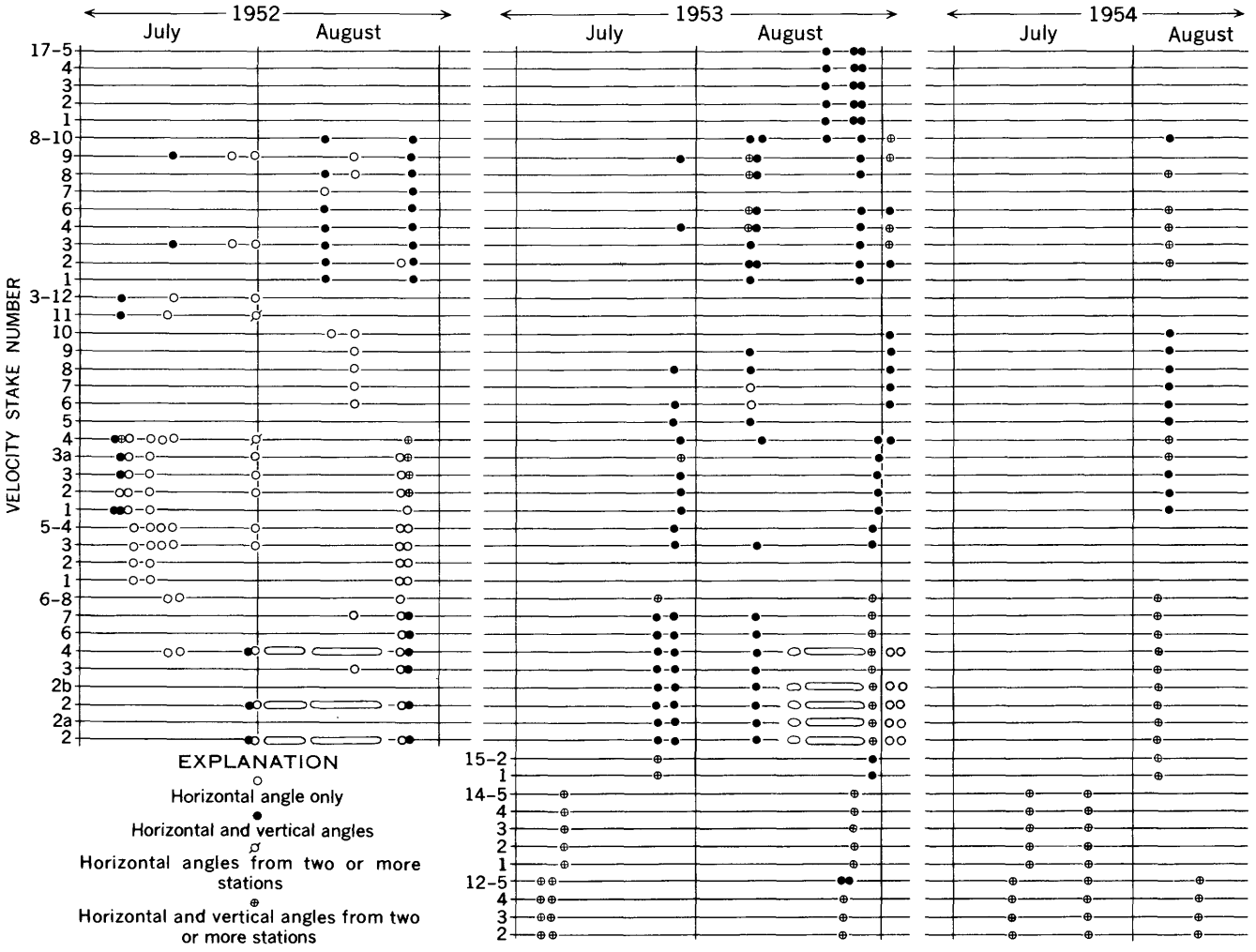

FIGURE 10.—Dates of survey of velocity stakes.

veyed at more frequent intervals to obtain detailed knowledge of the behavior of the velocity field as a function of time. The dates of survey of each stake are shown in figure 10. Measured summer and annual velocity components are reported in table 1, and coordinate locations of the stations at different times are given in table 10. All velocities are reported in feet per year; 1 fpy equals approximately 10^{-6} cm per second.

YEARLY CHANGES

Table 1 suggests a general deceleration from 1953 to 1954. Much of this apparent deceleration, however, was due to the movement of stations into locations of less velocity and does not indicate a general change in the field. However, there seems to be a slight residual deceleration (about 0.7 percent in the Castleguard sector) which is real. This could be due to the slight inequilibrium thinning because velocity of flow depends on a high power of ice thickness, but the effect is less than expected.[7]

SEASONAL VARIATIONS

In general, summer velocities are markedly greater than yearly average velocities. The percentage difference in the two velocities is apparently a function of position in the tongue (fig. 11) but the data do not show a consistent trend. The large variation in the data is probably due to short-interval jerkiness in the motion. Apparently summer and yearly velocities are nearly equal at the west end of Castleguard sector ($x' = 4{,}000$). The difference between yearly and summer velocity is greatest in the eastern part of Castleguard sector ($x' = 10{,}000$). Seasonal peaks

[7] Assuming Glen's experimental formula for creep (Glen, 1955, p. 528) and Nye's integrations for a glacier in a semicircular or very wide channel (Nye, 1952a, p. 84-85), the difference in velocity between surface and base should be approximately proportional to the 4th power of ice thickness. For the average observed thinning in Castleguard sector (6 years) this would suggest a 2 percent drop in differential velocity per year. The unknown effect of thinning on basal sliding must also be considered, however.

TABLE 1.—*Measured summer and annual velocity components, in feet per year*

[The location of each stake is shown on figure 9]

V_x = velocity component parallel to the x axis
V_y = velocity component parallel to the y axis
V_z = velocity component parallel to the z axis

Stake	1952 summer		1953 summer		1952-53 year*			1953-54 year*		
	V_x	V_z	V_x	V_z	V_x	V_y	V_z	V_x	V_y	V_z
17–5			[1][2] 209	[2] −28						
4			[1][2] 323	[2] −68						
3			[1][2] 378	[2] −45						
2			[1][2] 331	[2] −17						
1			[1][2] 305	[2] 3						
8–10			[1] 324							
9	285		244		253	17				
8	179	0	206	−17.4	182	−49	−13.4	215	−42	−15.3
7	[1] 185									
6	230		232	−11.2	232		[3] 9.1	238	−2.4	−9.1
4	266		255	−8.1	247		−8.1	246	12.7	−7.6
3	254	−12.5	[4] 252		[4] 241	[3] 14	−9.1	239	13.7	−7.9
2	239		[4] 235		231		[4] 6.2	230	19.7	−9.5
1	[1] 38	8.4			[1] 37		5.5			
3–12	[1] 212									
−11	[5] 194									
10	170				[1][2] 164			168		10.6
9					[1] 231			234		−3.4
8			[4] 204		230			235	18.5	−3.3
7					[1] 233			[1] 235		−2.7
6					[1] 243			[1] 244		−3.9
3–5								[1][4] 249		[3] −9.1
4	[6] 262	−21.5	253	−13.6	[4] 243	[4] −9.6	[3] −11.4	242	−6.0	−13.0
3a	222	−15.8	221	−9.8	[4] 204		[3] −12.0	206	−17.7	−10.2
3	[1] 156	−1.0	[1] 153	4.6	[1][4] 126		[3] 1.0	[1] 133		3.6
2	[1] 93				[1][4] 71			[1] 72		6.6
1	[1] 51		[1][4] 49		[1][4] 38		[3] 2.2	[1] 35		6.4
5–4	[1] 217	−10.1	[1] 241	−13.5						
3	[1] 213	−14.0	[1] 235	−13.4						
2	[1] 120	6.4								
1	[1] 67									
6–8			232	−4.3				183	40.3	−2.4
7			237	−13.9	[4] 186	[4] 19.3	[3] −5.3	194	23.2	−4.8
6			233	−12.9	214	1.6	−9.1	214		−11.5
4	237		225	−8.6	208	2.8	−10.4	[4] 209	[4] 18.6	−4.1
3			200	16.0	[4] 175			157.8	−6.8	3.3
2b			121	2.4				99.5	−17.5	7.8
2	129		119	10.5	[4] 99	[4] −22		98.3	−18.4	6.6
2a			109	10.3				86.4	−13.5	8.6
1	92	7.8	91	15.7	[4] 85	[4] −14.7		64.2	−17.4	7.8
15–2			[4] 141					143.2	73.1	1.9
1			[4] 44					38.5	20.7	6.2
14–5	122							120.3	54.1	2.3
4	104							94.9	40.6	1.6
3	118		[2] 137					107.5	45.8	1.8
2	118		[2] 125	[2] 17				98.6	37.0	1.6
1	98		[2] 65	[2] 6				85.4	33.5	9.0
5	53		25	1				38.4	5.3	−.8
4	45		26	−3				31.6	6.1	.6
3	22		19	−1				23.4	6.7	
2	20		11	−1				11.7	.5	3.8

[1] Horizontal flow direction assumed.
[2] Time interval 10 days or less.
[3] Uncertainty due to resetting ±1 fpy.
[4] Uncertainty due to resetting, ±3 fpy.
[5] $V_y = -71$.
[6] $V_y = 1.6$.

* The 1952–53 year and 1953–54 year values represent average velocities from late July or early August of the first year to a similar date in the second year.

509755 O - 60 - 3

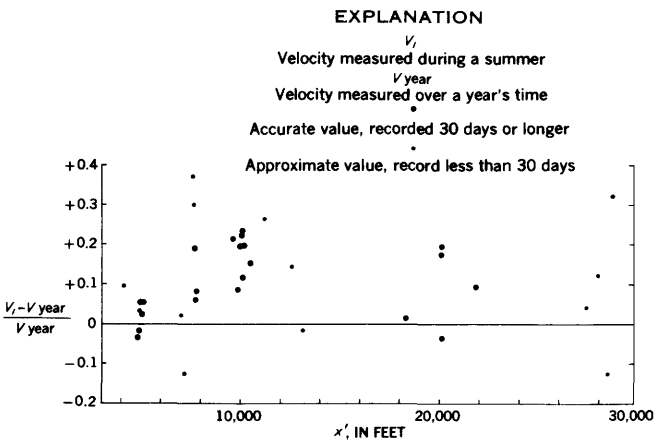

FIGURE 11.—Relative difference between summer and yearly velocity as a function of longitudinal position.

in velocity may progress from the firn, in winter, to the extreme terminus in fall in some valley glaciers (Hess, 1933, p. 73). It is possible that similar "waves" passed through the lower part of Castleguard sector during the July and August measuring periods.

SHORT-INTERVAL VARIATIONS

Glacier motion is known to be jerky with respect to measurements made on an hourly or daily schedule (Klebelsberg, 1948, p. 86–88), but the detailed form of the variations and their cause is not known. The velocity of stakes 6–1, 6–2, and 6–4 was measured once a day for 22 days in 1952 to obtain data on these short-interval fluctuations. A marked variation in flow rates was found (fig. 12).

In 1953 the measurements were continued at 12-hour intervals for 18 days (fig. 13) using 5 stakes arranged in a cross, one arm transverse and the other parallel to the direction of flow. Angles to the stakes were turned from a reference mark painted on the cliff near TP–9. Experimental error was greatly reduced by using a theodolite housed in a tent, and the precision of the measuring procedure was tested (see p. 64). Probable errors of measurement and the limits within which there is 95 percent confidence that the measurement was correct are shown with the velocity data in figure 13. Percent deviations from the mean velocity for each stake and the average deviation for each time interval of observation are shown in figure 14. Concurrently with the 1953 velocity measurements, atmospheric pressure at camp was recorded with a barograph, air temperature 4.5 feet above the ice at stake 6–2 was measured with a thermograph calibrated with a mercury thermometer, and synoptic observations of precipitation, cloud cover and wind were made at the time of each observation. These meteorological data are shown in figure 14. The standard deviation of velocity for each stake, expressed in feet per year and in percentage of the mean velocity, and the standard deviation of the velocity of each stake from the 5-stake average velocity during each time interval (s_{v-va}) is given in table 2.

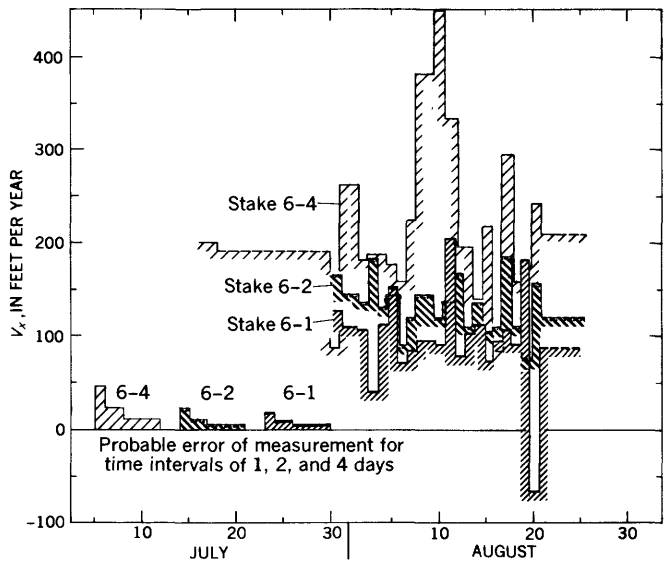

FIGURE 12.—Velocity variations in 1952.

TABLE 2.—*Standard deviation of velocity*

Stake	s_v (fpy)	s_v (percent)	s_{v-va} (percent)
6–1	0.127	51	18
2a	.210	77	42
2	.146	53	20
2b	.121	45	19
4	.309	57	40

These velocity data show profound fluctuations. Sudden increases in velocity up to 170 percent and decreases as large as 230 percent (resulting in backward motion) were recorded. As shown in table 2 the dispersion of velocity is greatest for the stake with the highest velocity (6–4). Percentagewise, however, a very slight increase in dispersion from margin (6–1) to midglacier (6–4) is shown. A profile downglacier, from 6–2b through 6–2 to 6–2a, shows a marked increase in dispersion. This effect could have been caused by a jerkiness predominantly in a direction more perpendicular to the line of sight of 6–2a than of 6–2b, or it might have been due to differences in the local structural environment. Stakes 6–2a and 6–4 moved independently, while stakes 6–1, 6–2 and 6–2b moved somewhat as a solid

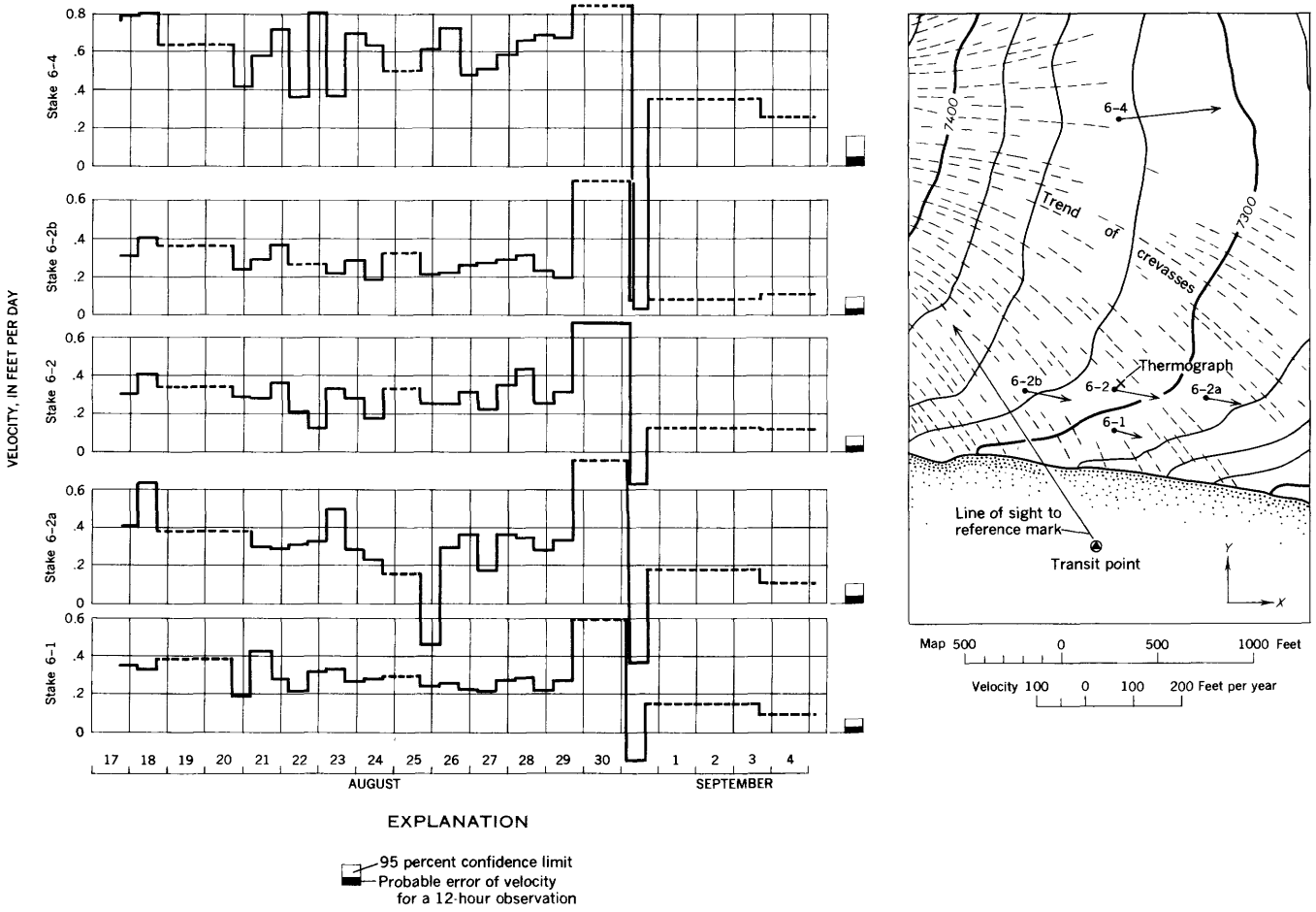

FIGURE 13.—Short-interval velocity variations in 1953.

unit (their dispersion from the 5-stake average motion averages only 19 percent).

Most of the erratic 12-hour fluctuations were not synchronous from one stake to another. However, fluctuations of 1.5 days or longer were often indicated simultaneously by all stakes. No evidence was found from the 1953 data that short-period "waves" of increased velocity traveled down or across the glacier, but there is a suggestion in the 1952 data that some major fluctuations in midglacier velocity were felt by the marginal stakes after a delay of 2 to 3 days.

A slight relation between air temperature and velocity is apparent. The air temperature was measured at a point 4.5 feet above the ice near stake 6–2, and is representative of the air temperature at this height at all 5 velocity stakes, but is not representative of the temperature at the measuring instrument location. Average velocity deviation is plotted as a function of temperature in figure 15. The correlation coefficient of these data to a linear relationship (fitted by the method of least-squares) is 0.307. By a standard statistical analysis (Hoel, 1947, p. 89) it was determined that this correlation was not significant and that there is about 1 chance in 6 that as good an apparent relation as this could be obtained from a random sampling of unrelated variables.

Precipitation seems to have some effect on velocity. Perhaps it is significant that the great increase in velocity shown by all stakes August 29 to 31 coincided with the heaviest rainfall. However, these rainfall data are not quantitative and no firm conclusions can be drawn. Barometric pressure, wind, and cloudiness show little or no relation to velocity. Incoming radiation from sky and sun is a function of the degree of cloud cover; so it seems that the velocity and radiation data are not related—contrary to many statements in the literature (Drygalski and Machatschek, 1942, p. 111–112; Klebelsberg, 1948, p. 86).

The jerky motion cannot be explained satisfactorily. The sharpest variations are not synchronous from stake to stake, therefore, they cannot be due to any general or regional effects such as weather

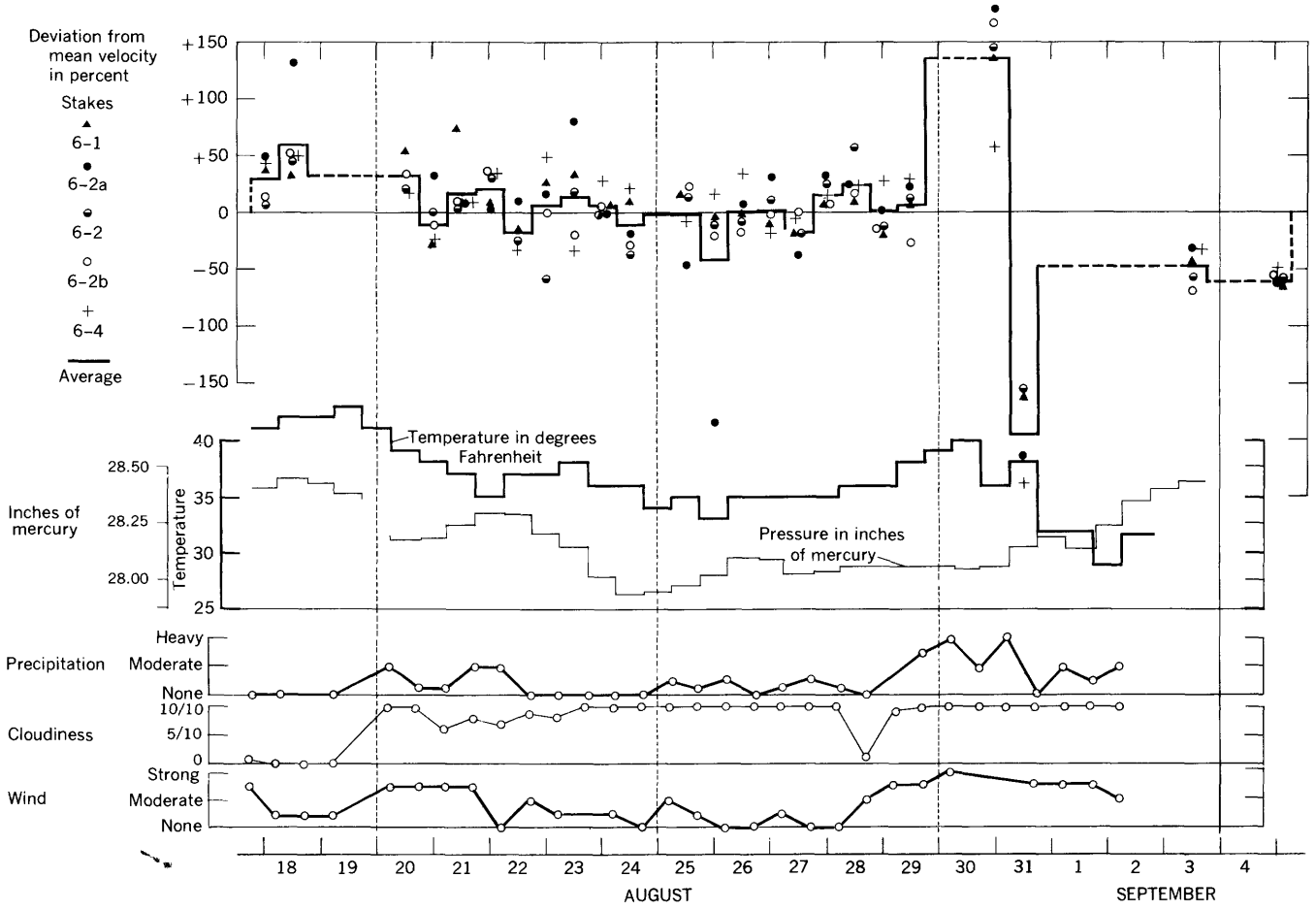

FIGURE 14.—Velocity deviations and meteorological observations, 1953.

changes. Longer variations might be caused, or aided, by lubrication of shear surfaces or the bedrock channel during warm or wet periods. The jerkiness involves domains of limited size (not more than a few hundreds of feet in horizontal dimension) because these domains cannot be larger than the distance between stakes. Therefore, irregular differential movements which may be due to irregular tilting or fracturing of blocks between crevasses, must take place within the ice. However the observation that dispersion increases from stake 6–2b to 6–2a suggests that the main direction of jerkiness (if there is one) is not perpendicular to the crevasses. If there was a preferred direction of jerkiness perpendicular to the crevasses, the dispersion would have appeared larger at stake 6–2b than at 6–2a because of the method of observation (fig. 13). Irregular rotations of the intercrevasse blocks may contribute to the jerkiness. Local domains of plastic shearing probably become active sporadically because ice shows negligible strain hardening. Behavior of this type has been observed along shear planes in an ice cliff in Greenland (White, 1956, p. 40–46) and in the Alps (Chamberlin, 1928, p. 16–19), and on a microscopic scale in laboratory experiments (Ivanov and Lavrov, 1950). This effect could have caused the observed velocity fluctuations.

SUMMARY OF TIME-DISPERSION OF VELOCITY

The velocity at a given point on the glacier surface shows a complete time spectrum of variations. Observations for months or years indicate variations that may be due to changes in melt water lubrication or changes in ice thickness and are generally synchronous between nearby points. Fluctuations having wavelengths sufficiently short to be detected in daily or twice-daily observations reflect irregular differential movements of small domains of ice and may be due to local sporadic shearing. The amount of the fluctuations decreases with increasing wavelength (period of observation) as shown in figure 16. This suggests two conclusions of great importance: (1) The accuracy of a single velocity observation, as a measure of "average" velocity, depends on the length

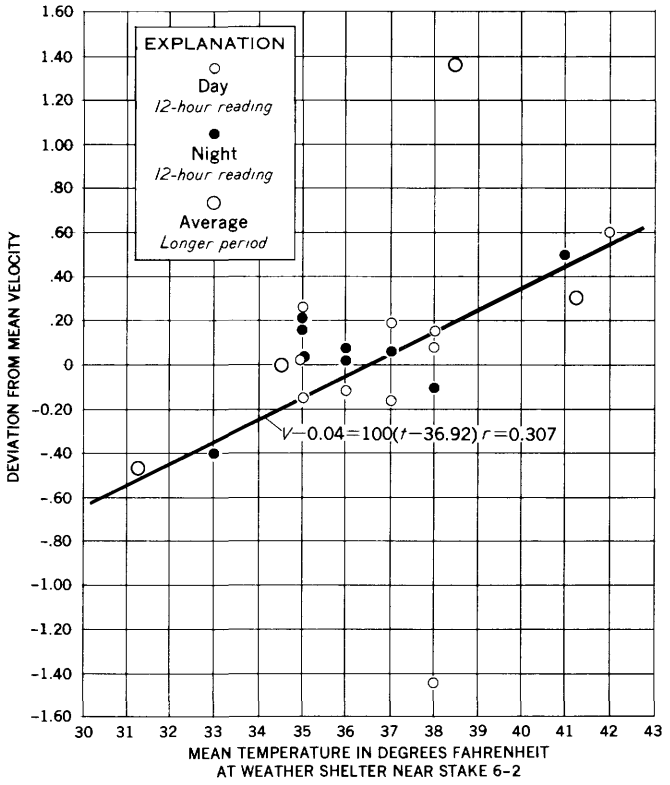

FIGURE 15.—Relation of deviation of velocity to temperature.

of the observation period even with perfect experimental procedure. (2) The flow appears to be comprised of a large number of individual short wavelength "pulses" or fluctuations. The relation between dispersion and wavelength might suggest the magnitude of individual fluctuations that make up the flow, but the dispersion values for long periods of observation are too crude for firm conclusions.

CONFIGURATION OF THE SURFACE VELOCITY FIELD

Accumulation or ablation represents a flux of ice through the surface of a glacier; therefore streamlines of ice flow are generally not parallel to the surface. The rates of accumulation or ablation and flow vary across a glacier; therefore streamlines of flow are generally not parallel to the valley walls. Thus measurement of three components of velocity of the ice at each point is necessary to define the velocity field. Components of velocity parallel to the x, y, and z coordinate axes were measured by triangulation and other components of the vector ($V_{x'}$, $V_{y'}$, V_d) resolved from these.

The following components are measured in a vertical direction. Upwards movement is considered positive. All components are referred to a coordinate system fixed in space unless otherwise specified.

V_z The velocity of a particle of ice.

V_a The velocity of accumulation or ablation (a positive value denotes accumulation, a negative value ablation), relative to a coordinate fixed in the ice very close to the surface.

V_d The velocity of rise of the glacier surface, due to ice motion, which would occur if there were no accumulation or ablation. This velocity component relates the moving coordinate system of V_a to the fixed coordinate system.

V_s The actual velocity of rise of the glacier surface, due to the action of both V_a and V_d. $V_s = V_a + V_d$.

These components are illustrated in figure 17. Measured and assumed values for the different components of the average velocity at each stake are reported, along with x' and y' coordinate locations and surface slope ($\tan \alpha$), in table 3. The observed variation of $V_{x'}$ and V_d over the whole of the tongue

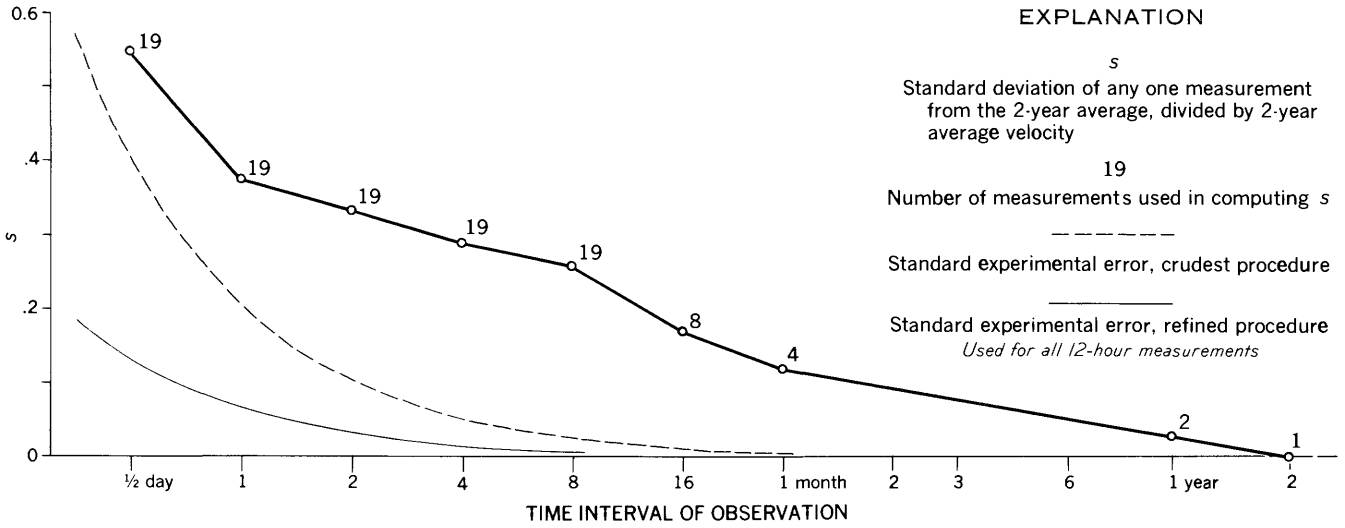

FIGURE 16.—Velocity dispersion spectrum at stake 6–4.

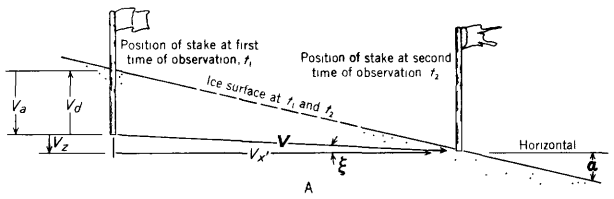

A. Special case of a point on the centerline of the flow of an equilibrium glacier The diagram is referred to an observer fixed in space These quantities are defined

$\boldsymbol{V}$ Velocity of a particle of ice, in general this refers to a particle of ice adjacent to the base of a velocity stake The scalar magnitude of $\boldsymbol{V}$ is given by V Both $\boldsymbol{V}$ and V are always considered positive

α Slope of the surface, measured from the horizontal in the direction of $\boldsymbol{V}$ This angle is considered negative if the surface slopes down in the direction of glacier movement

ξ Slope of $\boldsymbol{V}$, measured from the horizontal in the direction of $\boldsymbol{V}$, and considered positive if $\boldsymbol{V}$ points upwards in the direction of movement $\tan \xi = \frac{V_z}{V_{x'}}$

$V_{x'}$ Component of $\boldsymbol{V}$ in the direction of the x'-axis, taken positive in the direction of the $+x'$-axis $V_{x'} = V \cos \xi$ (See below)

V_z Component of $\boldsymbol{V}$ in the vertical direction, taken positive upwards $V_z = V \sin \xi$

V_a Component in a vertical direction of the velocity of surface accumulation (positive) or ablation (negative) This is measured by the change in position of the ice surface on a stake fixed in the ice This velocity is relative to a coordinate system moving through space with the ice

V_d Component in a vertical direction of velocity of rise (positive) or fall (negative) of the ice surface, due solely to ice motion, which would occur if there were no surface ablation or accumulation
$V_d = V_z - V_x \tan \alpha = V(\sin \xi - \tan \alpha \cos \xi)$

t_1, t_2 Two different times of observation, $t_2 > t_1$.

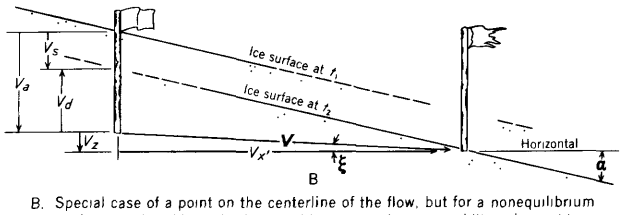

B. Special case of a point on the centerline of the flow, but for a nonequilibrium glacier In addition to the quantities given above, an additional quantity is defined

V_s Component in a vertical direction of the net velocity of rise (positive) or fall (negative) of the glacier surface, due to the action of both V_a and V_d
$V_s = V_a + V_d$

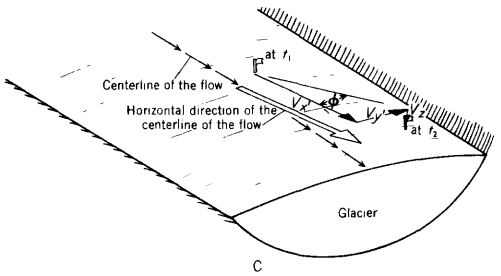

C General case for a point off the flow centerline for a nonequilibrium glacier The following additional components are defined and the formula for $V_{x'}$ is modified as follows

ϕ Angle between $\boldsymbol{V}$ and the x'-axis, measured in a horizontal plane, considered positive on the $+y'$ side of the x'-axis.

$V_{y'}$ Component of $\boldsymbol{V}$ in the direction of the y'-axis $V_{y'} = V \sin \phi$.

$V_{x'} = V \cos \xi \cos \phi$.

FIGURE 17.—Definition sketch of velocity components.

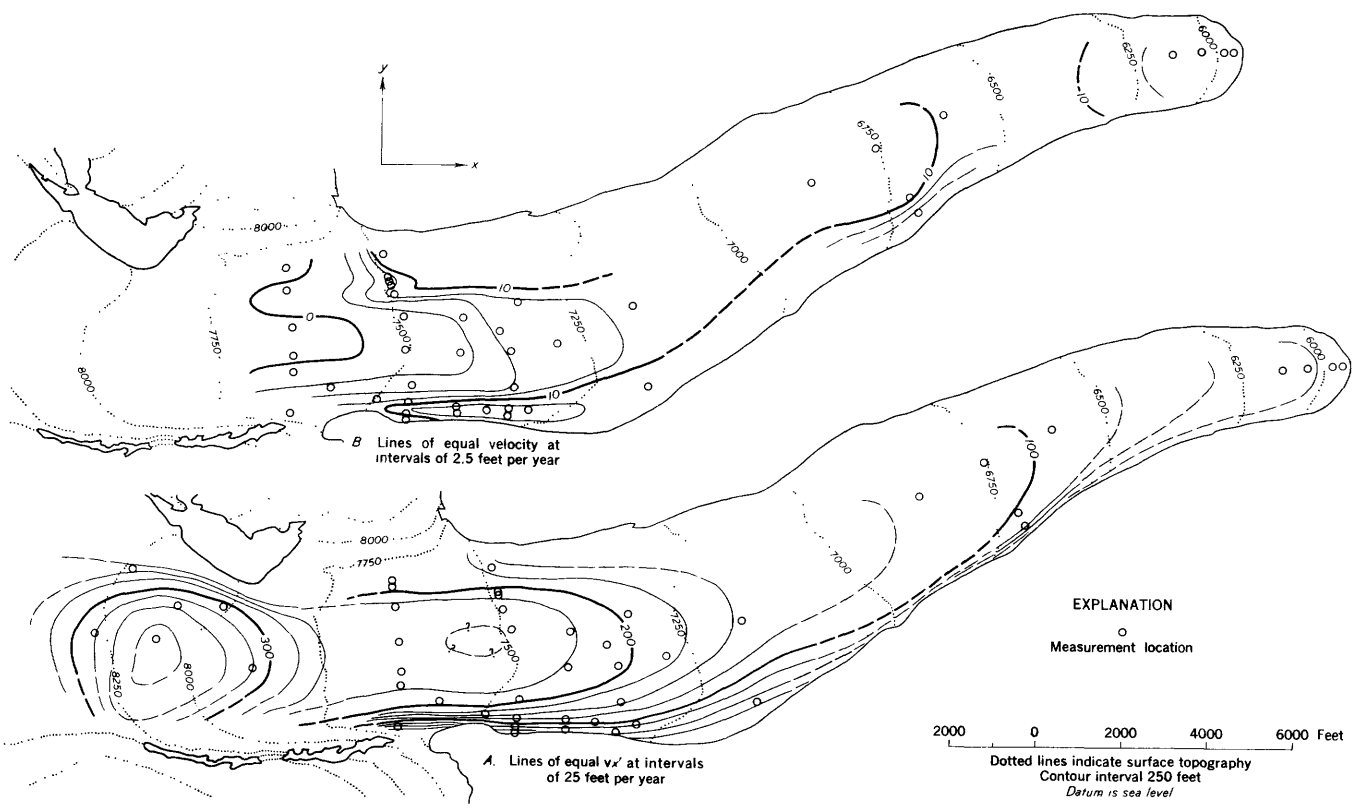

FIGURE 18.—Distribution of $V_{x'}$ and V_d on Saskatchewan Glacier. *A*, refers to $V_{x'}$; *B*, refers to V_d.

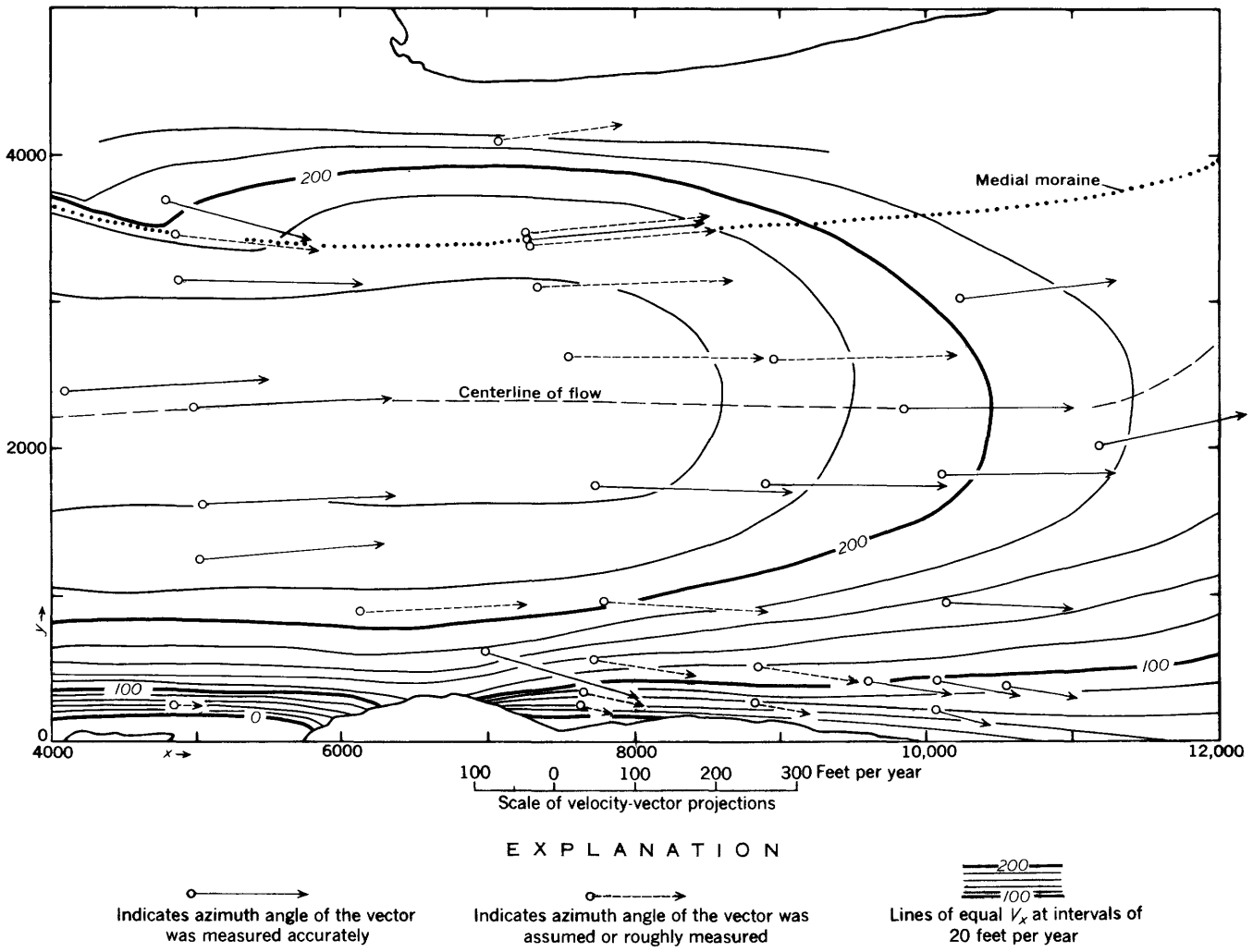

FIGURE 19.—Distribution of V_x, and horizontal projection of velocity vectors in Castleguard sector.

is shown in figure 18. For the Castleguard sector the variation of $V_{x'}$ is shown in figure 19, $V_{y'}$ in figure 20, V_z in figure 21 and V_d in figure 22. Profiles of $V_{x'}$, V_z, V_d and surface slope along the centerline are shown in figure 23. Transverse profiles of $V_{x'}$ in Castleguard sector are presented in figures 24 and 25.

HORIZONTAL DOWNGLACIER COMPONENT

This component ($V_{x'}$) ranges from 383 fpy at the firn limit to 12 fpy at the extreme terminus. The data show variations similar to that commonly observed on valley glaciers—gradual decrease from firn limit to terminus because of the decreasing quantity of ice transported, and a decrease from centerline toward margin because of the drag of the valley walls. The decrease along the centerline is uneven because of changes of surface slope (fig. 23). In Castleguard sector the velocity is constant within 10 percent across the central half of the glacier but falls off rapidly in the outer quarters of the width to a very small amount at the margins (fig. 24). Extrapolation of the transverse profiles shows that margin slip along the south border of the glacier in Castleguard sector is less than 5 percent of the centerline velocity (fig. 25) except where a resistant bedrock bulge constricts the flow between $x' = 6{,}000$ and $x' = 7{,}000$. In this area the valley wall is vertical, strongly polished and striated, and the marginal ice is highly crevassed and contorted; whereas elsewhere moraine-covered stagnant ice borders the flowing glacier, crevasses die out toward the margin, and the transition from flowing to stagnant ice occurs over a zone several feet wide.

HORIZONTAL SIDEWAYS COMPONENT

A transverse component of flow ($V_{y'}$) in the ablation zone of a valley glacier results from decreased marginal velocity in relation to average of the cross section (Nielsen, 1955, p. 11–21). This effect is clearly shown in the transverse profiles of

TABLE 3.—*Velocity components, slope, ablation, and surface lowering at velocity stakes*

Stake (fig. 9)	Quantities computed directly from the raw triangulation and topographic map data							Quantities computed from the data in the left-hand columns using formulas given in figure 17						Quantities which were directly observed		
	x' (feet)	y' (feet)	z (feet)	α	V_x (fpy)	V_y (fpy)	V_z (fpy)	ϵ	ϕ	V (fpy)	$V_{x'}$ (fpy)	$V_{y'}$ (fpy)	V_d (fpy)	V_a summer (fpd)	V_a year (fpy)	V_s (fpy)
17–5	−1,630	+1,700	8,237	−4°44′	209	−111	−28	−6°44′		239			−9			−9
4	−2,200	0	8,263	−4°14′	323	−25	−68	−11°52′	[2] 0	330	324	[1] 0	−50			−11.0
3	−770	+150	8,125	−6°44′	378	−53	−45	−6°42′	[2] 0	385	383	[1] 0	+3			−10.7
1	−790	+1,050	8,070	−8°52′	305	−59	+3	+0°34′		311			+48			−11.0
8–10	+1,580	−230	7,860	[2] −2°50′	324											
9	+4,080	+131		[2] −2°00′	253	+17										
8	+4,788	+1,432	7,697	−3°15′	196	−46	+14.3	+3°59′	−15°41′	204	196	−56.2	−3.0		[2] −6	−7.3
7	+4,800	+1,130			202	[3] −19						[3] −28.6				
6	+4,888	+903	7,667	−2°36′	235	−2.4	−9.1	−2°13′	−3°41′	236	235	15 − .1	+1.8		[2] −6	−8.5
4	−4,977	0	7,636	−1°43′	246.5	+12.7	−7.9	−1°50′	[1] 0	247	247	[1] 0	− .5		[2] −7	−8.3
3	+5,039	−627	7,650	−1°58′	240	+13.7	−8.4	−2°00′	+0°14′	241	241	+1.0	− .2	−0.177	−5.6	−7.3
2	+5,043	−993	7,662	−2°09′	230.5	+19.7	−7.8	−1°57′	+1°58′	231	231	+7.9	+.8		[2] −6	−6.5
1	+4,875	−1,985	[2] 7,680	[3] −0°00′	37	[3] 0	+5.5	+7°51′	[4] +22°00′	37	34	[3] +15	+5.5		[2] −10	−5.0
3–12	+6,323	−1,390	[2] 7,630	−4°05′	212	[3] +12										
11	+7,080	−1,700	[2] 7,490	−9°10′	172	−57										
10	+7,066	+1,790	[2] 7,507	−3°35′	168	[3] +20	+10.6	+3°37′		169			[2] +21.1		−7.6	
9	+7,254	+1,168		−2°24′	232.5	[3] +19.5	−3.4	−0°50′	+5°32′	233	232	+22.5	+6.3		−3.9	
8	+7,273	+1,119	7,515	−2°23′	232.5	+18.5	−3.3	−0°49′	+5°18′	233	232	+21.5	+6.4		−6.1	−5.4
7	+7,287	+1,076		−2°24′	234	[3] +17.5	−2.7	−0°40′	+5°00′	235	234	+20.5	+7.0		−4.4	
3–6	+7,338	+794	[2] 7,480	[2] −2°50′	243.5	[3] +9	−3.9	−0°55′	+2°49′	244	244	+12	[3] +8.3		−6.9	−5.4
5	+7,551	+313	7,507	[2] −2°24′	249	[3] 0	−9.1	−2°06′	+0°41′	249	249	+3	[3] +1.4		−5.2?	−7.0
4	+7,735	−550	7,500	−4°20′	242.5	−6.0	−12.2	−2°53′	−0°43′	243	243	−3	+6.2	−0.129	−7.4	−5.7
3a	+7,787	−1,320	7,450	−4°02′	205	[3] −10	−11.1	−3°06′	−2°31′	206	205	−9	+3.4		−8.6	−4.2
3	+7,730	−1,720	7,428	−2°42′	138	[3] −20	+2.3	+0°57′	−7°26′	139	138	−18	+8.8		−9.5	−7.0
2	+7,669	−1,954	7,420	−2°55′	71.5	[3] −13.7	+6.6	+5°11′	−10°14′	73	72	−13	+10.3		−12.5	−8.2
1	+7,624	−2,045	7,408	−2°42′	36.5	[3] −8.2	+6.4	+9°51′	12°32′	38	36	−8	+8.1		[2] −16	
5–4	+8,840	+320	[2] 7,468	−3°40′	228	[3] +5	−11.8	−2°58′	+1°15′	228	228	+5	+2.8			
3	+8,860	−500	[2] 7,454	−3°35′	223	[3] −1.5	−13.4	−3°27′	−0°23′	223	223	−1.5	+ .6		[2] −8	−6.0
2	+8,880	−1,755	[2] 7,393	−3°11′	125	[3] −17.4	+6.4	−2°54′	−7°56′	127	125	−17.4	+13.3		−9.3	
1	+8,830	−2,005	[2] 7,360		70	[3] −14.6			−11°47′		70	−14.6			[2] −11	
6–8	+11,200	−320	7,281	−2°45′	183	+40.5	−2.4	−0°44′		188			+6.6	−.164	[2] −10.5	−8.9
7	+10,245	+746	7,340	−3°40′	193	+23.2	−4.8	−1°25′	+6°27′	194	193	+21.8	+7.6		[2] −9	−6.3
6	+9,870	0	7,354	−4°24′	214	+1.6	−10.3	−2°46′	b0	214	214	[1] 0	+ 6.2			
4	+10,100	−427	7,329	−3°24′	209	+2.8	−7.3	−2°00′	+0°20′	209	209	+1.2	+5.1	−.184	[2] −9.7	−8.7
3	+10,129	−1,312	7,322	−3°01′	158	−6.8	+3.3	+1°12′	−2°54′	158	158	−8.0	+5.0		[2] −10	−5.5
2b	+9,614	−1,840	7,323	−3°24′	99.5	−17.0	+7.8	+4°24′	−10°03′	101	100	−17.7	+13.8	−.147	−14.8	−4.8
2	+10,068	−1,833	7,305	−3°24′	98.3	−18.4	+6.6	+3°47′	−11°02′	100	98	−19.1	+12.4	−.147	−15.0	−4.8
2a	+10,543	−1,874	7,287	−3°46′	86.4	−13.5	+8.6	+5°40′	−9°18′	88	86	−14.1	+14.3	−.187	−15.9	−4.6
1	+10,068	−2,035	7,290	−3°11′	64.2	−17.4	+7.8	+6°42′	−15°37′	67	64	−17.9	+11.4		−17	−3.7
15–2	+13,080	0	7,194	−2°35′	143.2	+73.1	+1.9	+0°41′	[1] 0	161	161	[1] 0	+9.2		[2] −10	−10.5
1	+12,570	−1,670	7,212		38.5	−20.7	+6.2	+8°05′	−0°57′	44	43.7	−1.1			[2] −11	
14–5	+18,300	+170	6,848	−3°20′	120.3	+54.1	+2.3	+1°00′	[1] 0	132	132	0	+9.9	−0.133	−11.2	−10.5
4	+21,800	0	6,622	−4°15′	94.9	+40.6	+2.7	+1°30′	[1] 0	103	103	[1] 0	+10.2	−.175	−13.8	−5.8
3	+20,120	0	6,753	−3°15′	107.5	+45.8	−1.8	+0°53′	[1] 0	117	117	[1] 0	+8.4	−.129	−11.2	−6.7
2	+20,150	+1,400	6,720	−4°25′	98.6	+37.0	+1.6	+0°52′	−2°43′	105	105	−5.0	+10.0	−.146	−12.3	−8.8
1	+20,150	+1,780	6,712	−4°35′	85.4	+33.5	+9.0	+5°38′	−1°49′	92	92	−2.9	+16	−.154	−14.2	−10.3
12–5	+27,493	0	6,098	−7°10′	38.4	+5.3	+1	+1°28′	[1] 0	39	39	[1] 0	+5.9	−.202	−19.3	−8.0
4	+27,990	0	6,040	−7°55′	31.6	+6.1	+1	+1°47′	+3°03′	32	32	+1.7	+5.5	−.220	−20.3	−11.0
3	+28,431	0	5,966	−10°45′	23.4	+6.7	[3] +2	+4°44′	+8°18′	24	24	+3.5	+6.5	−.224	−20.1	−13.0
2	+28,691	0	5,920	−10°50′	11.7	+.5	+3.8	+17°30′	−5°14′	12	12	−1.1	+6.1	−.227	−20.3	−15.0

[1] These points determine the flow centerline. [2] Approximate value. [3] Assumed value.

the 3, 6, 15, and 14-series (table 3). In the lowest of the profiles (the 14 series, $x' = 20{,}000$) the marginal flow diverges from the centerline by 4.0 fpy, but the angle the right margin makes with the centerline of the glacier is such that the horizontal velocity component normal to the margin is about 34 fpy. Opposite Castleguard camp ($x' = 10{,}000$) the transverse velocity along the south margin is about 18 fpy relative to the centerline (fig. 20) and 9 fpy relative to the margin. On the other hand, the lateral flow in the 8-series profile ($x' = 5{,}000$) is strongly convergent. This is undoubtedly due to the supply of ice from both margins at and upglacier from this profile, and the bedrock bulge at $x' = 6{,}500$ may have an influence. The transition from convergent to divergent flow occurs at $x' = 6{,}500$ and shows as a "saddle" in the map of $V_{y'}$ (fig. 20).

ABSOLUTE VERTICAL COMPONENT

This component (V_z) was measured in relation to a coordinate system fixed in space and thus records the absolute rate of change in elevation of a particle of ice. Along the centerline, the vertical velocity is negative (downwards) from the firn limit through Castleguard sector but slightly positive (about 2 fpy) and relatively constant over the lower half of the tongue (fig. 23). In transverse profiles the vertical velocity is invariably upwards along the margins, giving a pronounced transverse gradient in the upper parts of the glacier. In Castleguard sector a large

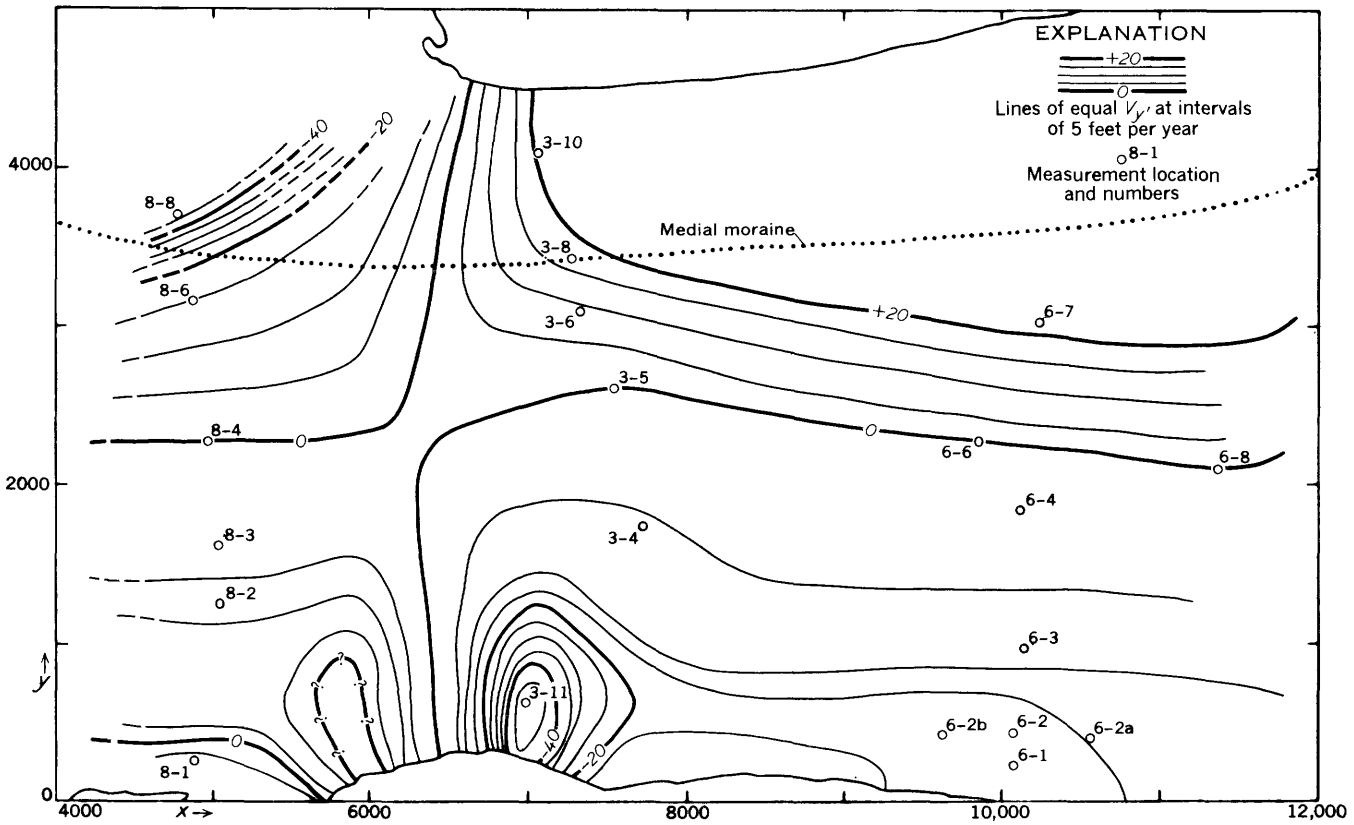

FIGURE 20.—Distribution of $V_{y'}$ in Castleguard sector.

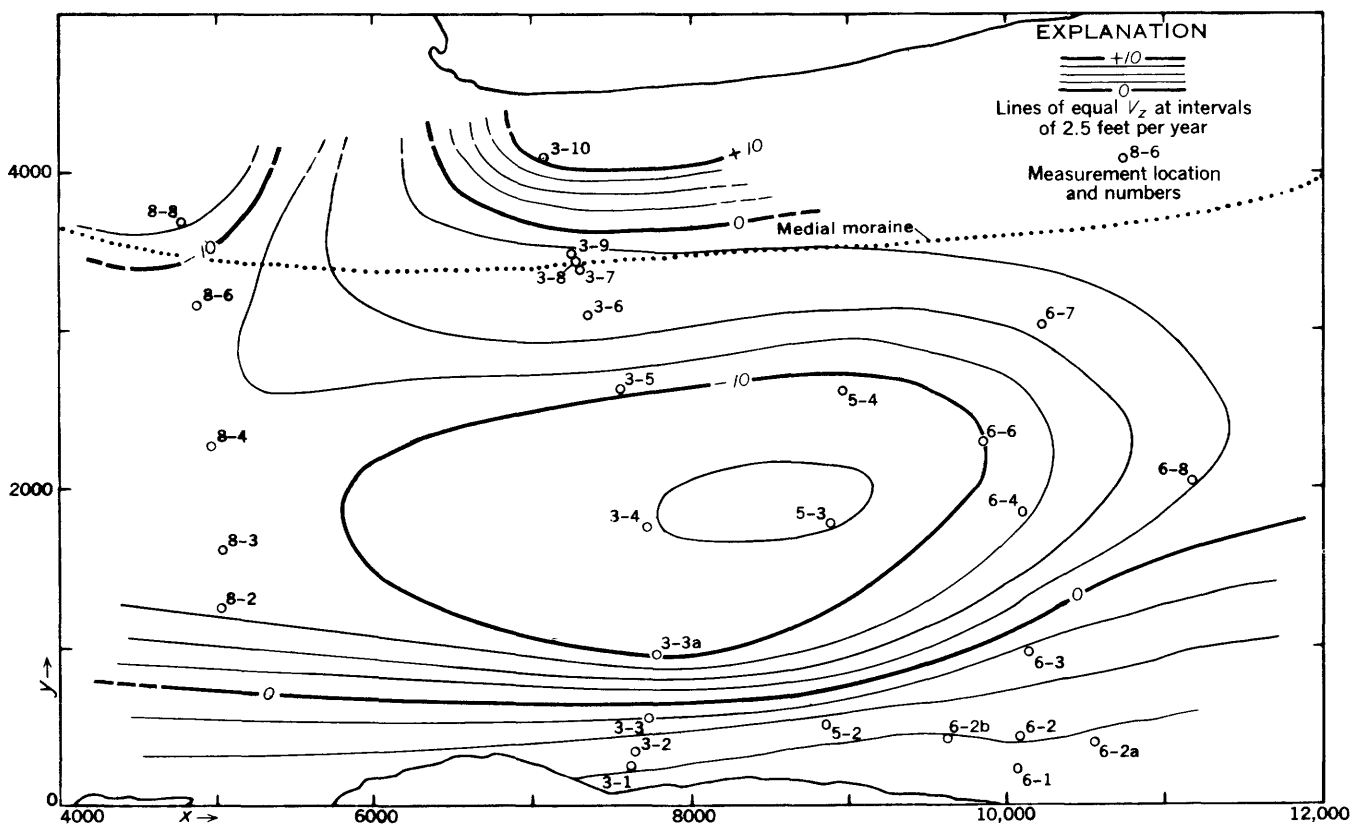

FIGURE 21.—Distribution of V_z in Castleguard sector.

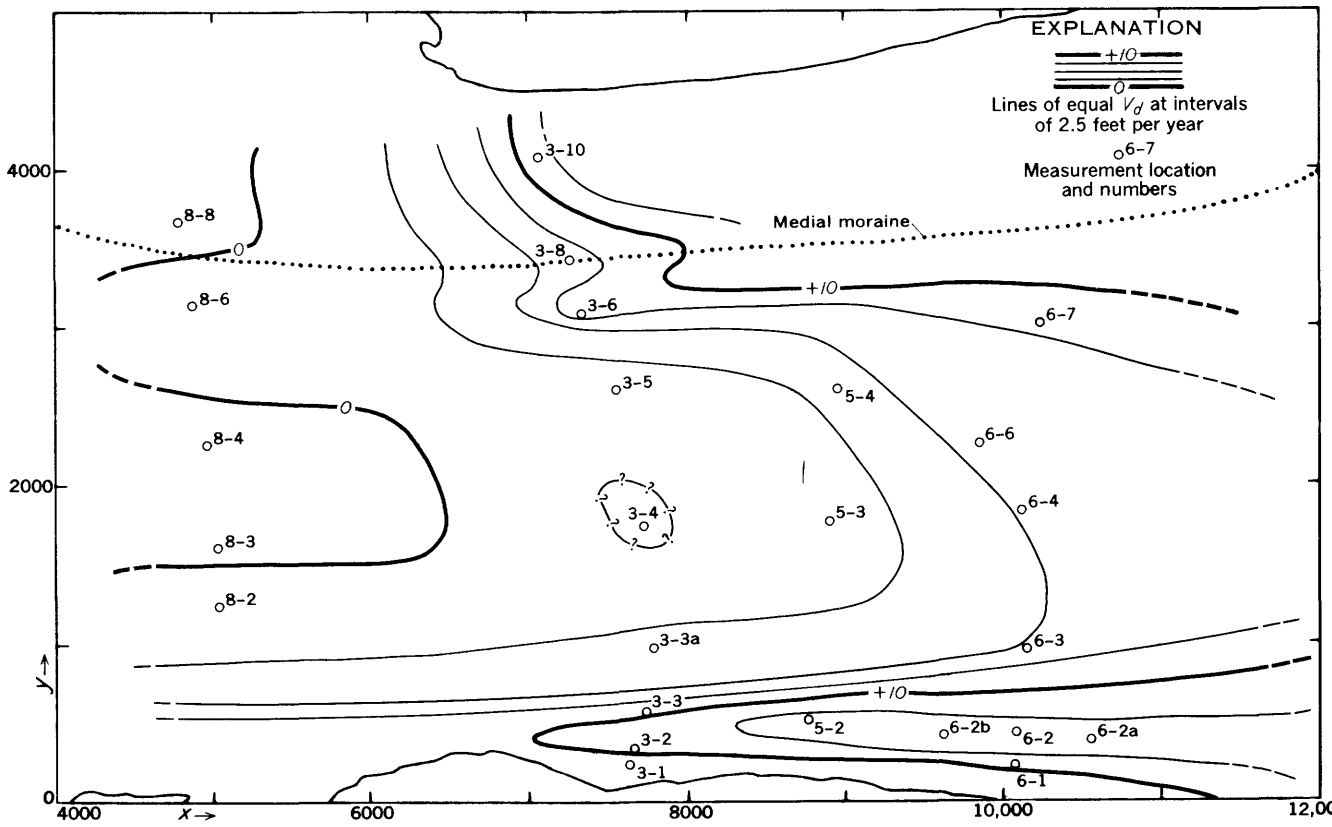

FIGURE 22.—Distribution of V_d in Castleguard sector.

oval-shaped area in midglacier shows negative vertical motion of more than 10 fpy (fig. 21).

COMPONENT OF SURFACE RISE DUE TO ICE MOTION

This component (V_d) is the velocity of rise or fall of the ice surface which would take place, due to ice motion, if there were no accumulation or ablation on the surface. With respect to a coordinate system fixed in space, it represents a flow of ice towards or away from the ice surface. Therefore it is not necessarily equal in magnitude to the flux of ice through the surface (the accumulation or ablation, V_a) because the surface is generally sweeping upwards or downwards in space. This component should not be confused with V_z (the absolute change in elevation of a particle of ice) which depends on the angle between the velocity vector and the horizontal. The component V_d depends on the angle between the velocity vector and the ice surface: If the velocity vector is inclined downwards more steeply than the surface slopes, V_d will show a flow of ice down and away from the surface (negative). If the velocity vector parallels the surface, V_d is zero. If the velocity vector plunges less steeply than the surface, or is horizontal, or is inclined upwards, V_d will show a flow of ice toward the surface (positive).

If the elevation of the ice surface is stationary in space for a long period (an equilibrium glacier), V_d and V_a (the accumulation velocity) are equal in magnitude but opposite in sign. Thus the component V_d in an equilibrium glacier compensates for accumulation or ablation at the ice surface. This relation has been pointed out by Reid (1896, p. 917–918; 1901, p. 750).

If the elevation of the ice surface is not stationary in space for a long period, the glacier is in a nonequilibrium condition. V_d over- or under-compensates the accumulation or ablation, resulting in a velocity of surface thickening or thinning (V_s) according to the relation

$$V_s = V_a + V_d$$

This relation follows directly from the vector diagram (fig. 17).

The quantity V_d can be postulated as the sum of a laminar-flow component and a component due to horizontal divergence of velocity. The laminar-flow component represents motion parallel to the bed and results in a surface change if the bed and surface are not parallel.

A glacier with negligible internal or basal ablation and composed of ice which does not change in density

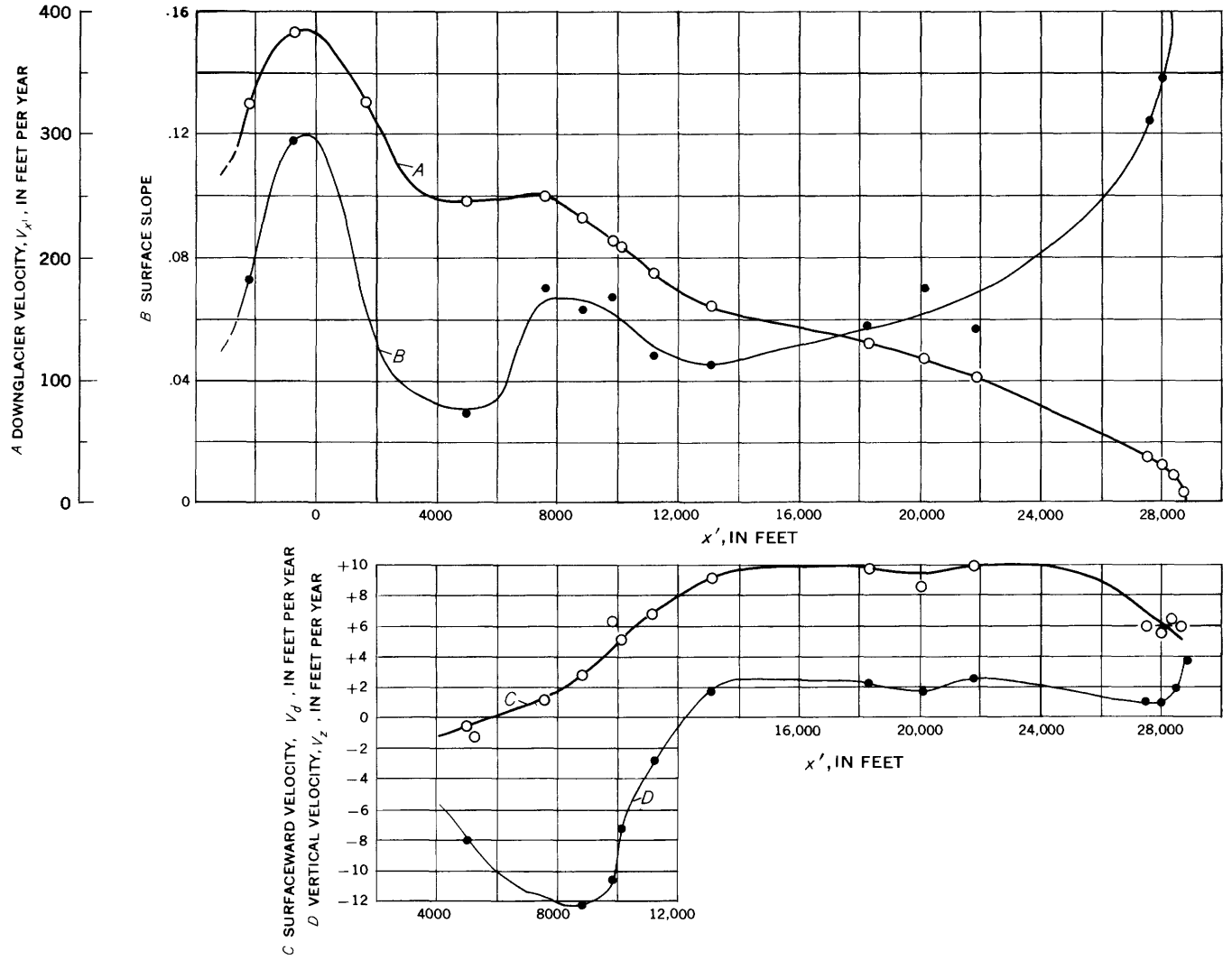

FIGURE 23.—Downglacier, surfaceward, and vertical velocities and surface slope along the flow centerline.

with time, measurements of V_d on the surface can be used to determine the ice flow into or out of specific parts of the glacier. This can be seen as follows: In the ensuing discussions of flow, attention will be directed on points or regions fixed in space, and the flow of material through these regions will be studied (the so-called Eulerian method of hydrodynamics). Consider a surface S parallel and in the same general vicinity as the glacier surface, but fixed in space and time. If the velocity of the ice is given by V, the velocity of flow through a small element of that surface δS is V·δS. If V and δS intersect a horizontal plane at angles of ξ and α respectively, the velocity of flow through δS is given by V·δS = V sin (ξ − α) δS wherein V and δS represent the scalar magnitudes of V and δS. The projection of δS onto a horizontal plane (a map) has the area δS cos α. From figure 17, $V_d = -V$ (tan α cos ξ − sin ξ). Therefore $V_d \cdot \delta S$ cos α = V·δS. Thus, the total flow velocity through S, that is the integral of V·δS evaluated over the irregular surface S, can be determined by the simple operation of summing products of V_d and map area. Unless there is appreciable density change or internal ablation, this sum measures the net flow of ice into the volume underlain by S because of the restriction of continuity. Therefore measurements of V_d can yield valuable information on ice discharge and velocity at depth.

Along the centerline, V_d is negative from the firn limit to x' = 6,000, but in Castleguard sector it increases downglacier to a value of +10 fpy at x' = 14,000, and is constant at this value for the lower half of the tongue except for a slight decrease at the terminus (figs. 18, 23). In transverse profiles V_d increases away from the centerline reaching a maximum near, but not at, the margin (fig. 22).

Actual lowering of the surface of Saskatchewan Glacier was measured during the interval 1948–54, showing that this glacier was in a nonequilibrium condition. Values of V_d can be compared with surface lowering and ablation (fig. 26). These three quantities were measured independently: V_d was

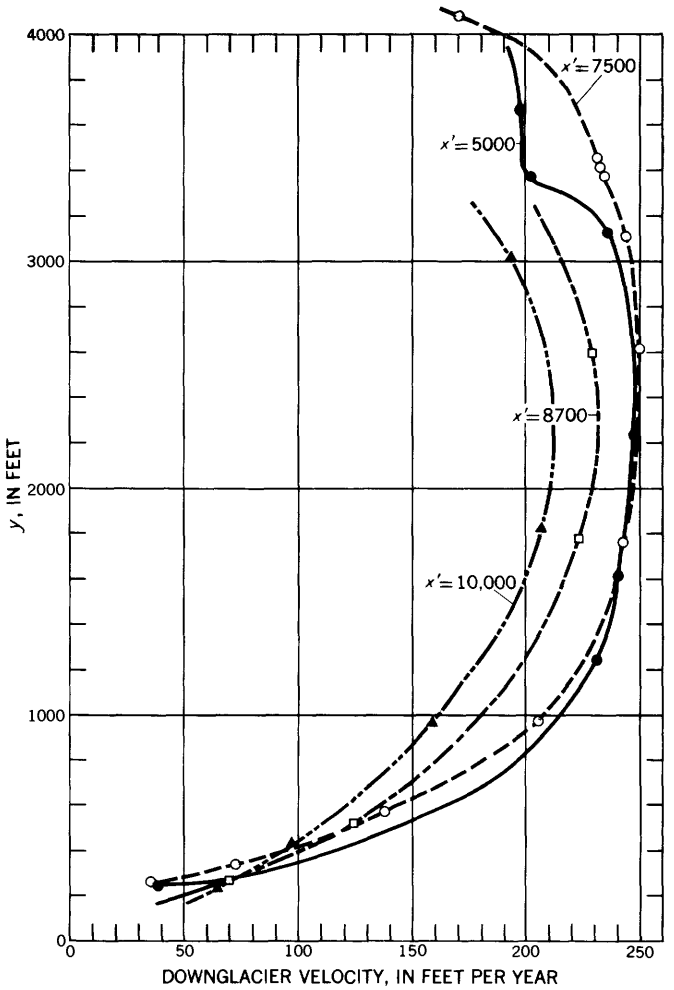

FIGURE 24.—Downglacier velocity along four transverse profiles in Castleguard sector.

measured by triangulation surveys of the movement of a stake in space, V_a by the depression of the ice surface down the length of the stake, and V_s by topographic surveys of the glacier at two different times. The poor correlation between the two sets of data is attributed to the relative inaccuracy of the lowering and ablation values. The surface-lowering velocity was measured from 1948 to 1954 whereas the other velocities were measured from 1952 to 1954. Probably the rate of surface lowering or the ablation has changed with time; these possibilities would also cause scatter in figure 26.

The average value of V_d obtained by measuring

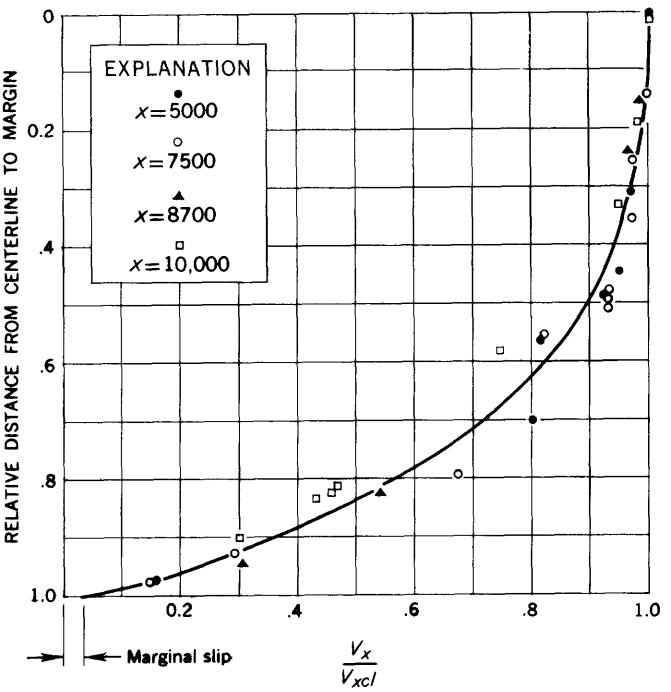

FIGURE 25.—Ratio of downglacier velocity (V_x) to centerline downglacier velocity (V_{xcl}) as a function of relative distance from the centerline for four transverse profiles.

areas within contours of V_d on figure 18 was 4.1 fpy in Castleguard sector and 9.9 fpy for the tongue below Castleguard sector. The average ablation for these two areas was 8.7 fpy and 13.2 fpy, respectively. The differences between these values 4.6 fpy and 3.3 fpy, reaffirm the previous conclusion that

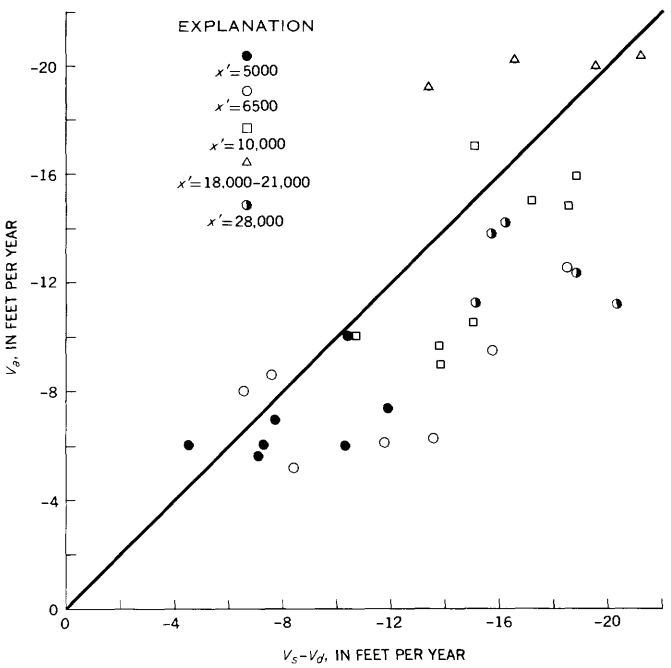

FIGURE 26.—Ablation velocity (V_a) compared with difference between surface lowering velocity (V_s) and surfaceward flow velocity (V_d).

thinning was actually slightly greater in Castleguard sector than in the lower part of the tongue.

DIRECTION OF THE VELOCITY VECTOR

The plunge of the velocity vector of a particle of ice shows a gradual change along the flow centerline from a slight negative angle in the Castleguard sector to a positive angle at the terminus (pl. 5). The plunge is slightly greater than the surface slope in the upper part of Castleguard sector. The angle between the ice surface and velocity vector increases steadily downglacier reflecting increase or constancy in V_d and decrease in $V_{x'}$ in this direction.

Velocity vectors in a map view converge in the upper part of Castleguard sector and diverge in the lower part, and the angular spreading increases slightly but steadily downglacier (fig. 19).

In a transverse profile perpendicular to the ice surface the velocity vectors spread away from the centerline (fig. 27). It is especially interesting to note that at the margin the vectors in this plane did not parallel the margin. This angular relationship is necessary so that ablated ice at the margin can be continually replenished.

VELOCITY PATTERN AT THE MEDIAL MORAINE

A medial moraine represents the contact between two separate streams of ice. Currents of ice in a single stream moving side by side at different velocities have been observed (Battle, 1951, p. 560), and it has been suggested that the ice streams on the two sides of a medial moraine might flow independently. This would cause severe shearing along the moraine. Foliation, a structure in the ice apparently caused by shear, is intense along and in the medial moraine of Saskatchewan Glacier. It is instructive to examine the velocity pattern there.

A sharp change in velocity at the moraine occurs at the highest transverse profile, $x' = 5{,}000$ (fig. 24). The trunk glacier flows 235 fpy at a point 200 feet from the medial moraine, only 11 fpy less than the centerline velocity. The velocity at the center of the moraine is only 202 fpy, and 300 feet farther north (well into the tributary ice stream) the velocity is 198 fpy. This indicates a strong transverse gradient in velocity along the trunk-glacier side of the medial moraine.

On the other hand, the transverse gradient in velocity at $x' = 7{,}500$ shows no great change at the medial moraine (fig. 24). Three stakes were placed in a 92-foot transverse profile across the moraine to measure shearing but the difference in horizontal velocity recorded between the end stakes is only 1.5 fpy, which is close to the experimental error. The difference in vertical velocity is only 0.7 fpy. This measuring location is not conveniently located for accurate triangulation so horizontal converging or spreading of velocity vectors across the moraine could not be measured.

These results show that the flow of the tributary glacier, which initially has no component parallel to the main glacier, is gradually picked up by the trunk glacier for a distance of less than 4,000 feet. Most of this eastward flow is imparted in the first 2,200 feet. Beyond the 4,000-foot interval the trunk and tributary glaciers flow together as a unit and the medial moraine ceases to mark a discontinuity in velocity.

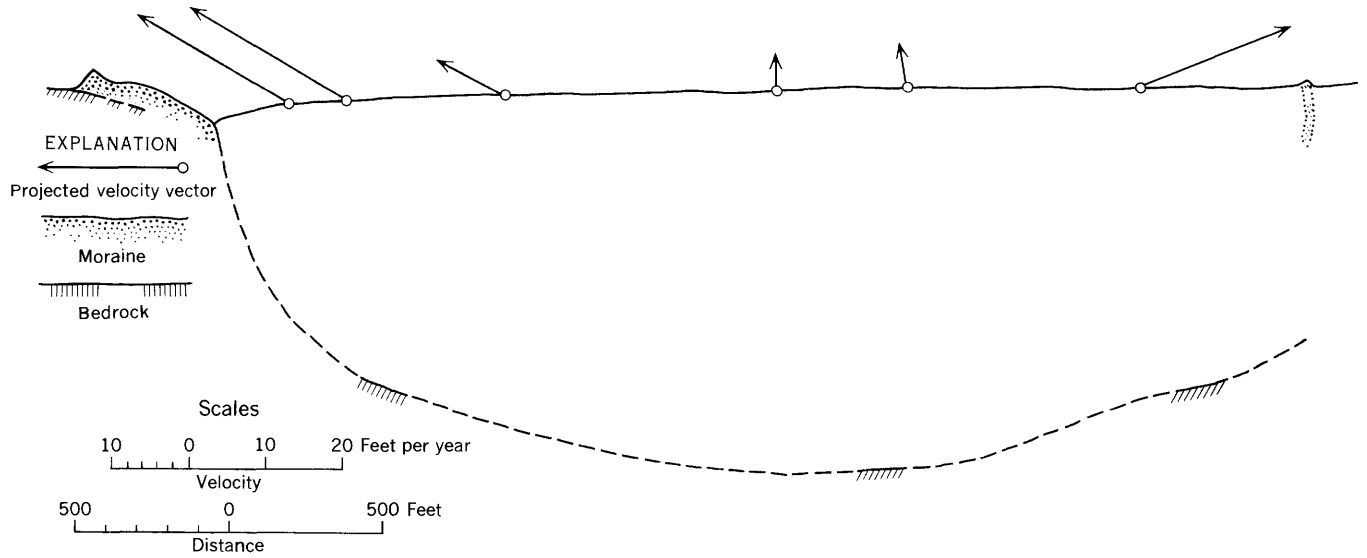

FIGURE 27.—Velocity vectors projected onto a transverse plane perpendicular to the glacier surface at $x' = 10{,}000$, viewed upglacier.

509755 O - 60 - 4

ENGLACIAL VELOCITY MEASUREMENTS

The velocity distribution within a flowing glacier has long been a matter of theoretical speculation but few actual measurements have been made. Gerrard, Perutz, and Roch (1952) measured the velocity distribution from surface to supposed bedrock in a firn basin near the Jungfraujoch in Switzerland. Sharp (1953) measured the velocity change with depth along a vertical line reaching halfway to bedrock in Malaspina Glacier, Alaska. McCall (1952) measured three-dimensional components of velocity in a horizontal tunnel to bedrock in a small cirque glacier. Some observations of various components of velocity have been made in tunnels within a small firn cap (Haefeli and Brentani, 1955–56) and in several icefalls (Haefeli, 1951; Glen, 1956). Apparently the velocity distribution at depth in a valley glacier flowing in a channel of simple configuration has never been measured. Such data would be of first-order importance for the framing and testing of theories of flow, because the approximate stress distribution at depths can be calculated. Therefore, a project to determine englacial velocity at depth in Saskatchewan Glacier was given highest priority.

SITES

Attempts to measure englacial velocities were made along the flow centerline in Castleguard sector, because the surface velocity and deformation fields and the bedrock configuration were known in greatest detail. The first location selected ($x = 9{,}660$, $y = 2{,}268$, $z = 7.370$ in 1952) is approximately opposite Castleguard camp. This point is designated as 6–6 (fig. 3). The following velocity and strain rate (ϵ, p. 32) components and slope were measured on the surface at this site:

$V_x' = 214$ fpy	$\dot{\epsilon}_{xx} = -0.014\ \mathrm{yr}^{-1}$
$V_y' = 0$	$\dot{\epsilon}_{yy} = +0.005\ \mathrm{yr}^{-1}$
$V_s = -10.3$ fpy	$\dot{\epsilon}_{xy} = 0$
$V_d = +6.2$ fpy	
$V_a = -9.5$ fpy	$\alpha = 4.41°$

This location is in a region of relatively steep surface slope and markedly nonlaminar "compressing flow" (p. 37). The cross section of the channel here is nearly elliptical and the depth is about 1,215 feet.

Attempts to measure englacial velocity were made in 1953 and 1954 at a site farthur upglacier ($x = 4{,}590$, $y = 1{,}920$, $z = 7{,}670$ in 1954) designated as stake 8–11 in 1954 (fig. 3). Velocity at this point was not measured directly, but components of velocity and strain rate have been interpolated from nearby stations 8–3 and 8–4 as follows:

$V_x' = 243$ fpy	$\dot{\epsilon}_{xx} = +0.001\ \mathrm{yr}^{-1}$
$V_y' = +0.5$ fpy	$\dot{\epsilon}_{yy} = -0.001\ \mathrm{yr}^{-1}$
$V_z = -8.2$ fpy	$\dot{\epsilon}_{xy} = +0.003\ \mathrm{yr}^{-1}$
$V_d = -0.3$ fpy	
$V_a = -6.5$ fpy	$\alpha = 1.84°$

This location, ideally suited for mathematical analysis, is in an area where the flow is neither extending nor compressing and the velocity vector is nearly parallel to the surface. The cross section is almost semicircular.

METHOD

The plan called for sinking a pipe vertically to the floor of the glacier and determining the subsequent deformation of the pipe by means of repeated inclinometer surveys, a procedure already used in other areas (Gerrard, Perutz, and Roch, 1952; Sharp. 1953). Aluminum pipe of inner diameter 1.38 inches and outer diameter 1.65 inches, in 10- or 12-foot sections joined by aluminum couplings, served as drill stem. The threads of the couplings were coated with calking compound, and little water leaked into the pipe. Aluminum was used instead of steel because it permitted use of a small-diameter inclinometer in which the bearings of inclination readings could be determined magnetically. Boring in the ice was made by electric hotpoints of 2.0 inches outside diameter (fig. 28). The source of power was a portable, 2,500-watt 220-volt a-c generator driven by a small gasoline engine. The pipe served as one conductor and the other was an insulated No. 8 stranded-wire cable strung inside the pipe with a pullout plug at the bottom. Normally the hotpoints were operated at 8.0 to 9.5 amperes, dissipating 1,020 to 1,450 watts at the bottom of the hole. Drilling speeds of 14.3 feet to a maximum of 16.6 feet per hour were generally obtained. A hole diameter of 2.7 inches for normal operation was computed on the assumption of no heat loss up the drill stem. A hole diameter of 2.85 inches actually formed at the surface, using a somewhat lower velocity of boring. Heat losses, therefore, were not important but some efficiency was lost in melting the sides of the hole by warm water.

After completion of boring and withdrawal of the cable, the orientation of the drill pipe was determined at 25-foot intervals with a small single-shot inclinometer generously loaned by the Parsons Survey Co.

The inclinometer measured the inclination of the pipe from a vertical direction. In this section, the term inclination or inclination angle refers to an angle measured from the vertical direction.

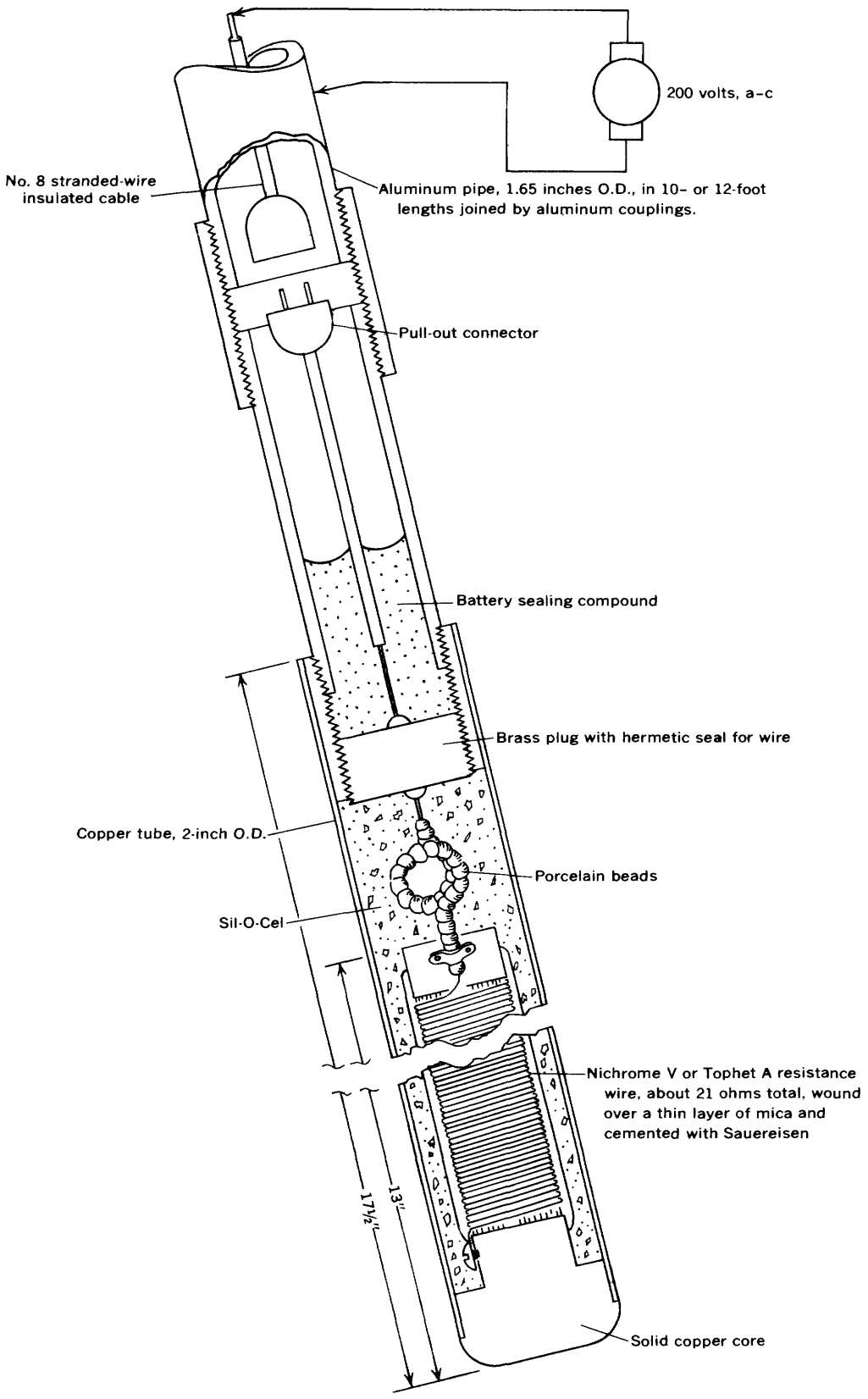

FIGURE 28.—Simplified sketch of hotpoint.

Relative displacements of points along the pipe were computed from the inclinometer data as follows: The inclination angles were first resolved into a plane parallel to the flow centerline by multiplying each inclination angle by the cosine of the horizontal angle between the direction of inclination and the direction of the flow centerline. The resolved configuration of the pipe was then computed to a first approximation by assuming that the resolved inclinations were constant from one point midway between two reading points to the next midpoint. The horizontal displacement of each midpoint differs from that of the next midpoint by the product of the distance along the pipe by the sine of the resolved inclination angle. This first-approximation configuration was then plotted on graph paper. A smooth curve, representing a better approximation to the true configuration, was drawn tangent to the known resolved inclination at each reading point (fig. 29). The relative displacements are given by the horizontal distances between two such curves taken at different times. The relative strain rates (the vertical gradients in V_x) are given by the relative displacements divided by the vertical distances and the time interval of measurement. The bottom of the pipe is considered as the fixed point, because pieces of pipe had to be removed from the top as ablation progressed.

In normal operation the inclinometer readings were reproducible to 0°05′ in inclination and 2° in azimuth. Other possible errors (such as the effect of ice streaming past the pipe, sagging of the pipe due to its own weight, and resistance of the couplings to flow along the pipe) are discussed by Gerrard, Perutz, and Roch (1952, p. 555–556). These errors are negligible for the Saskatchewan pipe owing to the extremely slight deformation.

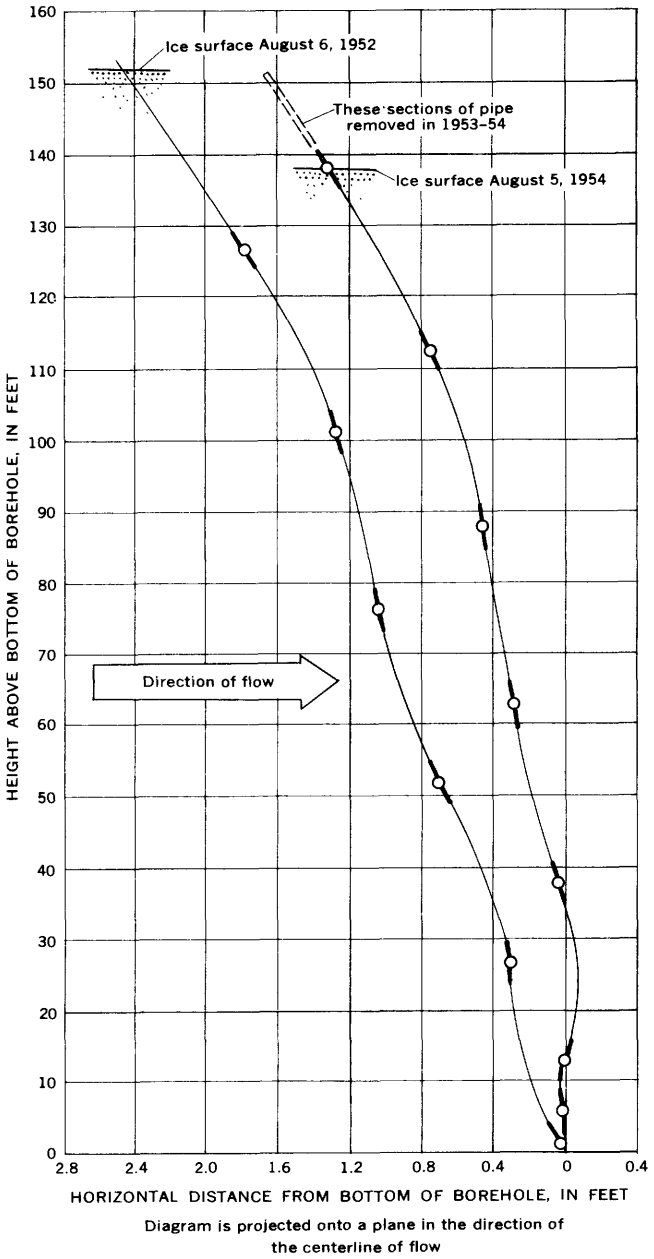

FIGURE 29.—Configuration of borehole 1 in 1952 and 1954.

BOREHOLES

The first borehole drilling in 1952, stopped at a depth of 85 feet owing to a burned-out hotpoint. A second borehole reached a depth of 155 feet, where penetration gradually slowed and eventually stopped, but electrical evidence indicated that the hotpoint was functioning properly. By the next morning the pipe was bound tightly in the hole; 2 hours work with full power applied to the hotpoint and 3 men pulling on the pipestem failed to free the unit. This unit was used in this condition for measurements. A third attempt at drilling was started 1,100 feet farther downglacier. After a few unsuccessful attempts caused by faulty hotpoint connections, normal drilling speeds were obtained. Penetration ceased with only 38 feet of pipe in the ice; again the hotpoint was apparently functioning correctly. After several hours work the pipe was forced past the obstruction, and drilling speeds of 7.51 and 10.9 feet per hour were reached. At a depth of 113 feet progress again ceased, and after 3 hours of operation failed to gain an additional inch. During this period the pipe was becoming increasingly tight in the hole. The pipe was extracted with great difficulty and had a noticeable kink 20 feet above the bottom. This hole was abandoned.

In 1953 a more favorable site was found farther

upglacier, where surface features suggested less active deformation. This operation also ended in failure when the deepest hole, 395 feet, was lost in the process of replacing a shorted-out hotpoint. Improper functioning of five electrical hotpoints was the principal cause of failure in 1953; but a gradual seizing near the surface, drifting into the side of the hole, and dropping a pipe wrench into a borehole contributed to the lack of success.

The 1954 field season was largely devoted to a final attempt at boring a deep hole at the 1953 site using improved, water-tight hotpoints. However, when boring was started on July 31, nearly 6 feet of snow and slush covered the ice, which is normally bare by early or middle July. The electrical equipment functioned satisfactorily and high drilling speeds were obtained. However, progress in the first hole stopped at a depth of 238 feet and a second hole reached only 290 feet. Failure was due to gradual seizing of the pipe in the hole, apparently at a shallow depth. This was probably due to a cold zone—perhaps a remnant of the previous winter's cold that was not ameliorated because of insulation by the heavy blanket of snow.

Three summers' work drilling with hotpoints resulted in the successful emplacement of one 150-foot pipe opposite Castleguard Pass (1952, 6–6) and the two pipes less than 300 feet long farther upglacier (1954, 8–11). (See fig. 3.) One of these latter pipes became useless when a connection was loosened allowing water to enter and freeze inside the pipe.

RESULTS

In the 2-year interval the 150-foot pipe was slightly tilted and bent; the top moved 0.71 foot farther downglacier than the base (fig. 29). The base moved 428 feet in these 2 years. The velocity decrease from top to base formed a smooth curve (fig. 30) similar to the curve found in the Jungfraufirn (Gerrard, Perutz, and Roch, 1952, p. 553).

This curve is significant in that it is entirely within the so-called "brittle crust" of the glacier. Matthes (1900, p. 190) and Demorest (1938, p. 724), among others, have suggested that a critical thickness of more than 100 feet of ice is necessary to start glacier flow. Matthes, (1942, p. 174), however, noticed that the gradual tilting of boring rods left in place in the Hintereisferner indicated some differential flow at shallower depths. The Saskatchewan data show evidence of shearing even in the upper 20 feet although the differential flow at such shallow depth is very slight. It is perhaps more significant that there is no evidence of a marked change in flow at any crit-

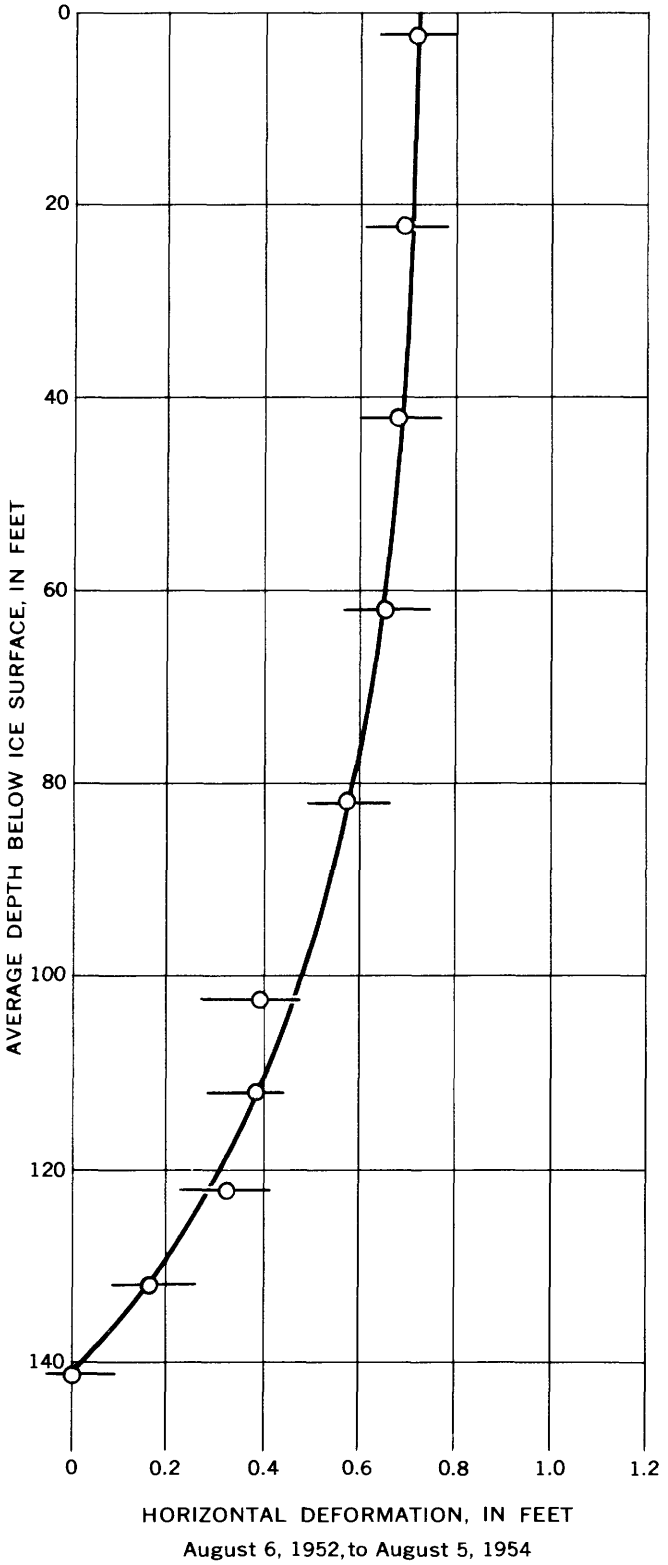

FIGURE 30.—Deformation of vertical borehole parallel to the centerline of flow. Circles indicate measurement points, short horizontal lines indicate approximate limits of measurement error.

ical depth. There is no possible suggestion of extrusion flow (Demorest, 1942, p. 31–38) in these results.

The inclinometer measurement data of the configuration of the 150-foot pipe in 1952, 1953, and 1954 and of the 238-foot pipe in 1954 are presented in table 11.

SOME INTERPRETATIONS OF THE VELOCITY DATA

SURFACE STRAIN-RATE FIELD

FUNDAMENTAL RELATIONS

The gradients of velocity on the surface of Saskatchewan Glacier furnish information on the deformation of the surface ice. Components (ϵ_{ij}) of the strain-rate tensor in terms of velocity components V_i relative to Cartesian coordinates x_i ($i = 1, 2, 3$) fixed in space are given by the relations (Nye, 1957, p. 115)

$$\dot{\epsilon}_{ij} = \frac{1}{2}\left(\frac{\partial V_i}{\partial x_j} + \frac{\partial V_j}{\partial x_i}\right) \qquad (1)$$

DEFORMATION OF THE SURFACE

Strain-rate components on the surface can be readily found if the surface velocity gradients are known. For this case relations (1) may be written

$$\dot{\epsilon}_{xx} = \frac{\partial V_x}{\partial x} \qquad (2a)$$

$$\dot{\epsilon}_{yy} = \frac{\partial V_y}{\partial y} \qquad (2b)$$

$$\dot{\epsilon}_{xy} = \frac{1}{2}\left(\frac{\partial V_x}{\partial y} + \frac{\partial V_y}{\partial x}\right) \qquad (2c)$$

where the coordinates (x, y) are as defined on page 10. Values of V_x and V_y were plotted on 4 transverse and 8 longitudinal profiles in the Castleguard sector, smooth curves were drawn through the points, and values of the 4 velocity gradients were determined at the 32 places where the profiles intersect (fig. 31). From these data the strain rates $\dot{\epsilon}_{xx}$, $\dot{\epsilon}_{yy}$, and $\dot{\epsilon}_{xy}$ were determined using relations (2). Values of the greatest principal elongation rate ($\dot{\epsilon}_1$) the least (most compressing) principal elongation rate ($\dot{\epsilon}_2$) and the maximum shearing deformation rate $\frac{1}{2}(\dot{\epsilon}_1 - \dot{\epsilon}_2)$ were determined by Mohr's circle constructions (fig. 32). These data are summarized in table 4 and are portrayed in terms of the orientations and magnitudes of the principal elongation rates in figure 33, trajectories of principal strain rate in figure 34, trajectories of maximum shearing strain

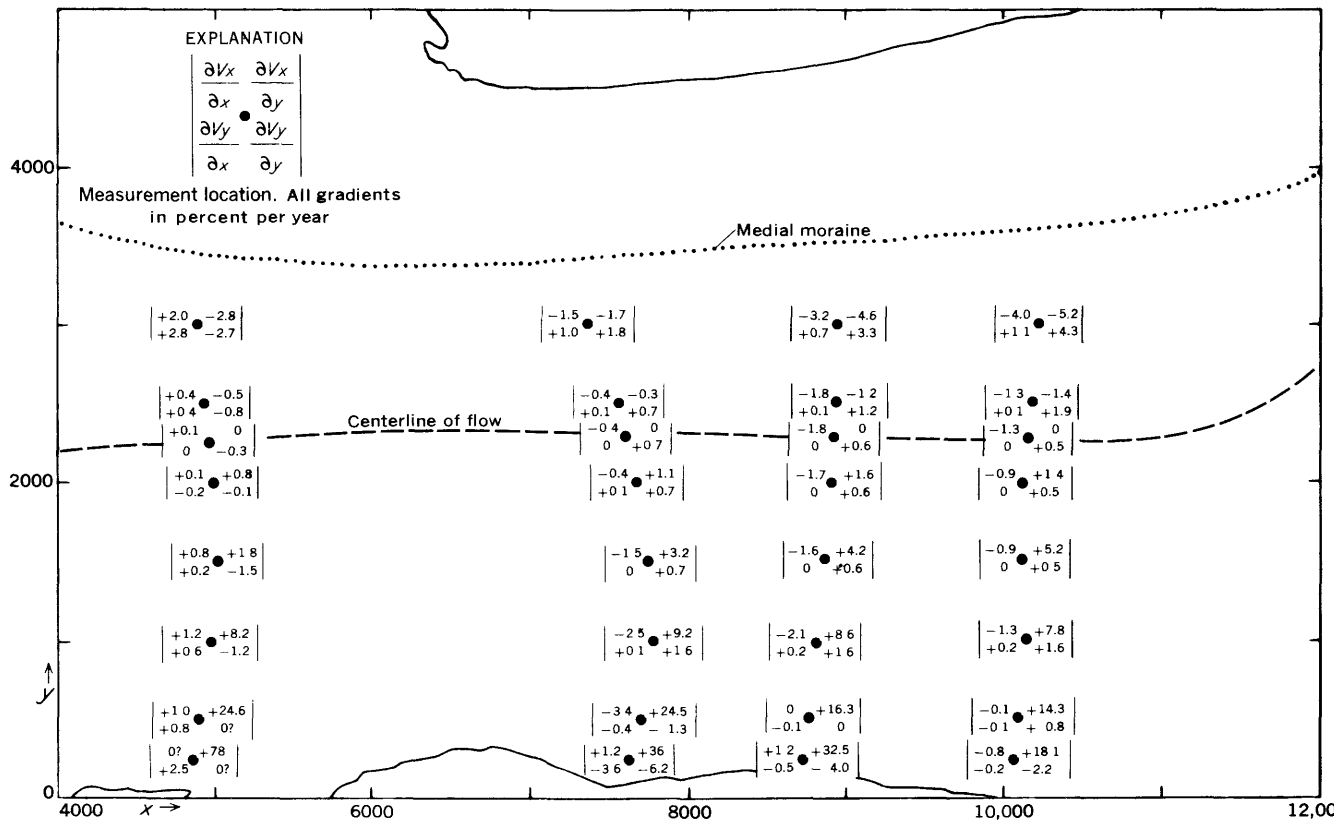

FIGURE 31.—Measured velocity gradients in Castleguard sector.

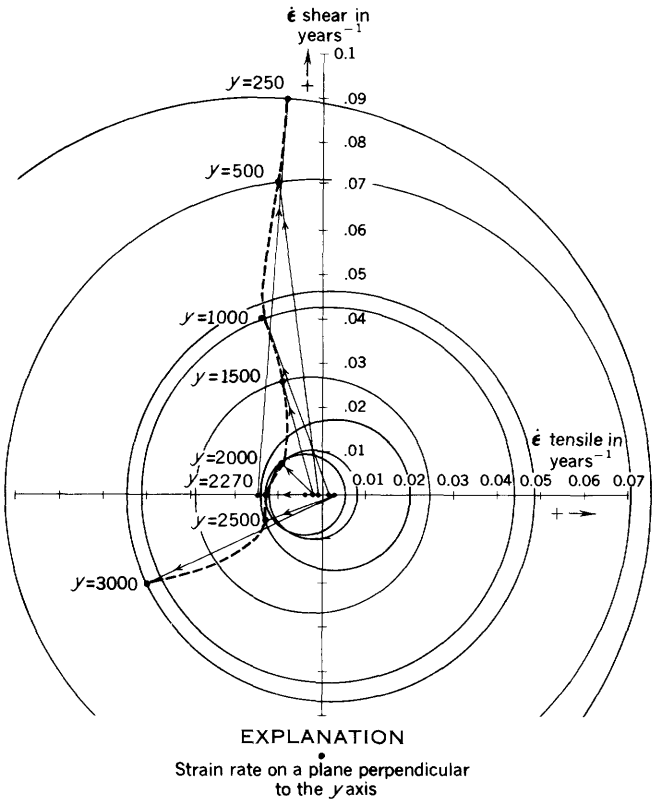

FIGURE 32.—Mohr's circle constructions showing changes in strain rate along a transverse profile at $x' = 10{,}000$.

rate in figure 35, and magnitudes of the normal strain rates parallel to the x- and y-axes in figure 36.

Many assumptions and approximations are involved in these computations. The more significant of these are:

Approximation of plane strain.—By this it is assumed that the vertical component of velocity is approximately constant independent of position. This assumption is necessary in order to compute the orientations of the principal strain rates. The following line of reasoning suggests that the deformation must be predominantly in the form of plane strain: The stress tensor must have a principal axis perpendicular to the surface because air can sustain no shear stress. The ice in Castleguard sector is approximately isotropic in mechanical properties except along the extreme margins and at the terminus (p. 5). For an isotropic material, it is generally assumed that the principal axes of stress and strain increment (or strain rate) coincide at all times (Hill, 1950, p. 38). Thus the strain-rate tensor probably has a principal axis perpendicular to the surface. Inspection of the velocity gradient data (fig. 31) shows that the sum $\epsilon_{xx} + \epsilon_{yy}$ does not equal zero at most points, and inspection of the map of V_z (fig. 21) shows that a slight horizontal gradient of

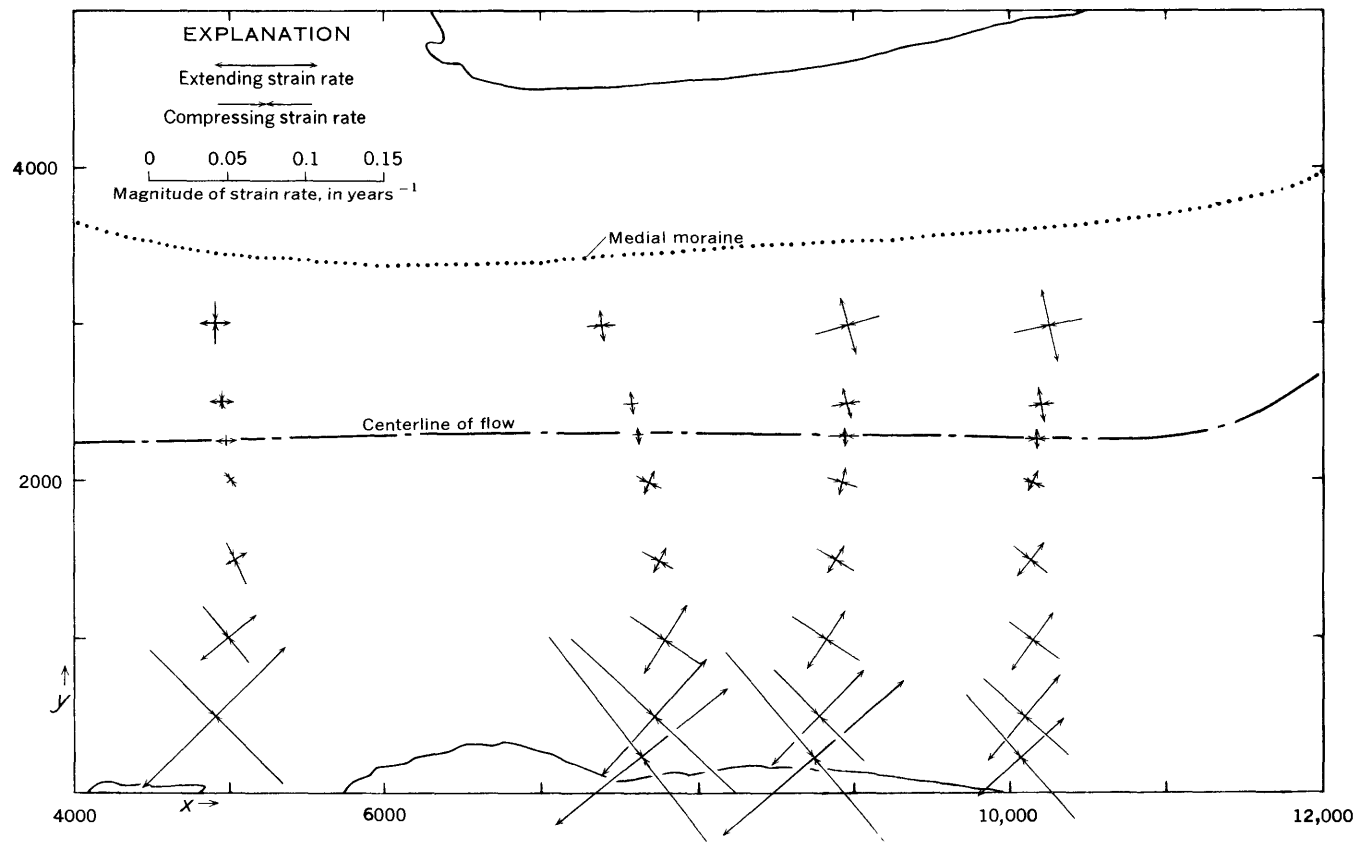

FIGURE 33.—Orientations and magnitudes of principal strain rates in Castleguard sector.

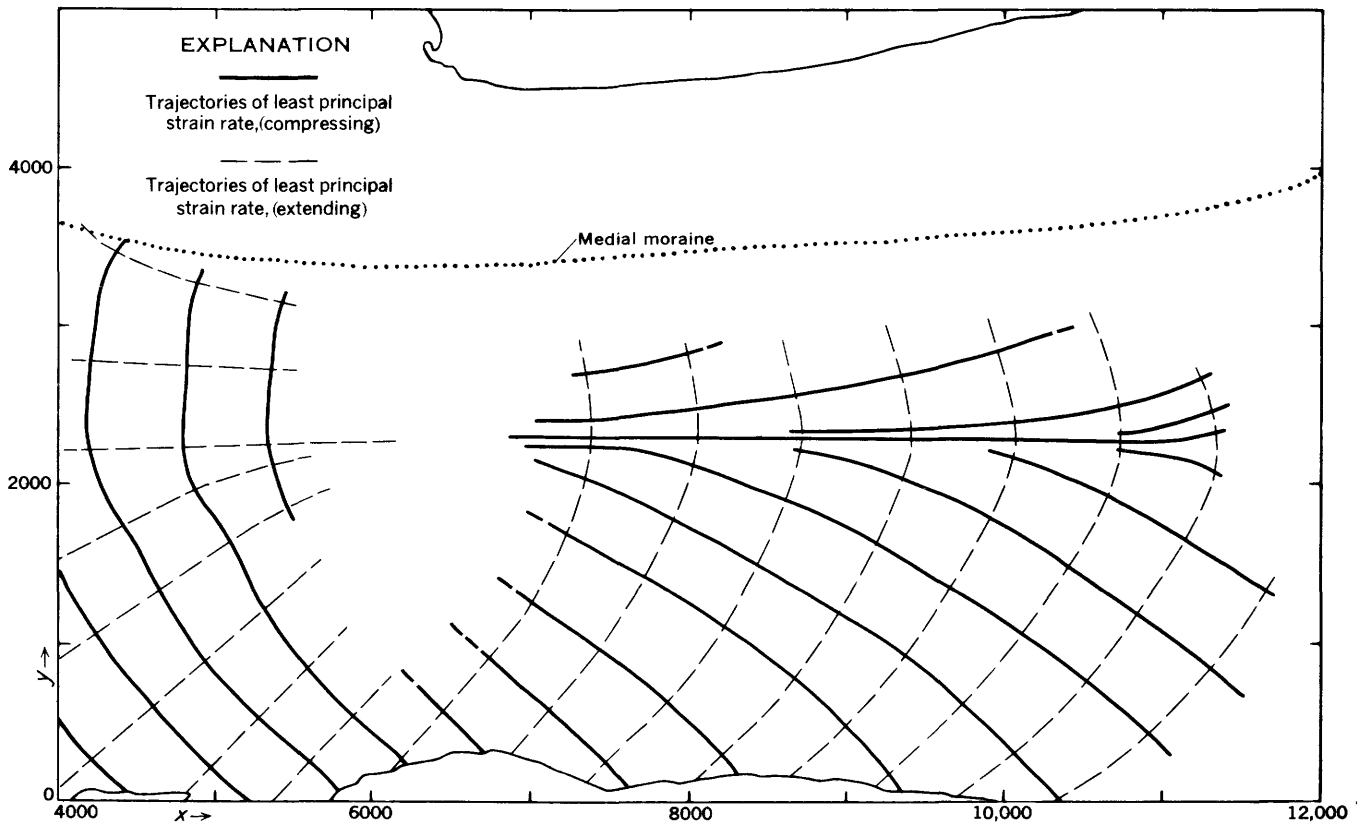

FIGURE 34.—Principal strain-rate trajectories in Castleguard sector.

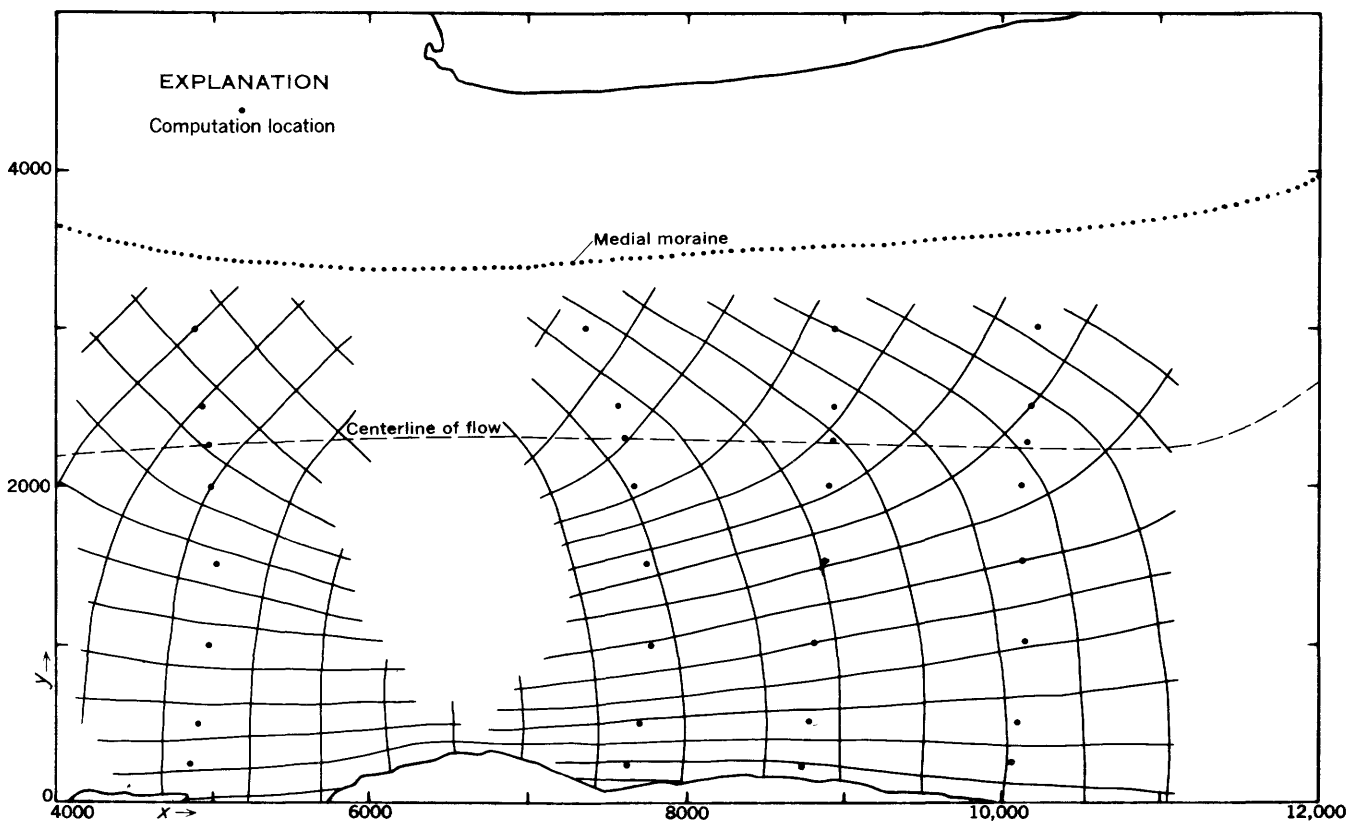

FIGURE 35.—Trajectories of greatest shear-strain rate in Castleguard sector.

TABLE 4.—*Strain-rate components*

[Columns 4–8, 10, and 12. Symbols for strain-rate and rotation-rate components are given on page 32. all values of strain-rate and rotation-rate components are given in percent per year. Column 9. Angle between ϵ_1 and the x axis, in degrees. Column 12. ω_{xy}, the rotation rate, is given by $\omega_{xy} = \frac{1}{2}\left[\frac{\partial V_x}{\partial y} + \frac{\partial^1 V_y}{\partial x}\right]$]

Point	x (feet)	y (feet)	$\dot{\epsilon}_{xx}$	$\dot{\epsilon}_{yy}$	$\dot{\epsilon}_{xy}$	$\dot{\epsilon}_1$	$\dot{\epsilon}_2$	θ	$\frac{1}{2}(\dot{\epsilon}_1 + \dot{\epsilon}_2)$	$\frac{1}{2}(\dot{\epsilon}_1 - \dot{\epsilon}_2)$	$\dot{\omega}_{xy}$
(1)	(2)	(3)	(4)	(5)	(6)	(7)	(8)	(9)	(10)	(11)	(12)
8–h	5,000	3,000	2.0	−2.7	0	2.0	−2.7	0	−0.4	2.4	−2.8
g	5,000	2,500	.4	−.8	0	.4	−.8	0	−.2	.6	−.4
f	5,000	2,260	.1	−.3	0	.1	−.3	0	−.1	.2	0
e	5,000	2,000	.1	−.1	0.3	.3	−.3	35.8	0	.3	.5
5	5,000	1,500	.8	−1.5	1.0	1.2	−2.7	24.5	−.4	1.5	.6
c	5,000	1,000	1.2	−1.2	4.4	4.6	−4.6	37.4	0	4.6	3.8
6	5,000	500	1.0	0	12.7	13.2	−12.2	42.8	.5	12.7	11.9
a	5,000	250	0?	0?	High	High	High	45.0	0	High	High
3–h	7,700	3,000	−1.5	1.8	−.4	1.8	−1.6	−83.2	.2	1.7	−2.0
g	7,700	2,500	−.4	.7	−.1	.7	−.4	−84.9	.2	.6	−.7
f	7,700	2,300	−.4	.7	0	.7	−.4	90	.2	.6	0
e	7,700	2,000	−.4	.7	.6	1.0	−.7	66.3	.2	.8	.7
d	7,700	1,500	−1.5	.7	1.6	1.5	−2.3	62.3	−.4	1.9	2.6
c	7,700	1,000	−2.5	1.6	4.6	5.2	−5.5	56.9	−.4	5.1	3.8
b	7,700	500	−3.4	−1.3	12.0	9.7	−14.4	47.6	−2.4	12.1	7.2
a	7,700	250	1.2	−6.2	16.2	14.1	−19.2	38.6	−2.5	16.6	9.2
5–h	8,850	3,000	−3.2	3.3	−2.0	3.9	−3.8	−74.2	0	3.8	−2.6
g	8,850	2,500	−1.8	1.2	−.6	1.3	−1.9	−79.1	−.3	1.6	−.6
f	8,850	2,280	−1.8	.6	0	.6	−1.8	90	−.6	1.2	0
e	8,850	2,000	−1.7	.6	.8	.9	−1.8	72.6	−.6	1.4	.8
d	8,850	1,500	−1.6	.6	2.1	1.9	−2.9	58.8	−.5	2.4	2.1
c	8,850	1,000	−2.1	1.6	4.4	4.5	−5.0	56.4	−.2	4.8	4.2
b	8,850	500	0	0	8.2	8.2	−8.2	45.0	0	8.2	8.4
a	8,850	250	1.2	−4.0	16.0	14.9	−17.7	40.4	−1.4	16.2	16.5
6–h	10,000	3,000	−4.0	4.3	−2.0	4.8	−4.5	−77.1	.1	4.6	−3.2
g	10,000	2,500	−1.3	1.9	−.6	2.0	−1.4	−79.7	.3	1.7	−.8
f	10,000	2,270	−1.3	.5	0	.5	−1.3	90	−.4	.9	0
e	10,000	2,000	−.9	.5	.7	.8	−1.2	67.2	−.2	1.0	.7
d	10,000	1,500	−.9	.5	2.6	2.5	−2.9	52.5	−.2	2.7	2.6
c	10,000	1,000	−1.3	1.6	4.0	4.4	−4.1	54.9	.1	4.3	3.8
b	10,000	500	−1.0	.8	7.1	7.1	−7.3	48.6	−.1	7.2	7.2
a	10,000	250	−.8	−2.2	9.0	7.5	−10.5	42.0	−1.5	9.0	9.2

V_z exists, so the measured strain rates do not indicate a perfect plane-strain condition. This is only partly due to the fact that V_z was not measured perpendicular to the surface.

Substitution of average for instantaneous velocities.—This occurs when finite displacements are divided by intervals of time in order to determine velocity. Actual strains up to 20 percent were measured in a year's time, and if velocity varies with time in these regions of high strain rate the resulting average velocity field will be inaccurate. However, the resulting strain-rate configuration probably is valid because (1) high rates of strain occur only very near the margin and (2) near the margin the deformation is nearly pure shear. In pure shear, gradients of velocity are small in the direction of the velocity vector, and the average velocity for an extended time interval is a good approximation of the instantaneous velocities.

Method of measuring velocity gradients.—Drawing a smooth curve through widely separated points is a subjective procedure, and gradients determined in this manner are certainly of questionable validity. Different curves through the same points determined values of strain-rate components differing as much as a strain rate of 0.3 percent per year of strain rate. In the vicinity of the flow centerline this is an appreciable fraction of the measured strain-rate components. Thus the strain-rate components in the central strip of the glacier are not precise but the general configuration must hold.

Assumption of a horizontal ice surface.—Velocity components parallel to the surface must be used if this computation is to be exact. Horizontal components were used instead. This is equivalent to assuming that the ice surface is horizontal. The surface slopes 3°23′ in the $+x'$ direction with a pronounced lateral slope only near the margins. Therefore the horizontal velocity components must not differ by more than 1 percent from the corresponding

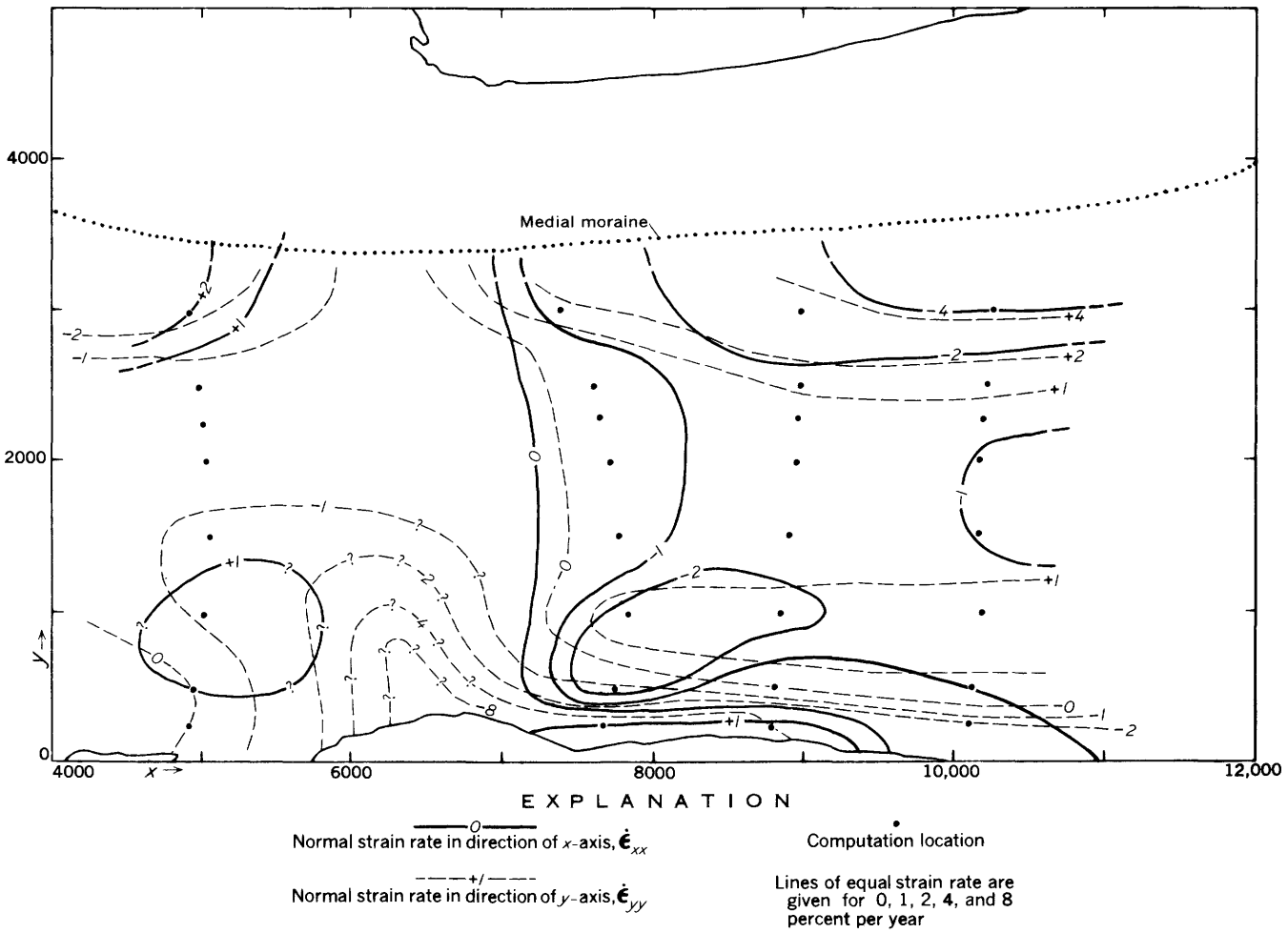

FIGURE 36.—Normal strain rates parallel to the x'- and y'-axes in Castleguard sector.

components parallel to the surface. Longitudinal distances along the surface, however, are incorrect by as much as 6 percent. Furthermore, the two principal strains on the surface are not exactly perpendicular when projected onto a horizontal plane. The combined error of all of these approximations cannot be greater than 10 percent for most points and general configuration should be valid.

The results show that most of the surface deformation is caused by the transverse gradient of longitudinal velocity and that all other velocity gradients are relatively small. The principal axes of deformation are, therefore, longitudinal and transverse to the flow along the centerline and intersect the margins at approximately 45° (figs. 33, 34). The influence on the orientation and magnitudes of the principal strain rates of this increase in ϵ_{xy} toward the margin is shown in the progressive changes in the Mohr's circle constructions along transverse profiles (fig. 32). Trajectories of maximum shearing-strain rate (analogous to slip lines) are almost parallel or perpendicular to the margin except near the flow centerline where they swing, abruptly, into a 45° relation to the flow (fig. 35).

In addition to this shearing deformation due to the drag of the valley walls, there are finite values of longitudinal (ϵ_{xx}) and transverse (ϵ_{yy}) normal elongations caused by other factors (fig. 36). In the upper part of Castleguard sector there is a very slight longitudinal extension along the centerline amounting to about 0.1 percent per year. This is "extending flow" in the terminology of Nye (1952a, p. 87), who has postulated that extending flow may develop in a very wide, plastic-rigid glacier if there is accumulation on the surface or a bedrock channel convex upwards in longitudinal profile (Nye, 1951, p. 561). This area is below the firn limit; therefore according to the postulate it must be assumed that the bedrock is markedly convex in longitudinal profile. The measured surface and bedrock profiles (pl. 1) show this.

At about $x' = 7{,}000$ the longitudinal normal strain

rate is zero and below this point it is negative ("compressing flow") reaching a maximum value of −1.8 percent at $x' = 9{,}000$ along the centerline. This is apparently due to ablation (Nye, 1951, p. 561).

The transverse normal strain rates change from compressive in the upper part of Castleguard sector to extending the lower part. This is due to a pinching of the channel at $x' = 6{,}500$ and the change from marginal accumulation above $x' = 5{,}000$ to pronounced marginal ablation below $x' = 7{,}000$.

The transition from longitudinal extension and transverse compression to longitudinal compression and transverse extension causes a strong warp in the strain-rate field with a branch point along the south margin at about $x' = 6{,}500$. This area sustains a complex fracture pattern: two sets of crevasses intersect with the formation of curving bands of contorted en echelon fractures (p. 56, 57).

The strain-rate data at most points show a net compression ($\dot{\epsilon}_{ii}$ is negative). The average value of $\dot{\epsilon}_{xx} + \dot{\epsilon}_{yy}$ for the 3 lower profiles is −0.23 percent per year. One can safely assume that there is no volumetric plastic compression of the ice because the density does not change appreciably. The compressing velocity in the x-y plane must be relieved by a vertical extending velocity in order to preserve incompressibility. If it is assumed that the horizontal compressing rate does not change with depth, and if the base and the surface slopes are the same, then the vertical extension rate for a vertical prism may be computed as

$$-(\dot{\epsilon}_{zz} + \dot{\epsilon}_{zz})\, d = {}_{zz}d = V_d \qquad (3)$$

where d is the thickness of the glacier (length of the prism). This vertical velocity is identical with the component V_d mentioned previously (p. 24). All quantities in equation (3) except d can be measured on the surface so this equation could be used to determine ice thickness. The Saskatchewan strain-rate data are too crude to use for quantitative depth measurements. For the south half of the Castleguard sector, the average value of V_d was measured as +4.1 fpy. The computed average depth is 1,740 feet. This is of the proper order of magnitude, but differs from the measured depth by nearly a factor of 2.

DEFORMATION IN THREE DIMENSIONS

Computation of all nine components of the strain-rate tensor on the surface requires knowledge of the vertical gradients of both horizontal velocity components. These data are not readily obtainable, and therefore little is known about the orientation and magnitudes of all axes of the rate of deformation tensor as a function of position.

The complete strain-rate tensor is known at the vertical borehole site on the centerline (stake 6–6). The following components were computed in percent per year:

$\dot{\epsilon}_{xx} = -1.3$	$\dot{\epsilon}_{yz} = 0$	$\dot{\epsilon}_{zz} = +0.1$
$\dot{\epsilon}_{xy} = 0$	$\dot{\epsilon}_{yy} = +0.5$	$\dot{\epsilon}_{zy} = 0$
$\dot{\epsilon}_{xz} = +0.1$	$\dot{\epsilon}_{yz} = 0$	$\dot{\epsilon}_{zz} = +0.8$

Within the limits of error, the principal axes of strain rate are oriented parallel and perpendicular to the surface at this point, and two principal axes are in the plane of the centerline. The greatest principal elongation is vertical, the greatest principal compression horizontal and longitudinal. Probably the deformation state is similar to this all along the centerline up to $x' = 7{,}700$. Farther upglacier, the relative values, but not the orientations, of the principal axes are different.

The principal axes are probably nearly perpendicular and parallel to the surface over most of the glacier surface. However, definite transverse gradients in vertical velocity were measured. A slight inclination of the principal axes is required to allow for this vertical shearing. The amount of inclination cannot be approximated because the vertical gradient in transverse velocity is not known and is probably appreciable.

FLOW LAW OF ICE

A flow law—"the quasi-viscous creep rate as a function of stress" (Nye, 1953, p. 477)—is the starting point for calculating the flow of glaciers. No flow law derived from theory for polycrystalline ice has been generally accepted, so recourse to experiments is necessary. A nonlinear empirical relation between shear stress and strain rate has been discovered for artificial polycrystalline ice in the laboratory (Glen, 1955) and for glacier ice in place (Gerrard, Perutz, and Roch, 1952, p. 554). However, the exact form of this relation and the values of the empirical coefficients have not been clearly established because different types of experiments have given inconsistent results. Furthermore, the possibility that strain rate may be a function of the mean stress ("hydrostatic pressure") in glaciers has not been investigated thoroughly.

Observations on Saskatchewan Glacier contribute to the understanding of the flow law for glacier ice. A flow law can be derived, with several broad assumptions, from a transverse velocity profile (where the mean stress is only atmospheric pressure), and from a short vertical profile of velocity (where mean

stress increases with depth). These data can be compared with each other and with data from two other vertical velocity profiles in glaciers, numerous tunnel closing-rate experiments and experimental deformation of ice.

FUNDAMENTAL RELATIONS

In order to compare these various experiments the stress and strain-rate data must be reduced to a uniform basis. Stress and strain rate can be related for a slowly flowing material if the material is isotropic and incompressible, because in this case the stress and strain-rate principal axes remain parallel during plastic flow (Hill, 1950, p. 34, 38). The yield criterion for metals and presumably most other polycrystalline substances is not affected by hydrostatic pressure (Hill, 1950, p. 16). In order to determine if this statement is valid for ice the assumption is made that it is, and then results from experiments involving different amounts of hydrostatic pressure are compared.

Nye's assumption (1953, p. 479), that the stress is not a function of the total plastic strain and that no strain hardening occurs is also adopted. It is then assumed that the strain rate is a function of the deviator of stress:

$$\dot{\epsilon}_{ij} = f(\sigma_{ij'})$$

where

$$\sigma_{ij}' = \sigma_{ij} - \frac{1}{3}\,\delta_{ij}\,\sigma_{kk} \qquad (4)$$

The magnitude of the deviator of stress is measured here by the octahedral shear stress σ_0 defined as

$$\sigma_0 = \frac{1}{3}\sqrt{(\sigma_1-\sigma_2)^2+(\sigma_2-\sigma_3)^2+(\sigma_3-\sigma_1)^2} \qquad (5)$$

where σ_1, σ_2, and σ_3 are the three principal stresses (Nadai, 1950, p. 103).

An octahedral shearing strain rate ϵ_0 is similarly defined as

$$\dot{\epsilon}_0 = \frac{1}{3}\sqrt{(\dot{\epsilon}_1-\dot{\epsilon}_2)^2+(\dot{\epsilon}_2-\dot{\epsilon}_3)^2+(\dot{\epsilon}_3-\dot{\epsilon}_1)^2} \qquad (6)$$

where ϵ_1, ϵ_2, and ϵ_3 are the 3 principal strain rates. The flow law relation to be measured and tested can then be written as

$$\dot{\epsilon}_0 = f'(\sigma_0) \qquad (7)$$

Strain rates are obtained directly from measured velocity gradients according to the relations (1). Stresses, on the other hand, must be computed and these computations require additional assumptions for each special case. It is important to note that the methods of Somigliana and Lagally (Lagally, 1929, p. 285–293) for computing stresses in a glacier cannot be used because they derive stress from predicted strains.

The more important assumptions made in this approach are summarized as follows:

1. Hydrostatic pressure has no effect on the flow.
2. The flow is determined only by the stress deviator.
3. Total plastic strain has no effect on the flow (neither strain hardening nor strain softening occurs).
4. The effects of transient creep are negligible.
5. The flow is slow and steady so that inertial forces are negligible.
6. Elastic strains are negligible compared with the plastic strains accumulated during the period of observation.
7. The ice is isotropic, homogeneous, and incompressible.

VERTICAL PROFILE

STRESS AND DEFORMATION IN LAMINAR FLOW

The simplest assumption that can be made about the state of deformation which produced the known velocity gradient is that the deformation occurred as simple shear in a direction parallel to the surface, and the only shear-stress components are those which produced the simple shear flow. This is equivalent to saying that the flow was laminar. The velocity vector did not quite parallel either the surface or the horizontal at the vertical profile measuring site and a longitudinal compression was measured, but this state of simple shear is a reasonable starting assumption. It is necessary to assume also that the simple shear planes were parallel at all depths.

Stress

The stress on a plane parallel to the surface for a unit width of ice (fig. 37)[8] can be computed as follows:

The shear stress σ_{zx} is approximately the tangential component of the pressure due to the weight of the column

$$\sigma_{zx} = \gamma z \sin\alpha$$

where γ is the specific weight of ice and α is the surface slope.

This formula is valid only if the glacier is infinitely wide. For a glacier flowing in a channel formed by half of a circular cylinder the flow has axial symmetry. In this case the increase of σ_{zx} with increasing depth is only half as great as for an infinitely wide

[8] Note that the x'- and z-axes are defined as parallel and perpendicular, respectively, to the surface. This is a difference definition than the one used in all other parts of this report, and applies only to this section on the vertical profile.

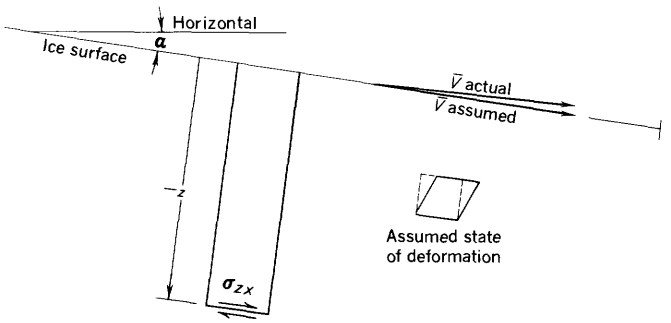

FIGURE 37.—Definition sketch for analysis of stress and deformation in a vertical profile.

glacier but is still linear (Nye, 1952a, p. 85). On a vertical plane through the axis of a semicircular channel

$$\sigma_{zx} = \frac{1}{2}\gamma z \sin \alpha$$

It seems logical to follow the *a priori* argument of Nye (1952a, p. 85–86) that these two cases can be expressed as special cases of a more general relation. A simple general relation is that the increase of stress along the centerline is always linear and that the rate of increase depends on a "shape factor" given by the ratio of hydraulic radius R to total depth d. This shape factor reduces to 1 for an infinitely wide glacier and to one-half for a semicircular cross section. In general it will be between these two limits for most valley glaciers. Thus we assume that

$$\sigma_{zx} = \frac{R}{d}\gamma z \sin \alpha$$

The principal stresses are $(\sigma_{zx} + \sigma, -\sigma_{zx} + \sigma, \sigma)$ where σ is the hydrostatic pressure. The octahedral shear stress is

$$\sigma_0 = \sqrt{\frac{2}{3}}\frac{R}{d}\gamma z \sin \alpha \qquad (8)$$

Strain Rate

The shearing strain rate from equations (1) is

$$\dot{\epsilon}_{zx} = \frac{1}{2}\frac{\partial V_x}{\partial z}$$

The principal strain rates are approximately $(\dot{\epsilon}_{zx}, -\dot{\epsilon}_{zx}, 0)$, and the equivalent octahedral shearing strain rate is

$$\dot{\epsilon}_0 = \sqrt{\frac{2}{3}}\dot{\epsilon}_{zx} = \sqrt{\frac{1}{6}}\frac{\partial V_x}{\partial z} \qquad (6)$$

Assumptions Used

In addition to the assumptions listed under "Fundamental relations," two major approximations have been added:

1. The increase of stress with depth is assumed to be linear and the gradient of stress increase was assumed to be proportional to a shape factor.
2. The deformation in the x, z-plane is assumed to be correctly shown in figure 37, V at all depths is parallel to V at the surface, and V does not increase or decrease in the x-direction.

RESULTS

Values of $\frac{\partial V_x}{\partial z}$ were computed from borehole displacements (fig. 30) and are shown in figure 38.

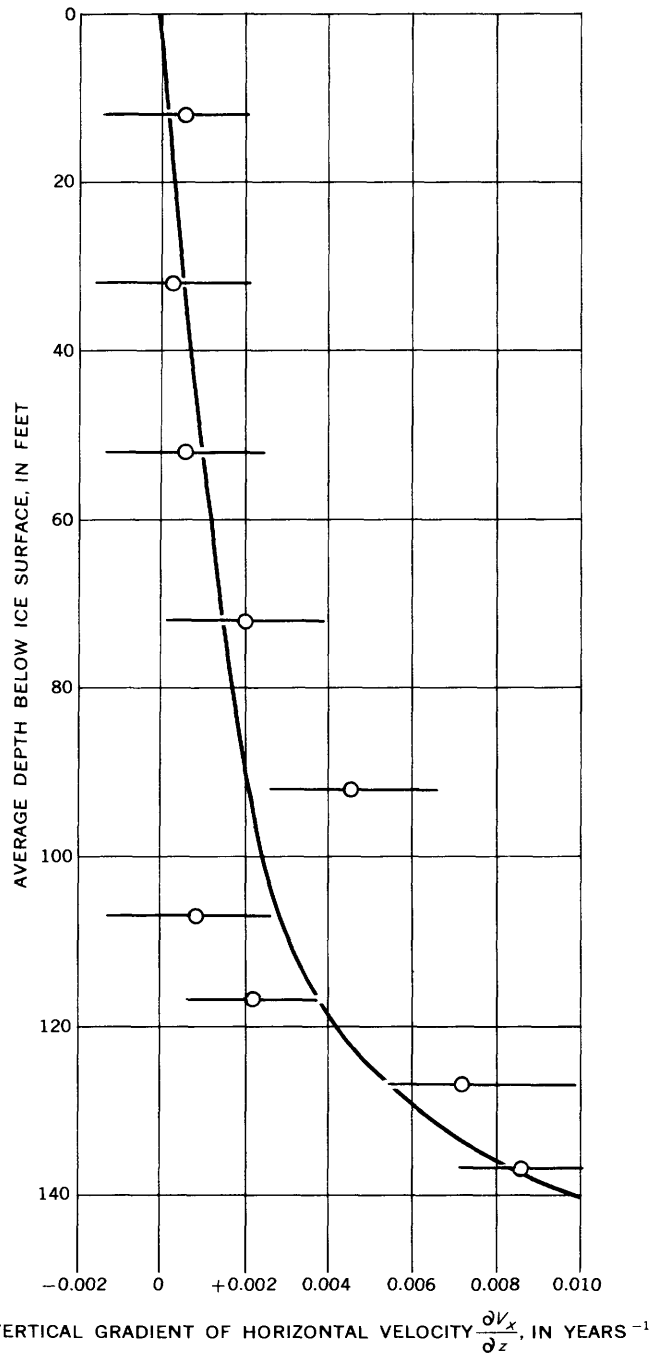

FIGURE 38.—Vertical gradient of horizontal velocity along vertical borehole. Circles indicate measurement points, short horizontal lines indicate approximate limits of measurement error.

509755 O - 60 - 5

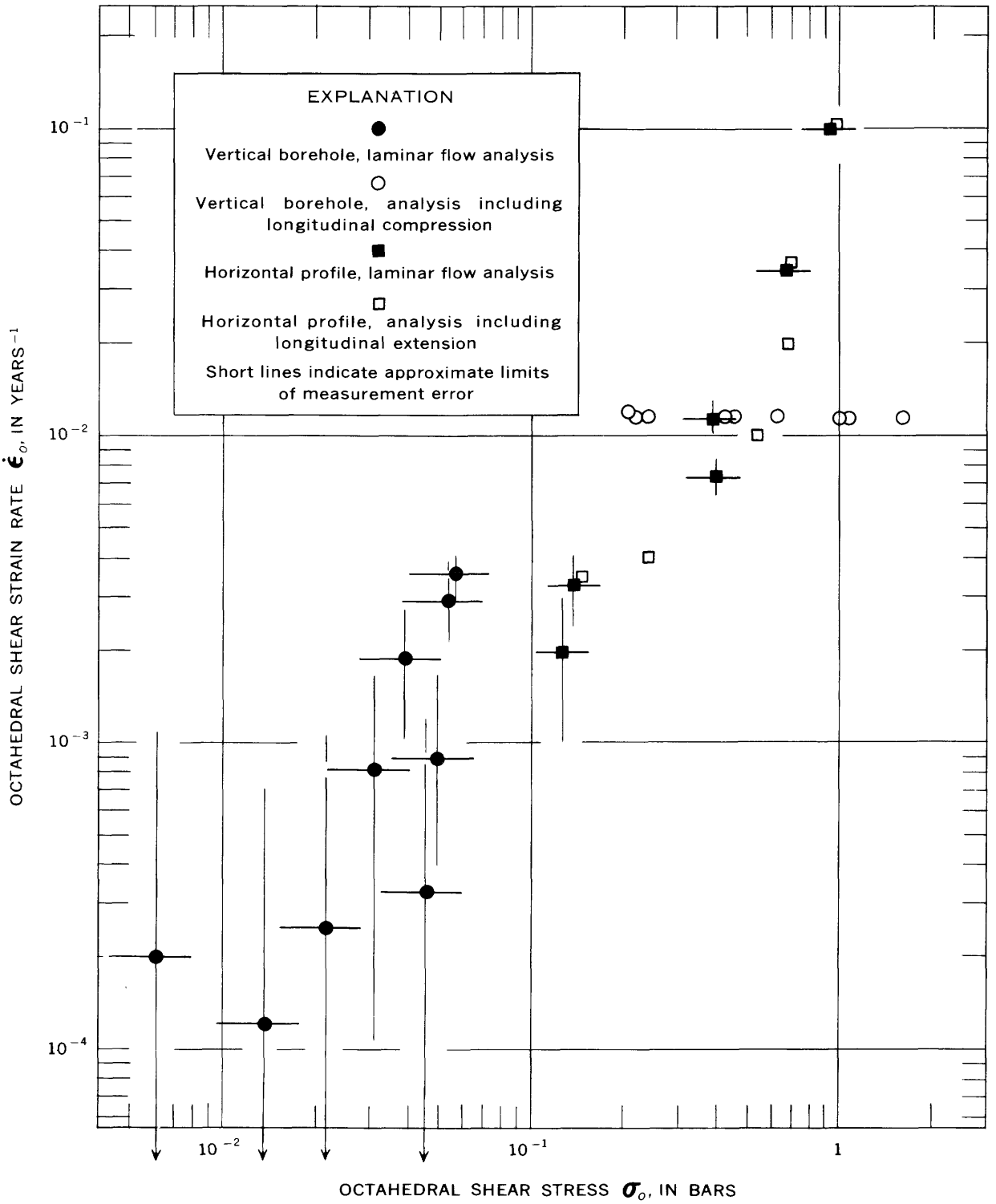

FIGURE 39.—Strain rate as a function of shear stress in Saskatchewan Glacier.

Values of σ_0 computed from equation (8) and $\dot{\epsilon}_0$ computed from equation (9) are presented in table 5 and in figure 39. It can be seen that the relation between these quantities is not linear.

No evidence of a yield stress appears in these data. The shearing rates at the lowest stresses (apparently the lowest which have yet been measured for ice) are somewhat faster than what one would predict from the behavior at higher stresses.

EFFECT OF LONGITUDINAL EXTENSION

When this borehole was emplaced and the results first analyzed, it was not possible to account for shearing stresses or strain rates due to horizontal extension or compression. In an analysis published subsequently, Nye has included horizontal longitudinal extension or compression within the framework of a general theory of stress and velocity in glaciers. He has also analyzed the Jungfraufirn borehole results (Gerrard, Perutz, and Roch, 1952) within this framework by using a trial assumption of a flow law. Some of his results can be applied to the Saskatchewan data.

TABLE 5.—*Stress and strain-rate data from vertical borehole*

[Formulas and definitions of symbols are given on p. 32, 42]

z (feet)	σ_0 (bars)*	σ_0' (bars)*	$\frac{\partial V_x}{\partial z}$ (years^{-1})	ϵ_0 (years^{-1})	ϵ_0 (years^{-1})
15.....	0.006	0.43	0.0005	0.0002	0.0114
35.....	.014	1.01	.0003	.0001	.0114
55.....	.022	1.08	.0006	.0002	.0114
75.....	.031	.44	.0020	.0008	.0115
95.....	.039	.24	.0046	.0019	.0116
110.....	.046	1.60	.0008	.0003	.0114
120.....	.050	.63	.0022	.0009	.0115
130.....	.054	.21	.0072	.0030	.0118
139.....	.057	.21	.0086	.0035	.0120

* 1 bar = 10^6 dynes per square centimeter = 14.5 pounds per square inch.

According to Nye's analysis (1957, p. 126), stress and strain-rate values can be deduced from a borehole experiment using the expressions

$$\sigma_0' = \sigma_0 \frac{\dot{\epsilon}_0'}{\dot{\epsilon}_0} = \sqrt{\frac{2}{3}} \frac{R}{d} \gamma z \sin \alpha \frac{\dot{\epsilon}_0'}{\dot{\epsilon}_0} \quad (8)$$

$$\dot{\epsilon}_0'^2 = \dot{\epsilon}_0^2 + \frac{2}{3} \dot{\epsilon}_{xx}^2 = \frac{1}{6}\left(\frac{\partial V_x}{\partial z}\right)^2 + \frac{2}{3}\left(\frac{\partial V_x}{\partial x}\right)^2$$

in which σ_0' and ϵ_0' are octahedral shear stress and octahedral shear rate modified to account for a longitudinal compressive strain rate $\dot{\epsilon}_{xx}$.[9] In addition to the assumptions given previously Nye assumes that no stresses or strains are active in the y-direction and that σ_{zx} and σ_0 are functions of x only and not of y. Transverse and vertical extending strain rates are known at the borehole site. These additional components of deformation could be considered by an extension of Nye's theory. However, in view of the lack of information on these components at depth, the inaccuracies in measurement, and the certain paucity of useful information in the final results, further refinement is not justified.

The effect of this modification of σ_0 and $\dot{\epsilon}_0$ is to seriously impair the usefulness of the Saskatchewan borehole data for deducing a flow law (table 5 and fig. 39). This is because the constant shear due to longitudinal compression overpowers the variable shears due to laminar flow, confining the spread of strain-rate values on a graph to an extremely small region. The lack of correspondence between relative values of σ_0 and σ_0' is noteworthy (table 5).

Nye has shown that if the flow law is of the form

$$\dot{\epsilon}_0 = k\sigma_0^n \quad (10)$$

where k and n are empirical coefficients, the effect of longitudinal extension on the Jungfraufirn results is to lower the apparent power-law coefficient n as calculated in a simple laminar-flow analysis. By assuming equation (10) one can show that the Saskatchewan data behave somewhat similarly. The average shearing-strain rate measured by the deformation of the borehole was only a tiny fraction of the prevailing shearing-strain rate due to longitudinal compression, and even at the bottom of the borehole the borehole deformation shear was only one-fourth of the compressional shear. This would suggest that if equation (10) were correct for ice, the simple analysis of the Saskatchewan data (p. 38–39) should have yielded an apparent flow law of the Newtonian viscous type. The fact that it did not do this (fig. 39) indicates that either equation (10) is not correct or that Nye's analysis does not apply perfectly. However, the basic approach we wish to use here is to first present the data and then see which type of flow-law relation best describes them.

TRANSVERSE PROFILE

STRESS AND DEFORMATION IN LAMINAR FLOW

The cross section of Saskatchewan Glacier at $x' = 5{,}000$ approximates a semicircle (fig. 6). This is the only cross-section shape for a valley glacier that is amenable to mathematical analysis at the present time. In this case surfaces of maximum shearing stress and strain rate form cylinders concentric about the flow centerline. We begin by assuming laminar flow. The complication of longitudinal

[9] These relations when combined with equations (8) and (9) and modified to use the symbols of this report are identical with Nye's equations except for a factor of $\sqrt{2/3}$. Nye reports his flow law data in terms of an effective shear stress and strain rate which are $\sqrt{3/2}$ times the octahedral shear stress and strain rate.

extension or compression is not pronounced at this location.

Stress

The shear stress on these cylindrical surfaces as given by Nye (1952a, p. 85) is

$$\sigma_{rx} = \frac{1}{2} r \gamma \sin \alpha \qquad (11)$$

where r is the distance from the centerline and α is the surface slope. The actual cross section is slightly elliptical. The eccentricity is slight, so it may be valid to allow for it by extending r slightly in the horizontal direction and compressing it slightly in the vertical direction as was done in equation (8). On the surface, equation (11) may be written as

$$\sigma_{yx} = \frac{R}{w} \gamma y' \sin \alpha$$

where w is the width of the glacier. The octahedral shear stress σ_0 is

$$\sigma_0 = \sqrt{\frac{2}{3}}\, \sigma_{yx} = \sqrt{\frac{2}{3}} \frac{R}{w} \gamma y' \sin \alpha \qquad (12)$$

Strain Rate

The shearing strain rate corresponding to equation (11) is given by relations (1) as

$$\dot{\epsilon}_{yx} = \frac{1}{2} \frac{\partial V_x}{\partial y}$$

and the octahedral shearing strain rate is

$$\dot{\epsilon}_0 = \sqrt{\frac{2}{3}}\, \dot{\epsilon}_{yx} = \sqrt{\frac{1}{6}} \frac{\partial V_x}{\partial y} \qquad (13)$$

Assumptions Used

1. It is assumed that the transverse gradient in shear stress is linear and is proportional to the gradient for a semicircular cross section.
2. It is also assumed that V is parallel to the surface and that the surface is level in a cross-glacier direction, and that there is no longitudinal or transverse extension or compression.

RESULTS

Values of stress computed from equation (12) and strain rate computed from equation (13) are shown in table 6 and in figure 39. These data follow the same flow-law trend found from the vertical profile, but they cover a range of higher stresses. Insufficient measuring points were available in the center of the glacier to define the strain gradient at low stresses so the ranges of stress do not overlap.

EFFECT OF LONGITUDINAL EXTENSION

The slight longitudinal extension which was measured along this profile can be considered similarly to the compression of the vertical borehole. In this case, equations (12) and (13) must be modified by use of equations (8′) and (9′) so that

$$\sigma_0' = \sqrt{\frac{2}{3}} \frac{R}{w} \gamma y' \sin \alpha \frac{\dot{\epsilon}_0'}{\dot{\epsilon}_0} \qquad (12')$$

$$\dot{\epsilon}_0'^2 = \frac{1}{6}\left(\frac{\partial V_x}{\partial y}\right)^2 + \frac{2}{3}\left(\frac{\partial V_x}{\partial x}\right)^2 \qquad (13')$$

The longitudinal extension rate $\frac{\partial V_x}{\partial x}$ varied along the profile, and these values are tabulated in table 6 along with values of σ_0' and ϵ_0' calculated according to equations (12′) and (13′). Transverse and vertical normal strain rates are also known along this profile, but the further refinement necessary to incorporate them is not justified for reasons similar to those given in the case of the vertical borehole.

The result of this modification of a laminar-flow analysis is to move several points toward slightly higher values of stress and strain rate (fig. 39). This does not appreciably change the indicated flow-law relation.

TABLE 6.—*Stress and strain-rate data from transverse surface profile*

[Formulas and definitions of symbols are given on p. 32, 42]

y' (feet)	σ_0 (bars)	σ_0' (bars)	$\frac{\partial V_x}{\partial y}$ (years)	$\frac{\partial V_x}{\partial x}$ (years^{-1})	ϵ_0 (years^{-1})	ϵ_0' (years^{-1})
−260	0.137	0.141	0.008	0.001	0.003	0.003
−760	.400	.540	.018	.008	.007	.010
−1260	.663	.690	.082	.012	.034	.036
−1760	.926	.926	.246	.010	.100	.100
+240	.126	.240	.005	.004	.002	.004
+740	.390	.680	.028	.020	.011	.020

DISCUSSION OF THE FLOW-LAW RESULTS

The relation between shear stress and shear-strain rate computed from vertical and transverse velocity profiles in Saskatchewan Glacier is shown on figure 40. Also shown on this graph are results from the Malaspina borehole (kindly supplied in advance of publication by R. P. Sharp), the Jungfraufirn borehole, McCall's Skauthöe, Glen's Austerdalsbre, and Haefeli's Z'Mutt and Arolla tunnel contraction data (as computed by Nye), and Glen's laboratory experiments at temperatures near the melting point. All of these data have been converted to octahedral shear stress and octahedral shear-strain rate.

Some uncertainty exists about the correct placement of Nye's and Glen's data on this diagram. Nye's stress data are reported in terms of an "effective shear stress" which is also called the "octahedral shear stress" and is defined as

$$2\,\sigma_0^2 = \sigma_{ij}'\,\sigma_{ij}'$$

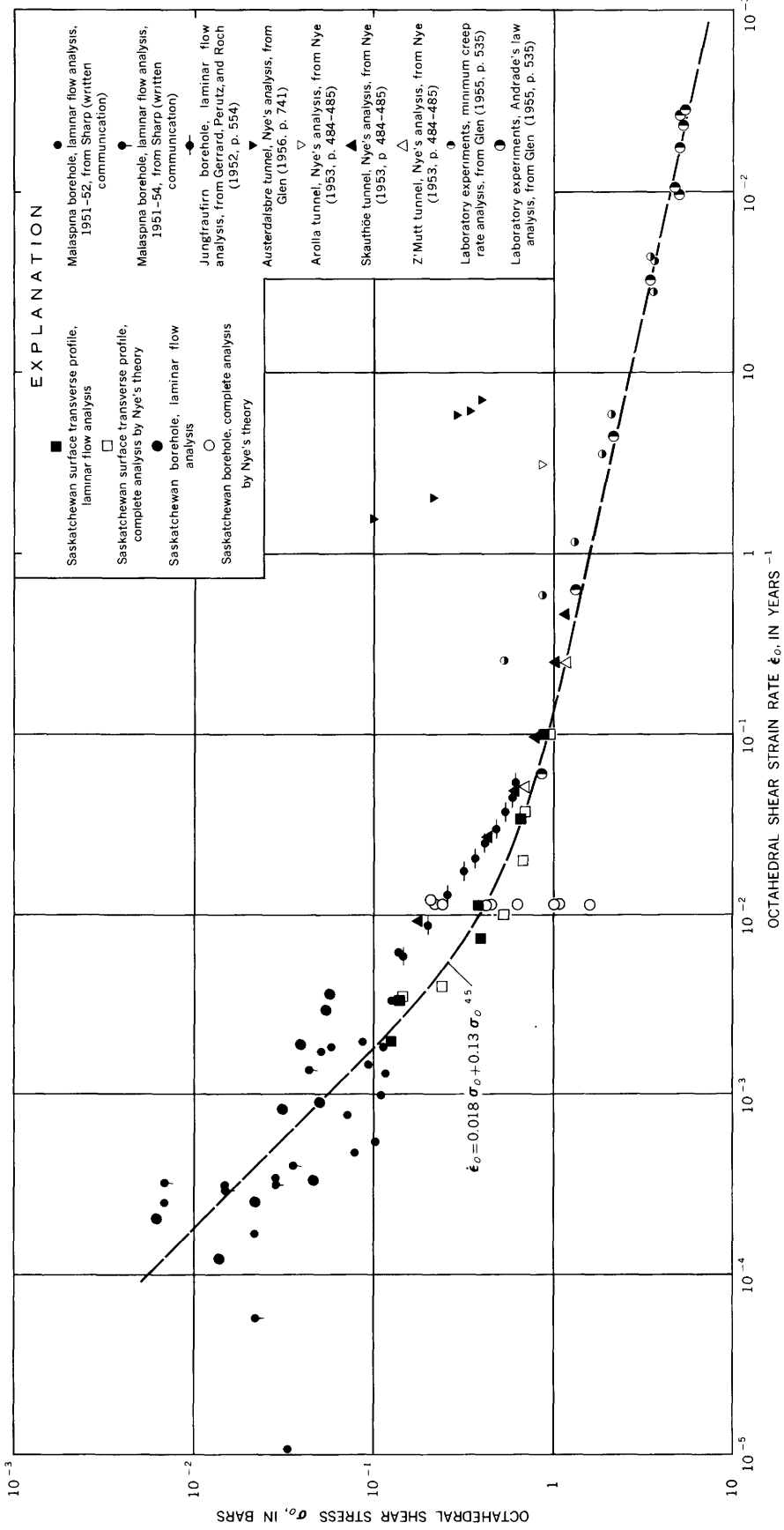

FIGURE 40.—Strain rate as a function of shear stress, data from numerous sources

where σ_{ij}' is the deviator of stress (1953, p. 478). Glen (1955, p. 536) analyzes his results "in the way described by Nye," and reports his data in terms of "octahedral shear stress." Strain rates are reported similarly by these investigators. However, these values of "octahedral shear stress" appear to be different by a factor of $\sqrt{2/3}$ from the shear stress on the octahedral planes as given by Nadai (1950, p. 103). The discrepancy is not too important because of the large scatter of the flow law data.

The tunnel data could not be placed directly on the diagram because a power-law relation must be assumed to convert from mean stress away from the tunnel to octahedral shear stress along the tunnel walls in Nye's method of computation. The Skauthöe and Z'Mutt mean stress and contraction rate data fit a power-law relation reasonably well (Nye, 1953, fig. 1). The tunnel data have been converted point by point assuming this relation.

Stress and strain-rate values were obtained independently in all other experiments.

In spite of the scatter of points and the many gross assumptions involved in the calculations, the data point toward several distinct conclusions:

1. Hydrostatic pressure has little effect on the flow rate, at least at shallow depths. This is indicated by the close similarity of the vertical and transverse profile data from Saskatchewan Glacier, and the similarity between the data from the Saskatchewan, Malaspina, and Jungfraufirn boreholes. These boreholes were drilled in glaciers of markedly different slope and therefore reached the same shear stress at markedly differing pressures. This conclusion agrees with recent laboratory results on the velocity of shear deformation of single ice crystals when the temperature difference between ice sample and melting point is kept constant (Rigsby, 1957).

2. Extending and compressing flow have minor effect on the flow-law relation except at low stresses. The Jungfraufirn borehole was in the center of an accumulation basin, in an area where the flow was markedly extended (0.14 years^{-1}). The Malaspina borehole was in an area of strong compressing flow, the Saskatchewan borehole was in an area of slight compressing flow (0.014 years^{-1}), and the Saskatchewan transverse profile was in an area of very slight extension (0.001 to 0.012 years^{-1}). These differences in environment do not cause a major displacement of the flow-law curves computed on a laminar-flow assumption.

3. All of the data give similar flow-law results except for those data from the Austerdalsbre and Arolla tunnels. This suggests that Nye's analysis of tunnel contraction breaks down when the general stress environment is not hydrostatic. In addition, the data suggest that Glen's analysis of creep curves using Andrade's law (Glen, 1955, p. 529) leads to results consistent with field relations. It is interesting to note that the actual measured points for the Skauthöe and Z'Mutt tunnels fit the general trend of results better than the power-law relation assumed by Nye (1953, p. 486).

4. There is no evidence for a yield stress of ice, even at stresses less than 0.01 bar. Movement along a glide plane in a single crystal probably occurs only when a critical shearing stress is reached on that plane (Turner, 1948, p. 229), and in the case of the ice crystal this stress may be about 5 bars (Bjerrum, 1952, p. 390). Therefore, intracrystalline deformation in ice must take place through the movement of dislocations—small imperfections in the crystal lattice.

5. The flow is more 'viscous" at low stresses and more "plastic" at high stresses, and the flow law seems to be more complex than a simple power-law relation.

Several analytical equations have been suggested by recent theoretical work on the flow of ice or metals. It is instructive to note how closely these equations fit the data. The theoretical equations of greatest interest have these forms:

$$\dot{\epsilon}_0 = \sigma_0^n \qquad (10)$$

$$\left.\begin{aligned} \dot{\epsilon}_0 &= \sigma_0^n \\ &\text{where} \\ k &= k_1 \text{ and } n = n_1 \text{ at } \sigma_0 \leqq \sigma_0 \text{ critical} \\ &\text{and} \\ k &= k_2 \text{ and } n = n_2 \text{ at } \sigma_0 > \sigma_0 \text{ critical} \end{aligned}\right\} \quad (10a)$$

$$\epsilon_0 = k_1 \sinh (k_2 \sigma_0) \qquad (10b)$$

Equation (10) was suggested as a good fit to laboratory results on the deformation of polycrystalline ice by Glen (1955, p. 528) and for single crystals by Steinemann (1954, p. 404). Subsequently, Weertman (1957) published a dislocation climb model for steady-state creep. This model does not require the formation of immobile dislocations and can therefore be applied to hexagonal crystals such as ice.[10] This theory (Weertman, 1957, p. 363) suggests equation (10) for low stresses in which the exponent n

[10] Considerable care must be used in interpreting the deformation of polycrystalline ice in terms of the behavior of single crystals. As far as is known, ice can glide only on its basal plane. Uniform plastic strain requires the simultaneous operation of five independent sets of planes if it is to be produced by slip alone (Hill, 1950, p. 8). Therefore contact between grains cannot be maintained by slip along basal planes alone, and effects at the grain boundaries must have an important influence on the flow.

has the value of 4.5. Figure 40 suggests that a simple power-law dependence (equation 10) is not quite correct. The Saskatchewan transverse profile and the laboratory results (Andrade's law analysis) of Glen both indicate that a real discrepancy at low stresses exists in spite of the effect of longitudinal extension or compression. Landauer (1957, p. 6) also suggests that a simple power-law relation is an over simplification.

Equation (10a) describes the flow law of aluminum at elevated temperatures (Servi and Grant, 1951, p. 911). This discontinuous behavior is attributed by these authors to an abrupt transition from grain boundary to intragranular creep. Many mechanisms have been suggested for the creep of ice (Sharp, 1954, p. 826–828) and the activation energy of creeping snow suggests that several mechanisms may act simultaneously (Landauer, 1955, p. 6). However, it is difficult to understand why any two possible creep mechanisms in ice should operate in this discontinuous manner. It would seem more logical for the two mechanisms to appear as separate terms in a flow-law equation. It must be noted that the strain softening observed by Steinemann (1954, p. 408), Griggs and Coles (1954, p. 10–20) and Glen (1955, p. 525) cannot be related to equation (10*a*) or to a break in slope on the stress-strain rate graph because the onset of strain softening is a function of the total strain, not the strain rate.

Equation (10*b*) states that the velocity of shear is proportional to the hyperbolic sine of the applied stress. This relation has been suggested on theoretical grounds by Eyring (Eyring, Glasstone, and Laidler, 1941, p. 483) for the laminar flow of a generalized fluid considered as a chemical-rate process. This theory has been applied to the flow of solid metals (Dushman, Dunbar, and Huthsteiner, 1944). Equation (10*b*) does not apply to the field data at the higher stresses, but affords a good fit at the lower stresses. A similar equation has been given for the creep of a single hexagonal crystal (Weertman, 1957, p. 363), but does not follow the data at higher stresses.

The flow data which have been assembled in figure 40 seem to indicate that two mechanisms of flow operate simultaneously. The relation

$$\dot{\epsilon}_0 = k_1 \sigma_0 + k_2 \sigma_0^n \qquad (10c)$$

seems to approximate the data quite well. This relation would be probable if steady-state creep in ice was due to two theoretically plausible mechanisms operating simultaneously: first, a Newtonian viscous flow due to grain-boundary creep (Jellinek and Brill, 1956, p. 1207; Cottrell, 1953, p. 210–211) and second, a power-law steady-state flow due to intracrystalline gliding produced by dislocation climb (Weertman, 1957). This suggested flow-law relation cannot be rigorously tested by the observed data, but it is not inconsistent with them. The following empirical coefficients are suggested:

$$k_1 = 0.018,\ k_2 = 0.13,\ n = 4.5$$

DISCHARGE RELATIONS

VELOCITY AT DEPTH

METHOD OF COMPUTATION

Velocity at depth can be calculated along the centerline of a valley glacier flowing in a simple channel if some assumptions about the stress are made, and information about the relation between stress and strain rates is available. Velocity distributions at depth have been calculated for other glaciers, but the situation for Saskatchewan Glacier is unique in that the calculation involves very few assumptions that have not been previously tested, and the results can be checked by several independent means.

The shearing stress that produces the shearing flow must first be determined. For simplicity, the stress on planes parallel to the surface will be computed. As can be seen on plate 5, the shear stress resolved on planes parallel to the surface is not very different from the stress resolved on planes parallel to the velocity vector or the streamlines. Consequently, equation (8) is applicable; this equation has been approximately verified by giving consistent flow law results (fig. 40). The cross section, surface slope and specific weight of ice are constant at any one vertical profile in Saskatchewan Glacier, so equation (8) can be written simply as

$$\sigma_0 = Cz \qquad (8')$$

where $C = \frac{R}{d}\,\gamma \sin \alpha$ and is expressed in pounds per cubic foot. The flow law relation is

$$\dot{\epsilon}_0 = f'(\sigma_0) \qquad (7)$$

and

$$\dot{\epsilon}_0 = \sqrt{\frac{2}{3}}\,\frac{\partial V_x}{\partial z} \qquad (9)$$

Therefore,

$$\frac{\partial V_x}{\partial z} = \sqrt{\frac{3}{2}}\, f'(Cz)$$

$$V_{z_0} - V_{z_z} = \sqrt{\frac{3}{2}} \int_0^{-z} f'(Cz)\, dz \qquad (14)$$

where $V_{x_0} = V_x$ at the surface and $V_{x_z} = V_x$ at depth $-z$.

RESULTS

Vertical velocity profiles at eight places along the longitudinal centerline profile of Saskatchewan Glacier are presented in plate 5. The curve for the highest profile (h) is a crude approximation because the cross-sectional characteristics could only be estimated. These results show that, in spite of the great differences in depth, slope and surface velocity, the curves all demonstrate a very low velocity at the bed. This bed velocity ranges from −11 fpy (probably due to a depth value that is slightly too large) to +50 fpy in absolute amount, or from −10 to +58 percent of the surface velocity. For the 7 best known cross sections the bed velocity averages 19.8 percent of the surface velocity.

The average velocity (area of the velocity-depth profile divided by the depth) ranges from 94 percent of the surface velocity at the terminus to 55 percent of the surface velocity in Castleguard sector (profiles f and g). There seems to be little justification for the frequently made assumption that the average velocity is approximately equal to the surface velocity (Nielson, 1955, p. 7–8). This seems to be true only where the ice is very thin such as at the terminus of Saskatchewan Glacier or under a thin cirque glacier (McCall, 1952, p. 126).

MASS BUDGET

FLOW INTO CASTLEGUARD SECTOR

The surface velocity and cross section at the upper part of Castleguard sector ($x' = 5{,}000$) are known with reasonable accuracy. Furthermore, the cross section here is amenable to stress calculation with few drastic assumptions, and the flow is nearly parallel to the surface. The discharge through this cross section can be computed with a reasonable assurance of accuracy.

Lines of equal velocity were drawn on a diagram of this cross section using as control the known distribution of velocity at the surface and the computed velocity (using fig. 41) at depth along the centerline (fig. 42). The total discharge through this cross section was computed by multiplying the area between each pair of equal-velocity lines by the average of the two velocity values and summing the results. This computation was done for the south half only, because of the complicated geometry and discharge relations along the north margin. The resulting discharge for the south half is 356×10^6 cfy, or 11.3 cfs.

SURFACEWARD FLOW

The discharge through a given cross section must be equal to the flux of ice toward the surface over the whole area of the glacier below that cross section. Thus the discharge and the depth of a glacier can be computed from measurements of the component V_d. (See p. 25.)

The total supply of ice to the south half of the glacier surface below $x' = 5{,}000$ was computed by graphically integrating the values of V_d given on figure 18. The result is 367×10^6 cfy. This agrees very well with the computed discharge through the cross section at $x' - 5{,}000$. The error of 3 percent is less than expected considering the crudeness of the V_d data along the sides of the glacier below Castleguard sector. The agreement in these values also indicates that the glacier is in a state of "constant unbalance": the ice that is being discharged into the tongue is just sufficient to maintain the present rate of thinning.

These and additional mass budget data are summarized in table 7.

STREAMLINES

METHOD OF DETERMINING

A streamline is a curve drawn so that its direction

TABLE 7.—*Mass-budget data for the south half of the tongue of Saskatchewan Glacier*

	Discharge (cfy × 10 ^{6})	Method of computation
At the firn limit....	360	Integral of Vd over tongue.
	553	Integral of ablation over tongue.
At x = 5,000	356	Double integral of measured velocity at surface and computed velocity at depth.
	367	Integral of Vd over area below this section.
	523	Integral of ablation over area below this section.
At x^1 = 10,000	317	Integral of Vd over area below this section.
	438	Integral of ablation over area below this section.
Deficit for the whole half-tongue.	186	Integral of ablation minus integral of Vd over the whole half-tongue.
Average contribution to stream-flow by ice melt during ablation season.	[1] 70.3	Integral of ablation expressed as cubic feet per second during a 3-month ablation season, assuming no losses.

[1] In cubic feet per second.

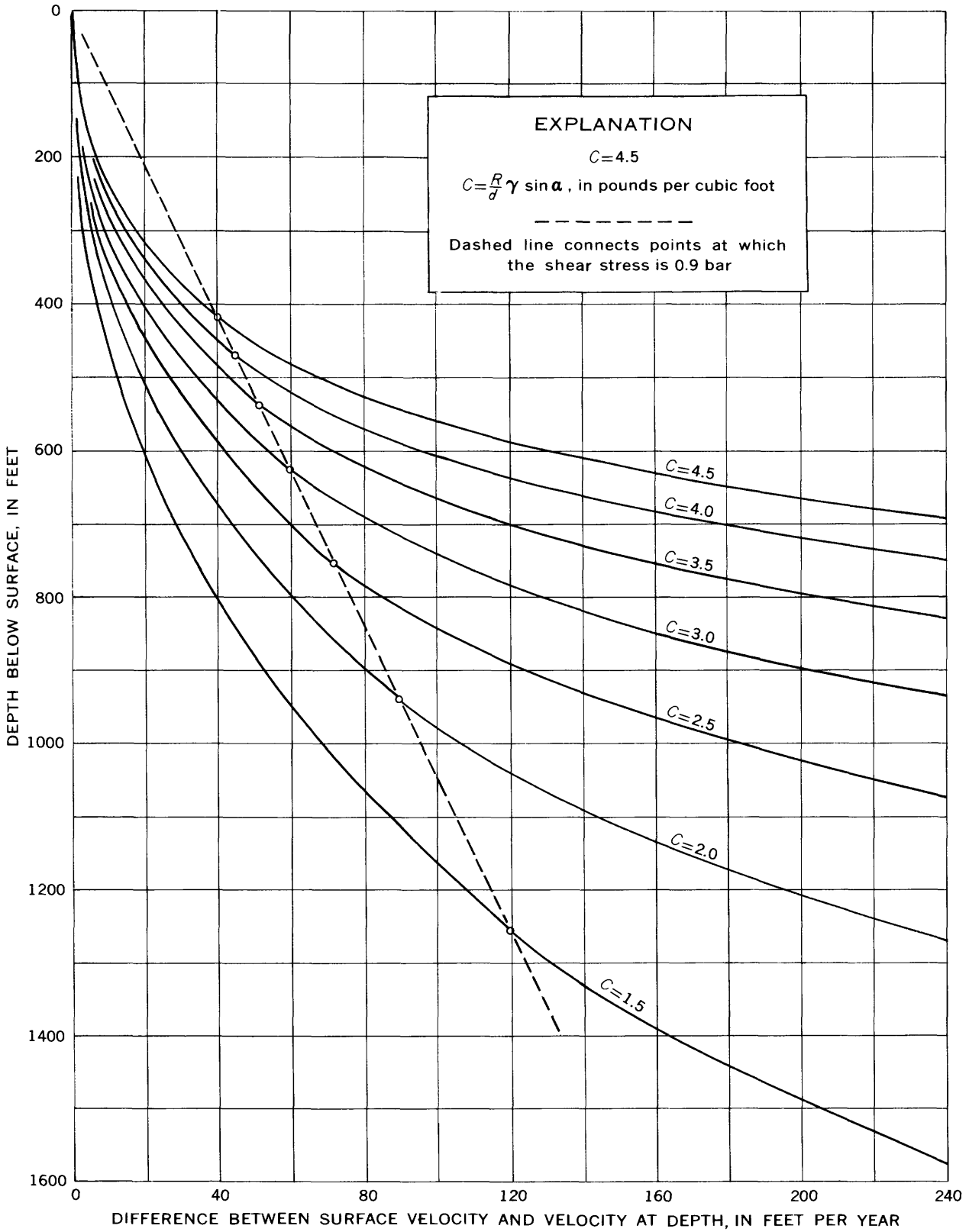

FIGURE 41.—Difference between velocity at the surface and velocity at depth as a function of depth.

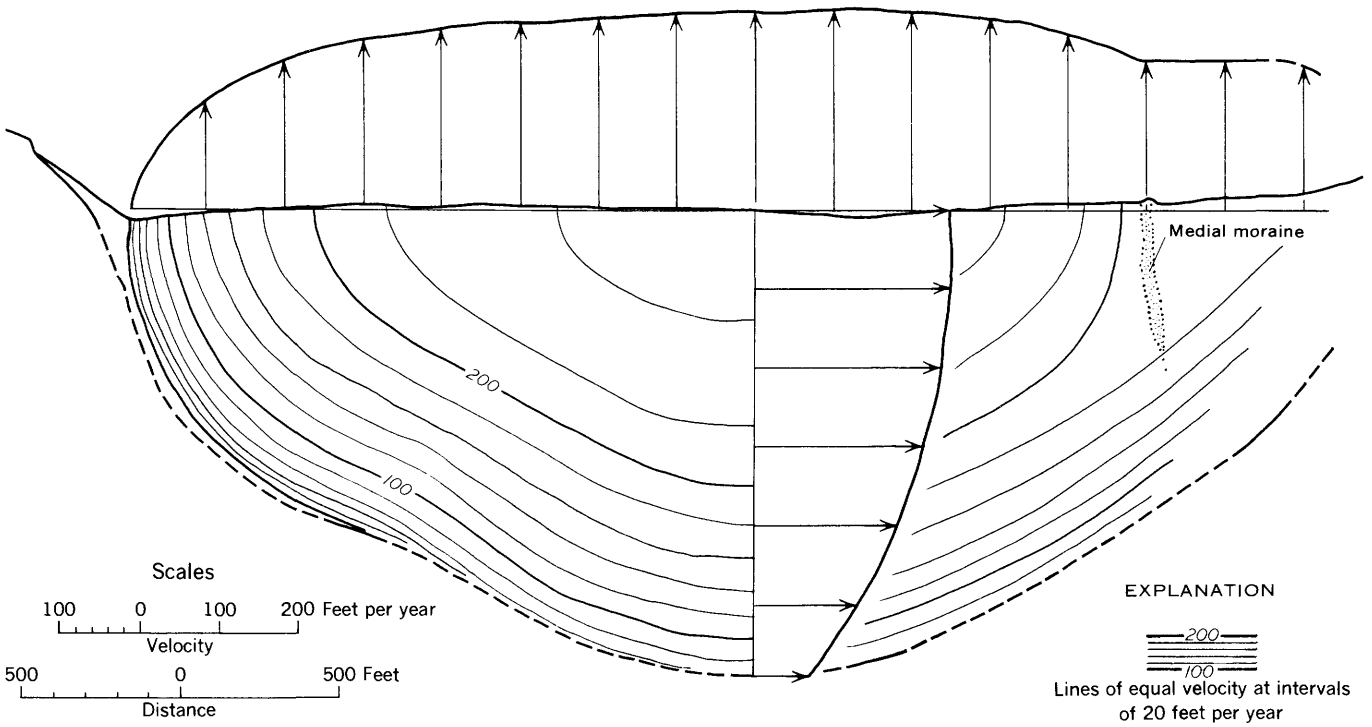

FIGURE 42.—Distribution of velocity in transverse section at $x' = 5{,}000$.

at every point coincides with the direction of the velocity vector. In steady flow (flow that does not vary in the course of time) the streamlines also coincide with the paths taken by separate particles (Prandtl and Tietjens, 1934, p. 73). The streamlines that pass through a closed curve collectively form a stream tube, and in steady flow no material can pass through the boundary of a stream tube. Thus the mass discharge through any stream tube must be constant. The flow of Saskatchewan Glacier is virtually steady, the ice is relatively constant in density, and very little internal ablation occurs, so the volume discharge through any stream tube must also be constant. Positions and shapes of streamlines along the centerline plane can be computed using this constancy of discharge relation. For simplicity of calculation, a unit width (in the y' direction) of flowing material is assumed throughout the calculations. This is not completely realistic because transverse extensions or compressions ($\dot{\varepsilon}_{yy}$) do occur. However, these effects along the flow centerline of Saskatchewan Glacier are small compared to the shears ($\dot{\varepsilon}_{zx}$) involved, and the simple analysis seems to offer a close approximation to the actual behavior.

The calculation proceeded as follows: The area under a graph of the vertical component of flow toward the surface (V_d) as a function of distance along the centerline (x', fig. 23*c*) was divided into 10 equal parts from the terminus back to $x' = 5{,}000$ feet. These equal parts represent equal discharges to the surface (see p. 24) of about 17.5×10^3 cubic feet per year per foot of width. Vertical profiles of the horizontal component of velocity were computed at or near 7 points marking multiples of these equal surfaceward discharges (pl. 5). The area of each of these profiles was divided into the same number of parts as the number of surfaceward discharge parts emerging downglacier from the profile. Lines were drawn dividing these equal parts of the discharge at depth so as to intersect the surface at points separating the equal surfaceward discharges. These lines represent streamlines of flow, and the volumes between adjacent pairs of lines and the unit width represent stream tubes handling constant discharges. These results are shown on plate 5.

CHECKS ON ACCURACY

The accuracy of these constructions can be checked several ways: First, the actual streamlines should crop out at the surface exactly parallel to the velocity vectors. The constructed streamlines with reasonable accuracy, as shown on plate 5. The streamlines and velocity profile at profile *C* are not very accurate because the cross section is not known exactly and there is some divergence between the velocity vectors and the streamlines in this area.

A second check on the entire construction (including the vertical velocity profiles) is that the dis-

charges represented by each of the vertical profiles should be equal to the discharge to the surface downglacier from that profile. The discharges through a vertical section are determined by V_x, on the surface, the depth, slope and cross section at that point. The discharges to the surface are determined by the integral of V_d times the area, and these values are computed from the surface profile, V_x, and V_z. Thus these two quantities are almost independent and can be compared. The increments of discharge to the surface were 17.5×10^3 cfy per foot of width. As shown in the tabulated data on plate 5, the incremental discharges at depth were similar to this value for most vertical profiles. The agreement is close considering the many approximations and assumptions involved in this calculation. Therefore we can assume that plate 5 gives a virtually correct interpretation of the distribution of streamlines at depth under the flow centerline.

CONCLUSIONS FROM THESE RESULTS

The two most striking features of the streamline distribution are (1) the close spacing near the surface and (2) the parallelism of streamlines to the bed profile.

The close spacing of streamlines near the surface is necessary because the velocity is greatest near the surface. However, in the several diagrammatic profiles showing hypothetical streamlines which have been published, close spacing has not always been considered. This spacing indicates that the ice which crops out 1½ miles upglacier from the terminus was never buried more deeply than one-half the total depth of the glacier. Thus the presence of slightly recrystallized ice still showing a primary stratification in the lower part of the tongue need not be considered unusual.

A more significant feature of the streamline distribution is the close parallelism between streamlines and bedrock. This parallelism is modified very slightly in the upper layers where the curvature of the streamlines is somewhat reduced. In general it seems that the shape of the streamlines is virtually independent of the thickness or speed of the glacier and is determined mainly by the long profile of the bedrock. The significance of this fact will be discussed in the next section.

LONGITUDINAL PROFILE

SIGNIFICANCE OF THE PROFILE

The length, thickness, and slope of a glacier are expressed in its longitudinal profile. Advances, recessions, and waves of thickening can be expressed quantitatively as transient changes in the profile. The shape of an equilibrium profile is ultimately determined only by the bedrock configuration and by the prevailing gradients of potential accumulation and ablation. Past climates might be quantitatively reconstructed from studies of old moraines if knowledge of bedrock topography and meteorological conditions could be used in predicting the longitudinal profile of a glacier which was in equilibrium with this environment. And likewise present-day climatic trends might be determined from present-day profiles. Glacial geology, paleoclimatology, and hydrology would benefit inestimably.

This prediction cannot be made at the present state of glaciological knowledge. The first task is to determine which geometrical factors are most important in shaping a longitudinal profile for a given discharge. The method which has been used most often in the past and the research that could be pursued in the future will be discussed in the following paragraphs.

CONSTANT BASAL SHEARING-STRESS CALCULATION

The profile of a large ice sheet resting on a horizontal floor has been calculated by Orowan (1949), Hill (see Nye, 1951, p. 571), and Nye (1951, p. 570–571; 1952a, p. 91–93) by assuming that the shear stress on the bed was everywhere constant. In a further calculation Nye (1952c) allowed the bed slope to change gradually along a line of flow. A similar analysis was applied to a valley glacier similar to Saskatchewan Glacier (Nye, 1952b).

These calculations gave good results along one profile in Greenland (Nye, 1952c, p. 531), but predicted a great depression of the bedrock over the northern half of Greenland which has not been confirmed by subsequent seismic and gravity measurements (Bruce and Bull, 1955). The valley-glacier profile, when adjusted by changing the "average shear stress on the bed" to the best fit for the glacier as a whole, did not give good results at the terminus and did not predict the proper length of the glacier.

The shear stress on the bed of a glacier is not constant, as has been shown for an icecap (Orvig, 1953) and for the Saskatchewan Glacier (pl. 5). This variability is a very significant objection to this theory because of the high sensitivity of flow rates to slight changes in shearing stress (fig. 40).

The most significant objection to this method of computing the profile of a glacier is the change in lengths and thicknesses of a glacier in response to changing climate. The constant basal shear stress theory cannot account for any changes in profile with

time. Even if this method could be modified to produce consistent results when applied to present-day glaciers, it would disclose nothing about the relation of glaciers to their climatic environment. Therefore further pursuant of this method of calculation seems fruitless.

HYPOTHESIS FOR THE LONGITUDINAL PROFILE

A few comments on how a long profile might be calculated are offered. The Saskatchewan data reveal two significant facts that provide a starting point for this calculation: (1) the streamline shapes are determined only by the bed and (2) the velocity at the bed is a minimum.

Visualize a field of streamlines fixed in space above a certain longitudinal bedrock profile. As a first approximation, the plunge of the streamlines ξ is equal to the slope of the bed β. At any one vertical section the surface slope α must cut these streamlines at the proper angle $\alpha - \xi$ so that $\frac{V \sin (\alpha - \xi)}{\cos \alpha} = -V_d$. For an equilibrium condition, $V_d = -V_a$. However, V is determined by α, z, and the cross-section shape, and V_a is also a function of z. The mathematical difficulties treating all of these interrelationships analytically preclude a simple solution to the problem at this time. Furthermore, the form of the flow-law relation (equations 10*a*, *b*, *c* or *d*) must be clarified. When these interrelationships can be stated in a usable analytic form so that actual glacier profiles can be constructed, it will be possible to relate glaciers to their climatic environment in a quantitative manner.

STRUCTURAL FEATURES

Glacier ice first accumulates as a sedimentary deposit. It is then metamorphosed by flowage and other agents, causing secondary flow structures to be impressed on the primary sedimentary features. Structural features form continually in this deforming material, and are of great interest because they illustrate the formation of many structures which occur in deformed rocks. The following discussion is included for a different reason: A study of the features produced by flow lends insight into the flow process. Furthermore, if the relation of structures to flow geometry can be demonstrated in certain areas, the structures can be used to predict the flow geometry in other areas where no flow measurements have been made. Structural studies, therefore, are a useful adjunct to a thorough investigation of glacier movement.

As in some thoroughly metamorphosed schists, it is often difficult to differentiate primary from secondary structures in glacier ice. After 3 years of observation on Saskatchewan Glacier and several years of study on other glaciers, the author could distinguish between primary and secondary structures with confidence only about 50 percent of the time. Structural studies and interpretations were handicapped by this uncertainty. Differentiation was obtained by classifying features solely on the basis of orientation groupings.

Structures were mapped in a reconnaissance over the entire tongue of Saskatchewan Glacier (pl. 2*A*). A detailed map of structures at the terminus was constructed by planetable means (pl. 3). Structures were studied most intensively in the lower part of Castleguard sector because the geometry was relatively simple and the flow was best known, but even here the minute complexity of features on the surface of this large area (nearly a square mile) made it necessary to sample, not map, them. In order to eliminate appreciable bias, the attitude and general appearance of structures at many sampling points were recorded. Attitudes were measured by Brunton compass. In some areas of low relief, dips were difficult to measure, and an inaccuracy of less than $\pm 5°$ could not be obtained.

With few exceptions, all of the structures observed can be placed in these five main classifications:

Stratification.—A primary sedimentary layering inherited from the firn.

Foliation.—A secondary compact layered structure produced by deformation.

Cracks.—Secondary planes of weakness distinguished by noticeable separation of the two walls.

Faults.—Secondary planes of weakness distinguished by appreciable shearing movement parallel to the walls and little separation of the walls.

Fold axes.—A preferred orientation of fold axes was the only lineation observed.

STRATIFICATION

APPEARANCE

Primary layering in this glacier is most easily recognized close to the firn limit. Here it appears as gently dipping layers of loose, granular, partly reconstituted firn alternating with ice layers and lenses formed by freezing of percolating melt water (pl. 7*A*, *B*). The granular layers are much too thick (as much as 6 feet) and variable to be a product of shearing. Sedimentary layers can be identified with certainty as far as 3 miles below the firn limit and with less certainty within 3,000 feet of the terminus. The layering is most easily recognized from a high

A, STRATIFICATION EXPOSED AT THE SURFACE 3.0 MILES BELOW FIRN LIMIT

A prominent stratum runs from lower left-hand corner to center horizon, dipping in direction of ice axe. The photograph shows vertical foliation that extends diagonally from upper left to lower right intersecting the stratification

B, PROMINENT STRATUM EXPOSED SOUTH OF CENTERLINE IN MID-GLACIER, 2.1 MILES BELOW FIRN LIMIT

Outcrop trace appears as short-line segments; individual parts of the stratum dip in direction of ice axe (toward the south margin and slightly downglacier)

C, OUTCROP PATTERN OF STRATIFICATION IN CASTLEGUARD SECTOR

View upglacier from cliff on south margin below Castleguard Pass. Splaying and en echelon crevasses are also visible

509755 O - 60 - 6

distant vantage point (pl. 7*C*), where it appears as zones or alternating bands of grayish and white ice. In some areas this broad tone banding can be traced over the glacier surface by an observer on foot and is seen to coincide with the layering of coarse- and fine-grained ice mentioned above. In many places the outcrop of granular layers appears distinct because fine mineral debris collects in the fine-grained intergranular depressions whereas it is washed off the smooth surface of coarse-grained ice layers. In fresh exposures made by digging, the fine-grained granular layers do not seem to contain any more dirt than the adjacent layers of coarse ice. It seems likely, though not certain, that the dirty appearance of the granular layers is due to a surficial deposit of silt, secondarily acquired from wind or melt water. Very fine grained granular layers are less common toward the terminus and contrasts between the appearance of adjacent layers are also less marked downglacier. This is evidently due to recrystallization. Little evidence of a rhythmic or cyclic repetition of bands was found, and annual layers of deposition could not be recognized.

OUTCROP PATTERN

The outcrop pattern of this stratification resembles that of truncated beds in a plunging fold (pls. 2*A*, 7*C*). The bands are most conspicuous in Castleguard sector and gradually become indistinguishable downglacier and toward the margins. None has been recognized in the area between the firn limit and $x' = 3{,}000$, but evidence indicates that they may have been hidden by unconformable overlying layers.

The main apex of the "fold" lies in the middle of the glacier and points downglacier. Spacing and width of the bands are not uniform and the sharpness of curvature and axial length of the curves increases downglacier because of faster movement in the center.

Many of the measured attitudes in Castleguard sector imply that the sedimantary layering has the shape of an anticline plunging downglacier (pl. 7*B*, *C*) with respect to the glacier surface. Older ice, which underlies younger ice, crops out farther downglacier; therefore an upglacier dip with respect to the glacier surface is expectable (fig. 43). A possible explanation of this puzzling outcrop pattern is exceptional thinning in Castleguard sector that has truncated nearly horizontal beds causing a local downglacier dip of stratification in relation to the present surface. An alternative and equally plausible explanation is that the apparent anticline is due to a biased sampling of attitudes and is not real.

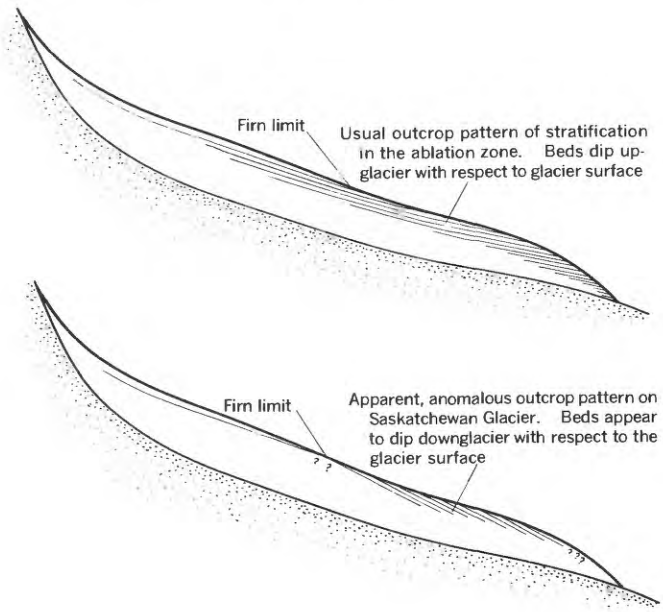

FIGURE 43.—Diagrammatic longitudinal sections of a glacier showing sedimentary layering.

Stratification here is nearly flat lying in broad aspect but highly wrinkled in detail and it is virtually impossible to measure the gross orientation from observations at a few points.

Although individual layers must crop out in broad zones that cross the glacier, stratification as seen on the glacier surface appears as discontinuous longitudinal lines (pl. 7*B*). This is apparently due to wrinkling parallel to longitudinal foliation. This change in outcrop pattern from transverse bands to longitudinal lines has been observed elsewhere (Kalesnik, 1939, p. 80). On Saskatchewan Glacier this wrinkling was probably formed when the broad sheets of firn from the Columbia Icefield were drawn through the narrow throat and into the valley occupied by the tongue.

FOLIATION

Much of the recrystallized surface ice of Saskatchewan Glacier shows a pronounced layered structure seemingly related to deformation. The name foliation is appropriate for this structure (Chamberlin and Salisbury, 1909, p. 247), and in this report the term will be restricted to compact secondary planar features caused by flow. In this sense, foliation may be identified with the "Feinbänderung" of Schwarzacher and Untersteiner (1953, p. 114–115), but prudence should be used in comparing it directly with banded structures in other glaciers described under diverse names such as "blue bands," longitudinal bands," "tectonic blue bands," "Bänderung,"

A, STRONG FOLIATION NEAR SOUTH MARGIN, 2.8 MILES BELOW FIRN LIMIT

Viewed upglacier. Foliation attitude is apparently conformable with valley wall to the left

B, GENTLY DIPPING STRATIFICATION, WRINKLED AND INTERSECTED BY NEARLY VERTICAL FOLIATION

Exposed on east wall of a crevasse, 2.8 miles below firn limit in midglacier

"Blätterung," "Pflugfurcheneis," "Druckschichtung," and "Scherflächen."

APPEARANCE

Foliation on Saskatchewan Glacier generally appears as alternating laminae of white bubbly ice and bluish clearer ice. Intercalated with these laminae are some thin layers of very fine grained, apparently brecciated ice. Locally, foliation is expressed by minor but abrupt differences in grain size. In some areas the foliated structure is obvious on either fresh or weathered surfaces (pl. 8*A*) and in such areas the thickness of individual folia is less than 1 inch. Over most of the glacier, however, foliation cannot be detected on a fresh ice surface and is only visible as a faint grain on the surface of weathered ice.

Many exposures show this layered structure as transecting (pl. 7*A*), wrinkling (pl. 8*B*), or offsetting (pl. 9*A*) other structures including primary stratification. In a few localities, however, the foliation appears to be truncated by sedimentary layering but these anomalous relations can be explained by differences in mechanical properties of adjacent ice layers. Shear strain in a mass of ice may form foliation in one layer by recrystallization and be taken up by undetectable intragranular movements in a less compact layer.

Criteria for differentiating foliation from primary stratification are presented in table 8.

TABLE 8.—*Criteria for distinguishing foliation from stratification*

Stratification	Foliation
1. Subtle, best seen from a high, distant vantage point. May not be visible in a close view.	1. Indistinct when viewed from a distance, usually obvious in a close view.
2. Contorted or obscured by shearing, and is therefore best observed in the middle of the glacier.	2. Definitely related to zones of great shearing and therefore strongest near margins and in medial moraines.
3. Layers generally not thin, but some ice layers 1 to 2 mm thick may be separated by much thicker layers of unrecrystallized firn.	3. Folia may be very close together (separated by less than a millimeter.
4. Layers may be obviously irregular or lenticular and less perfectly parallel.	4. Folia are generally planar and parallel except where secondarily contorted.
5. May include obvious structures inherited from the firn (ice lenses, glands).	5. Never includes ice lenses, glands, or other structures of the firn.
6. Usually recognizable on close inspection by contrasts in grain size, or by dirt content when viewed from a distance. Layers of fine-grained, loose grains (beds of only partially recrystallized firn) may be many feet thick.	6. Usually recognizable by contrasts in bubbliness of ice in adjacent folia. May also be grain size differences. Fine-grained, granulated ice only in very thin zones. Usually no conformable dirt.
7. Seldom causes other structures to be offset.	7. Often recognizable as a secondary structure by offsetting or transgressing other features.
8. Dips usually gentle except where severely contorted.	8. Attitude tends to parallel valley walls in strike and dip, hence steep.

OUTCROP PATTERN AND INTENSITY OF DEVELOPMENT

Foliation on Saskatchewan Glacier has a steeply dipping, longitudinal orientation (pl. 2*A*) except at the extreme terminus (pl. 3). Foliation parallels the valley wall at the margin, but dips are steeper in midglacier and nearly vertical dips predominate in the central third of the glacier. In Castleguard sector foliation dips about 75° toward the south margin in a strip 900 feet in from that margin. Folia are somewhat planar in the first 4 miles below the firn limit. Below that point the faint folia in midglacier are increasingly contorted (pl. 9*B*). Within 1,000 feet of the terminus the foliation forms a spoon-shaped structure dipping upglacier at a slight angle (pl. 3).

Foliation varies greatly in intensity of development, as expressed by closeness of spacing of folia, contrast in grain size, and contrast in bubble content across adjacent folia. Several degrees of foliation intensity are mapped in plate 2*B*. Foliation is most intense near the margins and along the medial moraine. Belts or zones of abnormally strong marginal foliation occur next to valley-wall bulges. These do not persist more than 1 mile below their apparent point of origin. Strongest foliation along the lower part of the medial moraine is in the tributary ice adjacent to but not under the moraine. In the upper part of Castleguard sector, however, foliation intensity is greatest under the center of the medial moraine. No difference in average foliation intensity across the glacier was detected from the upper part of Castleguard sector ($x' = 5{,}000$) to the terminus.

CRACKS

APPEARANCE

These planar structures are sharp discontinuities in the ice and they often have an air- or water-filled space between the walls. Some cracks are filled with ice crystals that have grown from the freezing of water that filled the crack after it had opened. These secondary "candle-ice" crystals are elongated perpendicular to the crack and are unlike ordinary glacier ice. It was easy to distinguish these features from foliation or stratification. Many cracks show shearing displacements. The strain on most of the surface of this glacier is strongly rotational (table 4), therefore all old cracks will show some shearing deformation. No effort was made to measure shear on open cracks or to classify them in this regard. Young closed fractures with appreciable shearing displacement are classed as faults and are discussed in the next section.

The cracks range in width from tiny, sharp fractures with openings of a millimeter or less

A, STRATFICATION(?) OFFSET BY FOLIATION
Viewed upglacier from a point 30 feet in from south margin, 2.5 miles below firn limit

B, FAINT CONTORTED FOLIATION, 0.8 MILE ABOVE TERMINUS, SLIGHTLY SOUTH OF CENTERLINE
Viewed downglacier. Foliation is nearly vertical and longitudinal in attitude. It appears as faintly wrinkled grain on the ice surface and trends directly away from the observer in the center of the field of view. Primary stratum crosses the field of view, dipping in the direction of the ice axe

C, EN ECHELON CREVASSE BELTS NEAR SOUTH MARGIN, 1.6 MILES BELOW FIRN LIMIT VIEWED NORTHWEST

("Haarrisse") to crevasses many yards wide. A distinction was made in the field between crevasses (more than 1 foot in width) and other cracks, but this distinction has no genetic or mechanical significance. The longest cracks extend for 1,000 feet; none less than about 20 feet was measured. Cracks are generally planar, although in the center of the glacier a few fractures of irregular shape were seen. The dip of cracks is almost invariably normal to the glacier surface. Crack depths were not measured.

PATTERN

The largest cracks (crevasses) form regular patterns on the glacier surface (fig. 44). Four different patterns are distinguished:

Splaying crevasses.—Crevasses having a longitudinal orientation in midglacier splay out toward the margin intersecting it at an angle slightly greater than 45° (fig. 44*A*). The apex of the acute angle at the margin always points downglacier. These crevasses are best displayed in Castleguard sector (pl. 7*C*). "Longitudinal crevasses," often mentioned in the literature, are merely splaying crevasses as observed in midglacier; true logitudinal crevasses cannot exist except along the centerline in a valley glacier.

Transverse crevasses.—These crevasses are convex upglacier and are normal to the flow direction in midglacier but curve to strike the margin at the same angle as splaying crevasses (fig. 44*B*). Where transverse and splaying crevasses occur together on a valley glacier they can be differentiated only in the central half. Transverse crevasses dominate a weaker pattern of splaying crevasses on and above the ice fall of the only tributary to Saskatchewan Glacier.

Chevron crevasses.—Straight crevasses (fig. 53*C*) extend from the margin toward the center of the glacier at a constant angle equal to the marginal acute angle mentioned under types (*A*) and (*B*). These do not extend to the centerline, and chevron crevasses from the two sides do not intersect. These crevasses are well formed just below Castleguard sector on Saskatchewan Glacier.

En echelon crevasses.—Short, wide crevasses ar-

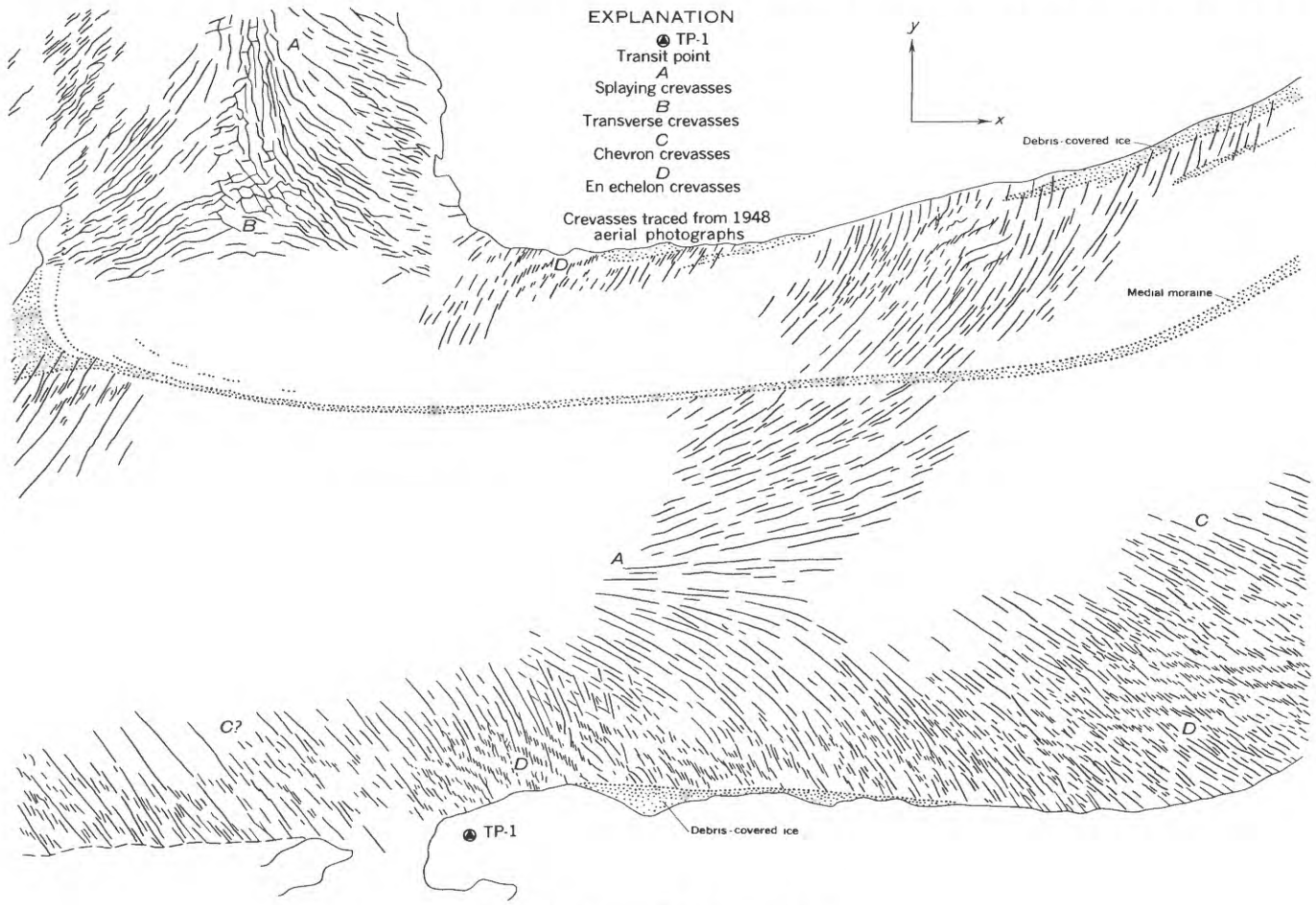

FIGURE 44.—Crevasses in Castleguard sector.

ranged in subequally spaced narrow belts (pls. 7*C*, 9*C*, fig. 44) are oriented en echelon. They are generally parallel in trend to one of the larger patterns. On Saskatchewan Glacier en echelon crevasses are best seen in three areas in Castleguard sector, where the narrow belts intersect the margin at acute angles of 20° to 35°.

In addition to the crevasses which form these different patterns, many minor cracks with apparently random orientation are seen on the surface of Saskatchewan Glacier. These define specific patterns, but a statistical approach must be used, and description of these features is postponed to the discussion of an area of detailed study.

FAULTS

Faults are fractures or discontinuities having noticeable shearing displacement and little or no normal separation of the two bounding blocks. They may be associated with the "Scherrisse" of the Alpine literature (Klebelsberg, 1948, p. 62–69). Left-hand strike-slip faults are common along the south margin just below Castleguard sector, where the glacier is shoved to the left by a curving valley wall. Most of the faults show horizontal displacements of a foot or less, and many of them also show slight dip-slip displacements (downglacier block had moved down). These are nearly vertical in dip and curve in strike from nearly parallel to the valley wall at the edge (the sharp acute angle pointed upglacier) to a nearly transverse orientation a few hundred feet in on the glacier. None could be traced farther. Other faults occur in Castleguard sector (pl. 3c).

FOLD AXES

Several types of linear structures, such as elongated grains and bubbles, have been observed in glacier ice (Schwarzacher and Untersteiner, 1953, p. 115). None of these is obvious on Saskatchewan Glacier, and the only lineation recorded is that formed by the axes of folds in contorted stratification. The plunge of these axes could not be measured except in fortuituous situations; consequently the nine measurements are too few to be statistically significant.

All measured fold axes plunge against the direction of flow, generally at angles much steeper (as much as 56°) than the velocity vector. Clearly, this lineation is not parallel to the direction of transport of the ice. Indirect evidence (the stratification outcrop pattern) suggests that the majority of fold axes near the flow centerline are nearly parallel to the glacier surface, but few measurements could be made. The lineation apparently lies in or near the plane of the associated foliation.

STRUCTURES OF CASTLEGUARD SECTOR

In order to study the myriads of small cracks and folia in an area where the surface deformation and flow conditions were known, structural information was obtained by a sampling technique in Castleguard sector. A total of 78 points were spaced at equal intervals (about 100 feet) on 3 transverse profiles extending from the south margin to within 800 feet of the medial moraine. All structures visible within about 20 feet of each point were measured. The total area covered was divided into three longitudinal strips (pl. 2*A*), one along the margin, one spanning the flow centerline and one covering the intermediate area. All measured structural attitudes from within each strip were collated onto an equal-area projection diagram (pl. 2*C*). No consistent differences in attitude could be detected by comparing data from the highest to the lowest transverse profile. Thus each of the three resulting diagrams shows the attitudes of structures within an area of reasonably uniform flow conditions. A similar plotting technique has been used by Untersteiner (1955, p. 504–505).

All observed structures were tentatively classified in the field as "crevasses," "cracks," "folia," "dirt layers," or "fold axes," and these field identifications have been indicated on plate 2*C*. However, with this method of plotting the distribution of orientation maxima can be studied without recourse to subjective identifications.

The density of points on each of these diagrams is contoured in order to bring out the various maxima more clearly (fig. 45). Orientation of the average velocity vector, surface strain-rate tensor and surface slope for each strip are also presented in figure 45.

These data show several clear maxima indicating preferred orientations of structural features. These preferred orientations can be followed with changing strain-rate tensor orientations from the margin to the centerline. The characteristics of each maximum are summarized in table 9.

The attitude diagram for the flow centerline shows orthorhombic, almost tetragonal, symmetry reflecting a symmetry of flow about the centerline. The diagram for the marginal strip is triclinic, almost monoclinic.

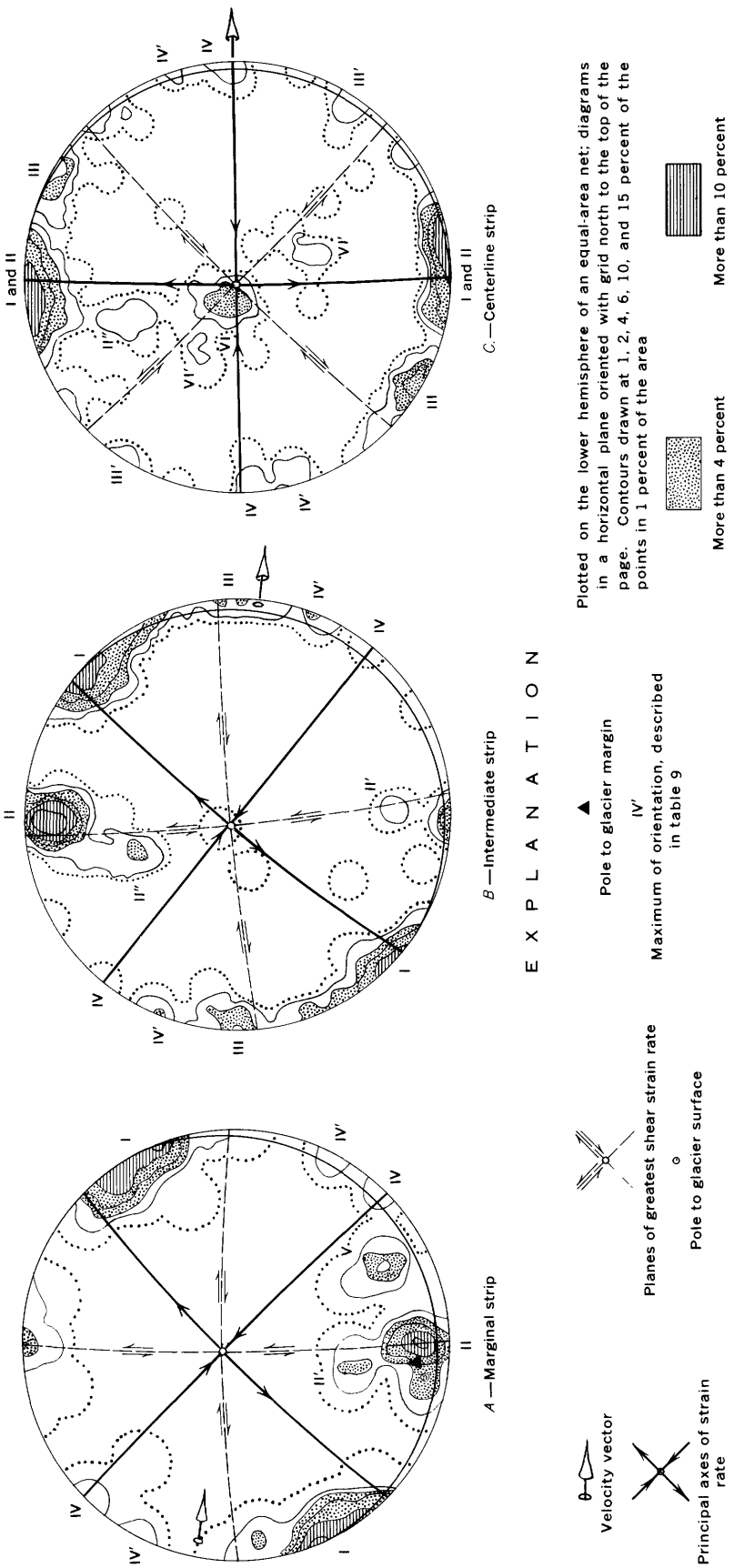

FIGURE 45.—Orientation of structural features in Castleguard sector.

ORIGIN OF TECTONIC FEATURES

FOLIATION

The origin of foliation has been a subject of considerable speculation. Recent studies have been made of the relation of crystal axes orientations to foliation (Bader, 1951; Rigsby, 1951; Schwarzacher and Untersteiner, 1953), but the results have been perplexing, and the mechanism of the origin of both this structure and the crystal orientations is still in doubt. On Saskatchewan Glacier additional important data (known strain geometry) was brought to bear on the problem, but only a few additional conclusions were forthcoming, as follows:

Foliation is related to shearing deformation.—This is evident from the warping or wrinkling of sedimentary layers (pls. 8*B*, 9*A*). Plunging fold axes that lay in the foliation plane (fig. 45*A*, *B*) also suggest a relation to shearing.

Foliation does not always form parallel to planes of greatest shearing strain.—The planes of maximum shearing strain rate intersect the principal strain rate axes at 45°. From symmetry considerations it is apparent that at the flow centerline one principal strain rate must always be directed along the centerline, both at the surface and at depth. Foliation which crops out on the surface at the plane of symmetry must have originated somewhere on that same plane of symmetry. Therefore the conclusion necessarily follows that foliation which stands parallel to a principal strain-rate plane where observed along the flow centerline could not have formed parallel to a maximum shearing strain-rate plane *either at its point of observation or at any logical place of origin.* Furthermore, there is no rotation so that planes of maximum shearing *strain* should not be different in orientation from the planes of maximum shearing *strain rate* along the flow centerline.

Further evidence suggests that foliation and maximum shearing strain-rate planes do not correspond. In the intermediate strip south of the centerline (fig. 45*B*) foliation dips to the south. The nearest plane of maximum shear stands approximately vertical at the surface, and at depth it must dip north in order to swing into approximate parallelism with the bedrock channel. Thus a discrepancy in attitude of the two planes is apparent.[11]

Feinbänderung on the Pasterze Glacier, which is apparently the same as foliation on Saskatchewan Glacier, seems to originate nearly perpendicular to the compressing principal strain-rate plane in midglacier (Untersteiner, 1954, table 1, profile 10, p. 238). Glen (1956, p. 740–742) observed a banded structure at the foot of an icefall in Norway that was within 5° of perpendicular to the compressing principal strain rate. Possibly the foliation in midglacier in Castleguard sector could have originated in this manner farther upglacier where a transverse compression occurred. However, this explanation does not apply to marginal foliation. It also seems unlikely that marginal foliation and midglacier foliation had different causes, because there was no evidence of any discontinuity in appearance or attitude.

Although it is not possible to state what actually

[11] This discrepancy may, however, be explained in another way: An icefall supplies ice to the south margin of the glacier below the normal firn limit. This ice is first superimposed (Sharp, 1948, p. 182) on the trunk glacier and its nearly horizontal stratification, but quickly sinks into the surrounding ice and becomes inset. Probably the preexisting stratification is bent down in the process to a steep south dip. Farther downglacier this relic stratification might be mistaken for foliation, or anisotropy due to the stratification might control the orientation of a later foliation. One argument against this is that the supply of ice from this icefall seems insufficient to account for such a large inset tributary.

TABLE 9.—*Characteristics of orientation maxima*

Designation	Strength	Orientation	Field identification	Comments on origin
I	Strong	Perpendicular to $\dot{\epsilon}$, *but smeared clockwise	Cracks and crevasses.	Chiefly tensile fractures. (This is the main crevasse system.)
II	...do	Very steep dip, parallel to **V** in strike, attitude essentially independent of strain rate tensor axes.	Folia and few dirt layers.	Not related to strain or stress tensor at point of observation. (This is the main foliation.)
II′	Moderate	Dip 45°–60°, parallel to **V** in strike, separated from II by 31°–40° rotation.	Folia	Apparently independent of strain tensor and related to II.
II″	...do	Dip 45°–50°, parallel to **V** in strike, separated from II by 36°–49° rotation in opposite sense from II′.	Folia, some dirt layers.	Do.
III	...do	Vertical, 45° to $\dot{\epsilon}_1$, missing in marginal strip	Cracks	Failure on planes of maximum shear almost perpendicular to the margin and foliation. Not developed in marginal strip becuase of restricting conditions at margin.
III′	Weak	Vertical, 45° to $\dot{\epsilon}_1$* (90° to III)	...do	Failure on other set of planes of maximum shear. Noticed only where not obscured by foliation.
IV	...do	Vertical, perpendicular to $\dot{\epsilon}_2$	...do	Plattungesbene? Or, cold weather construction cracks?
IV′	...do	Vertical, 15°–18° counterclockwise from IV	...do	Origin unknown, probably related to IV.
V	Strong	Strike N. 62° E., ** dip 67° N., appears only in marginal strip.	Folia and dirt layers.	Distorted primary stratification or a relic foliation? Origin unknown.
VI	Moderate	Almost parallel to surface, slight dip downglacier. Apparent only in central strip.	Dirt layers	Primary stratification.
VI′	Weak	Strike about N. 45° E., ** dip 20°–350° either north or south.	...do	Perhaps just a smearing out of VI by wrinkles with flat-lying axes.

* $\dot{\epsilon}_1$ = greatest (most extending principal strain rate.
$\dot{\epsilon}_2$ = least (most compressing) principal strain rate.
V = velocity vector.
** Strike referred to grid north (*y*-axis).

determines the orientation of foliation, recognition of the fact that foliation does not necessarily indicate plans of maximum shearing stress or strain rate may be an important step in the understanding of the mechanics of crystal axis orientation.

Foliation appears to form—or be preserved—only at shallow depths.—Maps of foliation attitude and intensity suggest that foliation forms only at shallow depths (pl. 2*A*, *B*). Had foliation been formed by shearing drag of the bed it would crop out as spoon-shaped surfaces crossing the flow centerline. No such folia were observed anywhere along the centerline except within 2,000 feet of the terminus where the ice is thin. Intense transverse compression probably would subsequently crumple the spoon-shaped surfaces to unrecognizable isoclinal folds, but it is difficult to find either a mechanism for this below the firn limit or evidence of such compression in the strain rate data or in crevasse arrangements. Additional evidence that foliation is not formed—or preserved—at great depth is offered by the belts of abnormally strong foliation which apparently disappear less than a mile below their point of origin.

This conclusion is in direct contradiction with the observation of Untersteiner that the Pasterze Glacier foliation (Feinbänderung), once formed, rode passively down the whole length of the tongue and could be identified even in the oldest ice of the terminus (Untersteiner, 1954, p. 239). Merrill (1956, p. 61), however, suggests that foliation in the northern Greenland icecap is easily obliterated by recrystallization and does not generally persist. Some of the petrofabric data from Pasterze Glacier suggest recrystallization at the surface (Schwarzacher and Untersteiner, 1953, p. 116), but presumably this has not been sufficient to obliterate the Feinbänderung.

If foliation forms or is preserved only at shallow depths, some change in the mechanical properties of ice with increasing hydrostatic pressure must be assumed. Such a change has been suggested repeatedly in the literature (Demorest, 1942, p. 36–37; Haefeli, 1948, p. 197), but it has also been challenged (Hess, 1937, p. 3–5; Nye, 1953, p. 489). The flow-law data from Saskatchewan Glacier show no effects that could be related to hydrostatic pressure (p. 44), and apparently no laboratory experiments have detected any influence of hydrostatic pressure on strain rates. Observations at points of local concentration of pressure and shearing strain beneath glaciers (Carol, 1947; Meier, 1951a, p. 112 and 1951b, p. 130–134) have shown that under these conditions ice can become so soft and "spongy" that a small mass curls and settles under its own weight. Laboratory experiments (Steinemann, 1954, p. 408) show that after a shearing strain of 10 to 20 percent a single ice crystal abruptly softens and remains soft, even after removal of stress, until recrystallized. This strain-softening behavior suggests a pronounced instability in the flow of ice and indicates the great effect of recrystallization on the flow.

A speculative mechanism for the origin of foliation is offered. Under an applied stress, ice begins to yield by plastic flow (grain boundary creep and intracrystalline gliding, see p. 45). Some local areas will strain more rapidly than others because of slight differences in grain shapes and orientations. When the critical strain necessary for crystal softening is reached in any small region, that region becomes locally a weak zone which tends to propagate by capturing more strain. These soft zones may grow most rapidly in a specific planar direction, so that layers of soft ice alternate with layers of hard ice, producing a foliated structure. The larger plastic strain in the soft ice may drive air bubbles into the neighboring ice, alter the grain sizes and shapes, and produce a preferred crystal axes orientation pattern. The soft layers need not be oriented parallel to the direction of maximum shearing strain and their orientation may be controlled by a minor prevailing anisotropy in the ice. The relative amounts of hard and soft ice which will exist at any one time in any one place will depend on (a) the total plastic strain, (b) the strain rate, and (c) the rate of recrystallization.

If the rate of recrystallization is a function of depth or hydrostatic pressure, a mechanism is produced for the observed distribution of foliation. If the rate of recrystallization increases with depth, at a critical depth it will be great enough to prevent the propagation of soft zones and the resulting ice will be homogeneous and unfoliated. If the rate of recrystallization decreases with depth, the zones of soft ice may increase to the point of eliminating all of the hard ice and the resulting ice will again be homogeneous and unfoliated. What determines recrystallization in glacier ice is not fully understood and it may be presumptious to assume that recrystallization rates vary with depth, but this seems to be the most reasonable explanation for the conclusion that foliation forms only at shallow depths.

MAIN CRACK SYSTEM (CREVASSES)

It is generally assumed that crevasses break at right angles to the greatest principal elongation or stress (Lagally, 1929, p. 293; Nye, 1952a, p. 90–91;

Untersteiner, 1955, p. 505). On the other hand, the fracture condition for metals (Nadai, 1950, p. 207–228), dry sand (Hubbert, 1951, p. 360–362), wind-packed snow (Haefeli, 1948, p. 681), and granitic rocks (Robertson, 1955, p. 1295–1304) involves both normal and shearing stresses. Data from northern Greenland (Meier, 1956) suggest that crevasses in firn form at an angle to the greatest principal elongation rate in an environment where the other principal strain rate is compressing.

As shown on figures 45 and 46, the cracks and crevasses on Saskatchewan Glacier approach but do not exactly coincide in attitude with the principal axes of strain rate. However, four effects mitigate against a direct comparison: (a) after a crevasse forms it is rotated passively in the deforming ice until it has melted out and disappears;[12] (b) the ice is somewhat anisotropic owing to foliation near the margins; (c) minor differences in stress or strength environments cause some variation in fracture orientations; and (d) the measured principal strain rate orientations in midglacier are not precise (see p. 35).

The results from this study of cracks and crevasses in a limited area can be extended qualitatively to all crevasse patterns. The following method of analysis is similar to that used by Hopkins (1862) and Nye (1952a, p. 89–91). In order to explain a crevasse pattern, the stress distribution on the surface must be described.

The splaying crevasses in Castleguard sector indicate transverse tension at the flow centerline. This is probably caused by transverse expansion of the glacier after passing a constriction in the channel at $x' = 6{,}000$. The margin of a glacier must be identified with a plane of greatest shearing stress so that the principal stresses must swing to a nearly 45° orientation at the margin. Crevasses may be of any orientation in midglacier but toward the margin a shear stress parallel to the valley wall must be dominant and crevasses will intersect the margins diagonally. In Castleguard sector this changing orientation of principal stress and strain-rate axes can be followed from the centerline to the margin both in the Mohr's circle constructions (fig. 32) and the map of principal strain rate trajectories (fig. 34).

[12] The effect of rotation can be estimated by the following sample computation at $y = 1{,}000$, $x = 7{,}000$. The greatest elongating strain rate here is 0.052 per year. This would cause crevasses to form to a depth of 31 feet according to a formula suggested by Nye for temperate ice (Nye, p. 513) and approximately cofirmed by field measurements in polar ice (Meier, 1956). After removal of stress these crevasses would have a life of 3.3 years under the measured rate of ablation. The rotation rate measured here was 0.039 radians per year. Therefore, if a crevasse formed instantly and was not widened further, it would be rotated through about 7.3° before disappearing.

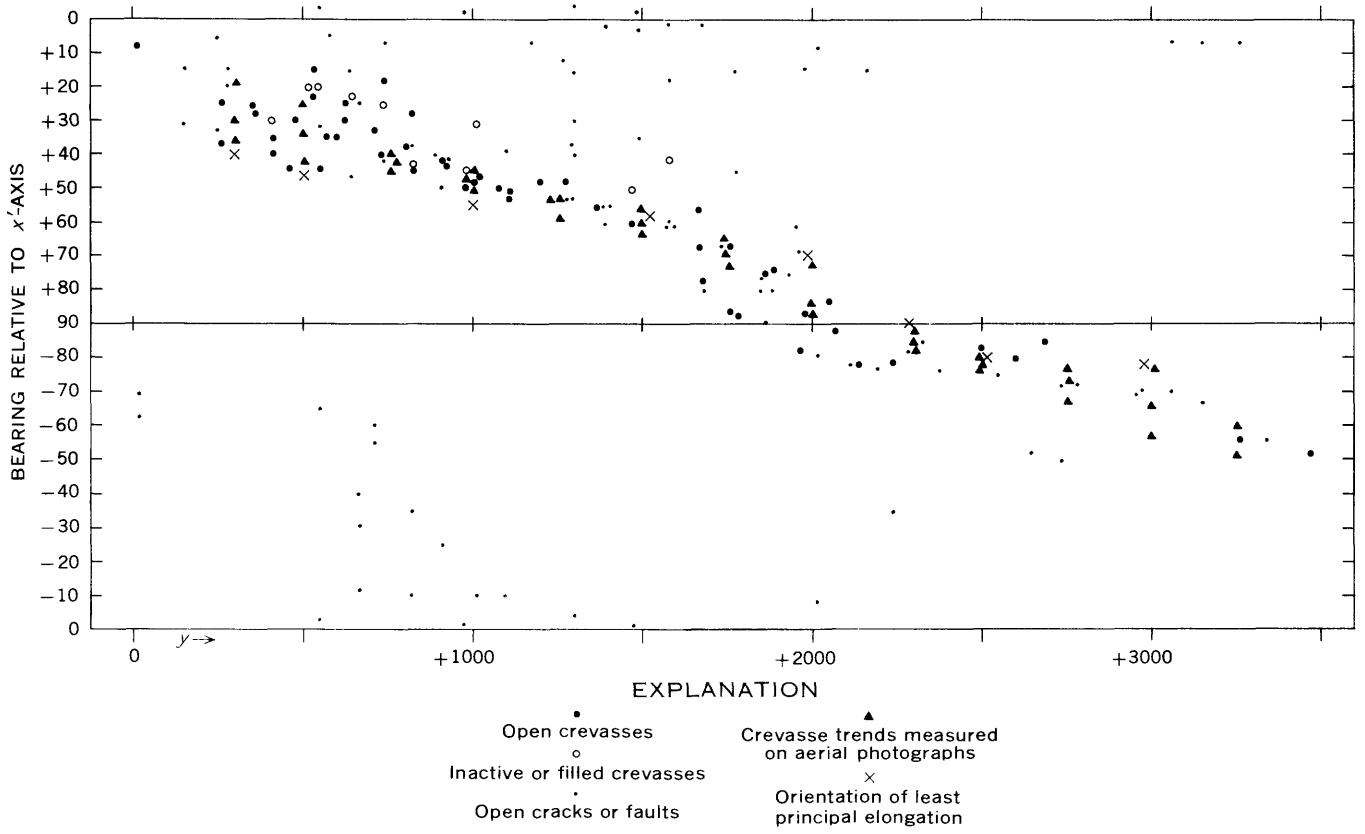

FIGURE 46.—Crevasse and open-crack orientations as a function of transverse location.

The transverse tension which causes splaying crevasses on the icefall of the only tributary glacier (fig. 44) must be due to a different mechanism because here the glacier's boundaries do not diverge. The upper reach of this ice stream is confined in a broad valley but the lower half flows in an unconfined course down the steep wall of the trunk valley; in effect it becomes a "wall-sided glacier" (Ahlman, 1940, p. 192). This probably causes a transverse spreading of the surface on the lower half, forming splaying crevasses.

Transverse crevasses on the icefall of this tributary glacier (fig. 44) indicate a longitudinal principal tension at the centerline. This is caused by the convex longitudinal bed profile. These transverse crevasses intersect the margin at the same angle as playing crevasses, and for the same reasons as given above.

Both transverse and splaying crevasses occur in midglacier on this tributary icefall, so both principal stresses must be tensile there. This condition can generally exist only in midglacier: the pure shear component introduced by marginal shear will cancel one of the principal tensions along the sides of the glacier. Intersecting crevasses, then, must be rare along glacier margins except where the stress field is greatly warped. The longitudinal tension is apparently stronger than the transverse tension on the centerline of the tributary icefall, because the transverse crevasses are dominant and continuous and the splaying crevasses die out near the margin.

The third major crevasse type—chevron crevasses —are related to pure shear caused by the drag of the valley walls. These crevasses indicate that the principal stresses are either zero or exactly equal. This stress field is probably rare.

The last, and most unusual, type of crevasse pattern which must be explained are en echelon crevasses. These indicate the intersection of two crevasse patterns or trends, but the crevasses do not intersect for the reasons given above. In echelon crevasses the stress field at depth must be strongly warped so that continuous surfaces cannot be formed that are everywhere perpendicular to the axis of principal tension. This is a general property of stress fields in three dimensions (Lagally, 1929, p. 294–295), and it must be assumed that long, even crevasses (such as the splaying crevasses in Castleguard sector) indicate little change in stress with depth except for the addition of hydrostatic pressure.

En echelon fractures have been commonly assumed in the geological literature to indicate a major shear at depth. The crevasse bands on Saskatchewan Glacier, however, are not parallel to a direction of great shearing strain but are more nearly parallel to a direction of principal elongation.

The en echelon crevasse pattern along the south margin at $x = 6{,}000$ (pl. 9*C*, fig. 44) suggests that the stress field at depth is oriented so as to produce splaying crevasses at the surface. The stress field at the surface is different and suggests chevron crevasses generated at the margin which intersect it at a steeper angle. These chevron crevasses are evidently related to the nearly vertical bulge in the valley wall. Irregular surfaces perpendicular to the suggested principal tension axes (fig. 47) would outcrop on the surface with a pattern similar to that of the en echelon crevasses. The crevasses seem to be twisted at depth in the manner shown in figure 47.

SIGNIFICANT FINDINGS

The flow of Saskatchewan Glacier was studied from several viewpoints. The velocity of the ice at points on the surface was measured both in regard to spatial configuration and to variation in time; some information was obtained on the change of velocity with depth along a shallow borehole; and studies were made of the structures produced by flow. In addition, the bedrock and ice and surface topography was measured and ablation data were obtained. Although measurement of these items over the entire glacier surface was not possible, the sampling of data was adequate to define the velocity and deformation fields and the structural patterns on the surface. Consequently Saskatchewan Glacier is the first glacier in the Western Hemisphere for which sufficient data were collected to provide a valid basis for conclusions on flow law, discharge at depth, and geometry of flow. The following conclusions are of the greatest significance:

1. Saskatchewan Glacier in the years 1952–54 showed a type of behavior which might be described as "constant unbalance." It was not in equilibrium because the surface was lowering, but the lowering proceeded at a nearly constant rate in time and space. The rate of lowering from terminus to firn limit was remarkably uniform (parallel downwasting). Furthermore, the discharge of ice through a high cross section was the exact amount to keep the rest of the tongue thinning at the prevailing rate. Thus there was no suggestion of any forthcoming change in the glacier's behavior.

2. Velocity measured at any one point depends on the time interval of observation. Very little time

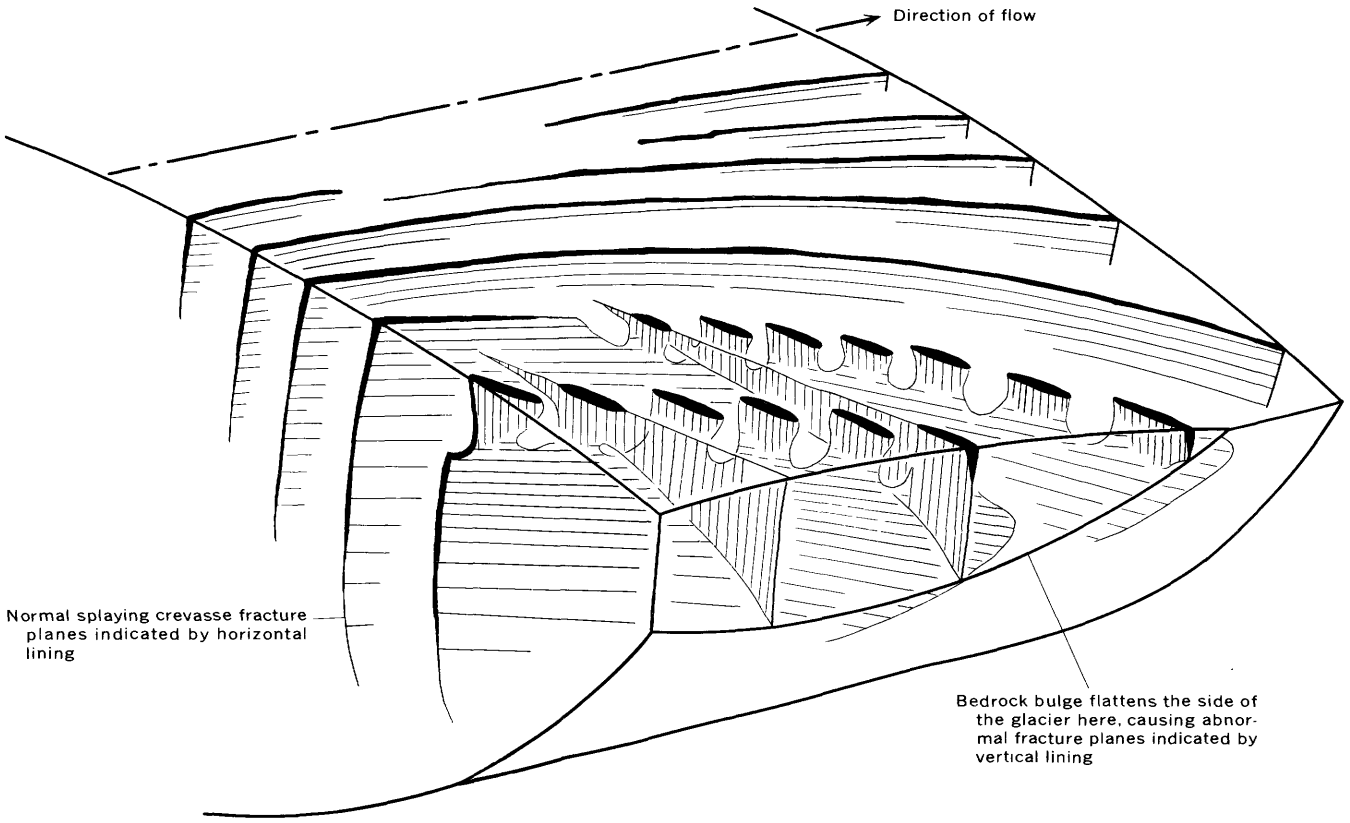

FIGURE 47.—Phantom view of part of Saskatchewan Glacier showing possible fracture planes leading to formation of en echelon crevasses at the surface.

variation can be detected in the velocity field over a long period except for a slight deceleration due to thinning. However, erratic fluctuations are noticed when velocity readings are made at shorter and shorter intervals. Fluctuations of more than 100 percent of the average velocity are not uncommon in measurements made over 12-hour intervals. The size of the fluctuations is inversely proportional to the logarithm of the time interval of measurement. It is suggested that the total flow is built up from many minor jumps or jerks along shearing planes; it is probable that the jerkiness is not due to the erratic opening or closing of crevasses.

3. The absolute value of velocity decreases down-glacier along the centerline and toward the margins. This causes a prevailing compressing strain rate in a longitudinal direction along the centerline which near the edge is outweighed by a shearing strain rate parallel to the margin. Thus, one principal axis of strain rate parallels the centerline at the centerline, and both principal strain-rate axes intersect the margin at 45°. Generally there is a component of velocity toward the margins. This prevailing deformation pattern is locally modified in the upper part of Castleguard sector: a flux of ice in from the margins and a slight constriction in the channel makes the velocity vectors converge in map view, causing a transverse compression and a longitudinal extension in spite of reverse slope in the bedrock channel and very low surface slope. Thus the amount of extending or compressing flow along the centerline is sensitive to changes in width. The orientations of the principal axes of strain rate are computed from known velocity gradients, and the results are checked against the orientations of crevasses.

4. A component of velocity (V_d) is defined which represents the rise or fall of the ice surface which would take place if there were no accumulation or ablation. This tendency for the elevation of the surface to change is due solely to translational and deformational motions of the ice. If the glacier is in equilibrium, V_d is equal in magnitude but opposite in direction to the surface accumulation or ablation V_a averaged over a year's time. The response, or state of health, of a glacier at any instant is given by the difference between V_a, which is a function only of the current climate, and V_d, which is a function only of the glacier's current dimensions.[13] Thus V_d is a

[13] In the case of polar and subpolar glaciers this statement is not true because the prevailing climate has an important effect on the thermodynamics of the flow process, and therefore on V_d. This effect probably is not important in the case of temperate glaciers such as the Saskatchewan because the temperature distribution within the bulk of the glacier is virtually unchanging with time.

509755 O - 60 - 7

factor of greatest significance in any study of the response or adjustment of a glacier to its climatic environment. The component V_d was also shown to be useful for computing discharge and velocity distribution at depth.

5. The flow law (shear strain rate as a function of stress) of ice was investigated using data compiled from Saskatchewan Glacier and other sources. The results show that:

(*a*) Hydrostatic pressure has no appreciable effect on the flow law relation.

(*b*) There is a transition in behavior from a nearly viscous flow at low stresses to a plastic flow at high stresses; the transition occurs at a stress of about 0.7 bar. Glen's formula for creep does not apply at low stresses.

(*c*) Probably two mechanisms of flow operate simultaneously. At low stresses the flow may take place largely by grain-boundary creep; at high stresses intracrystalline gliding may predominate.

6. Streamlines of flow on a plane along the centerline generally parallel the bedrock. This suggests that the longitudinal profile of a glacier tends to adjust itself so that V_d (determined by the depth, surface slope and streamline slope) just balances the ablation at each altitude. This hypothesis has not yet been stated in usable form. Considerable research effort along these lines is justified because determination of the longitudinal profile is the important link to an understanding of glaciers as climatic indicators, and because existing schemes of calculation (such as the constant basal shearing stress theory) lead to wrong or unusable results.

7. Several different types of structures can be distinguished in the ice of Saskatchewan Glacier. The following three structures are of greatest interest to this study of flow:

(*a*) Primary stratification, a planar structure inherited from the firn, rides passively down the tongue until obliterated by deformation or recrystallization.

(*b*) Secondary foliation, a planar tectonic structure formed by shearing, is sometimes difficult to distinguish from primary stratification because both structures are manifest by differences in grain size or ice texture. Foliation seems to form, or to be preserved, only near the surface and could not always be related to planes of maximum shearing strain. Foliation may be due to local zones of intense plastic flow separated by zones that are only slightly strained because ice exhibits strain-softening behavior. Recrystallization probably has an important influence on its formation, and the fact that recrystallization rates may be a function of depth might explain the lack of foliation in basal ice. The origin of foliation is still an unsolved problem, and much remains to be done. This problem is closely related to the problem of defining and explaining the flow-law relation.

(*c*) Cracks of several types were recognized. The major crevasse systems are related in orientation to the greatest principal strain rate although there is some suggestion of slight differences in angle. Several minor crack systems are related to planes of greatest shearing strain rate, and in one surprising case to the axis of least (most compressing) strain rate. Cracks can be of great value in determining stress and strain-rate axes orientations.

ACCURACY OF THE VELOCITY DATA

Two important questions should be asked about this, or any other, method of glacier velocity measurements: First, how exact are the final velocity data as indicators of the actual ice motion at the time? Secondly, how exact are the true average velocities measured for a certain time interval as indicators of the average ice motion for a different time interval? In order to answer the first question a series of tests was made on the reproducibility of the instrumental and computational methods; in answer to the second question, observations were made on the variation of the velocity field with time. (See table 10.)

In 1952 the velocity stations were surveyed using a 20-second engineers transit; horizontal angles were generally repeated four times and vertical angles read in both erect and inverted positions of the telescope. In 1953 and 1954 a T2 1-second optical theodolite was used; horizontal and vertical angles were generally read twice by two operators.

The survey data were analyzed three different ways:

(1) For all stations with reliable triangulation information, coordinate locations were determined once or twice each summer using 8-place trigonometric tables (or rarely, 6-place logarithms). From these data and the resetting data, velocity components parallel to the coordinate axes were readily obtained.

(2) For these same stations, velocity components at shorter intervals (½ day to 1 month) were obtained by computations of slide-rule accu-

racy, using increments of arc and assuming that the stake moved along the path found by the precise calculation.

(3) Insufficient data were available from some stakes to define accurately the direction of travel. For these, a direction was assumed by reference to nearby stakes, and calculation was done to slide-rule accuracy. Transverse velocity profiles were generally arranged directly opposite transit points, so that lack of information on the direction of ice motion would have minimum effect on computed longitudinal and vertical components of velocity.

Precision of measurement is determined by the accuracy of setup, pointing, reading and the inherent precision of the instrument; stability of instrument, transit point and sighting point; varying atmospheric refraction; resetting measurement precision; computational precision and accuracy; and human errors.

In order to determine the precision of the horizontal measuring procedure, a fixed angle between two bedrock points on the north side of the glacier was measured from a transit point on the south side. One line of sight barely grazed the flat surface of the glacier so that atmospheric effects would have a large influence on the results. The instrument (T2) was enclosed in a tent for protection against wind and direct sunlight, in the same manner as was used for a series of short-interval measurements in 1953. The fixed angle was measured 50 times by different operators under what was believed to be a representative sampling of different weather conditions and with several setups. The results, therefore, reflect the combined effects of instrumental error, precision in setup, sighting and reading, and atmospheric refraction. The data when plotted on arithmetic probability paper (fig. 48) show a normal error distribution with a standard deviation of angle of 3.0 seconds. This value is of the same order of magnitude as the reproducibility of pointing and reading the instrument, suggesting that other errors have negligible influence. From these data and tests of the reproducibility of readings with other setups, it is assumed that the probable angular error (0.67 times the standard deviation) of measurement ranges from about 6 seconds for the unshielded engineer's transit to 2 seconds for refined measurement with the T2. The probable error in locating the instrument horizontally over a point is negligible for the T2 (0.005 to 0.01 foot) but reaches a maximum of 0.05 foot (or more in a very high wind) for the transit.

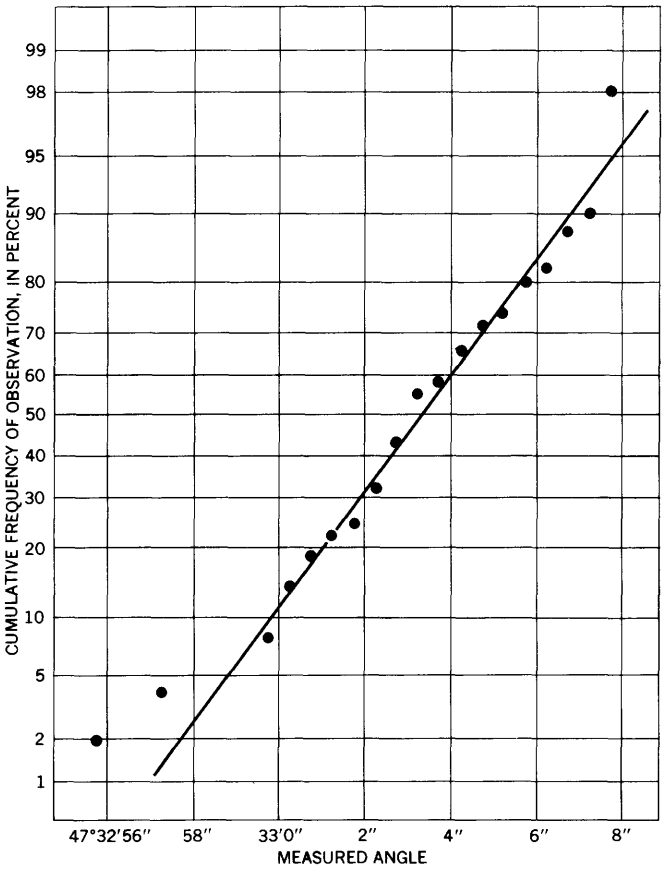

FIGURE 48.—Error distribution for 50 measurements of a fixed angle.

On this basis the probable error in longitudinal horizontal location for stations in midglacier ranges from about 0.05 to 0.7 foot, depending on the instrument used and the refiement of measuring procedure. For these same stakes the probable error in transverse location is estimated to range from 0.2 to 1.2 foot. Longitudinal locations are much more precise and transverse locations slightly more precise for stakes near the margin.

Vertical locations are less accurate. Changing atmospheric refraction and poor reproducibility of measuring vertical angles with the transit causes great variability of results; errors from all other causes are relatively negligible. Comparison between stake locations, measured simultaneously from two transit stations and elevations determined on successive days from the same station, suggested that the probable error in vertical location may have been as great as 1 foot for many stations. This was an appreciable fraction of the yearly vertical movement for some stations.

Other sources of error in location or velocity are difficult to evaluate. Some transit points on old moraines may have moved, but no suggestions of

such movement appears in the data, and a precise experiment to measure movement of TP–6 in 1952 gave completely negative results. Some stakes, after considerable ablation, were visibly vibrating in the wind at the time of observation, but it is not likely that an error greater than 0.1 foot was caused by this. Measurements made of the new positions as stakes were reset were generally as accurate as the surveyed locations. However, in 1953 the field party failed to record this information, completely or in part, for several stakes in the 8, 3 and 6 series. In a few places the missing information was obtained by surveys just before and just after resetting; in other places the data had to be estimated causing an error of up to 3 feet in location. Those data were discarded in which lack of resetting measurements caused an uncertainty in the velocity values of more than a few percent, and all other data with appreciable uncertainty are so specified. Computational precision was kept within the limits of instrumental inaccuracy, and the possibility of undiscovered human error in the triangulation computations was eliminated by a double calculation scheme.

In general, it is assumed that the yearly velocities reported here are correctly measured to within 1 fpy for the horizontal component and 2 fpy for the vertical component, unless otherwise specified. Summer and short-interval velocities were not as accurate. Actually, the inaccuracy of measurement of horizontal velocity over a summer's or year's time is only a negligible fraction of the probable error introduced by assuming that that measurement is representative of the mean velocity over a longer period of time.

TABLE 10.—*Coordinates of velocity stakes*

Stake	Date	x	y	z
17–5	Aug. 29, 1953	1,300 ±5	3,898 ±5	8,237 ±2
4	....do	2,160 ±5	2,305 ±5	8,263 ±2
3	....do	727 ±5	2,219 ±5	8,125 ±2
2	....do	221 ±5	2,991 ±5	8,097 ±2
1	....do	856 ±5	2,908 ±5	8,070 ±2
8–10	....do	1,570 ±10	1,584 ±5	7,860 ±2
9	Sept. 3, 1953	4,080.0	2,371.4	.....
9	Sept. 3, 1953	4,080.0	2,371.4	.....
8	Aug. 12, 1952	4,603.0	3,723.0	7,709.0
	Aug. 10, 1953	4,788 ±1	3,672 ±1	7,697 ±1
	Aug. 7, 1954	4,999.9	3,629.9	7,683.2
7	Aug. 12, 1952	4,615 ±5	3,370 ±10	.....
6	....do	4,650 ±5	3,148 ±5	7,680 ±5
	Aug. 29, 1953	4,887.7	3,143.0	7,667.2
	Aug. 7, 1954	5,112.0	3,140.7	7,658.6
4	Aug. 12, 1952	4,720 ±5	2,229 ±5	7,647 ±5
	Aug. 29, 1953	4,976.6	2,240.3	7,636.1
	Aug. 7, 1954	5,208.2	2,252.2	7,629.0
3	Aug. 12, 1952	4,774.2	1,593.0	7,673.5
	Aug. 29, 1953	5,039.2	1,613.0	7,649.6
	Aug. 7, 1954	5,264.2	1,625.9	7,642.2
2	Aug. 12, 1952	4,801 ±1	1,238 ±1	7,682 ±5
	Aug. 29, 1953	5,042.6	1,247.3	7,662.1
	Aug. 7, 1954	5,260.8	1,265.8	7,653.2
1	Aug. 12, 1952	4,837 ±2	258 ±5	7,684 ±2

TABLE 10.—*Coordinates of velocity stakes*—Continued

Stake	Date	x	y	z
3–12	July 8, 1952	6,102 ±2	899 ±2	7,639 ±2
11	....do	6,968 ±2	637 ±2	7,499 ±2
	July 7, 1952	6,981 ±2	636 ±2	.....
10	Aug. 17, 1952	6,898 ±2	4,070 ±5	7,497 ±2
9	....do	7,024 ±5	3,448 ±5	.....
8	....do	7,043 ±2	3,401 ±5	7,501 ±2
	Aug. 10, 1953	7,272.9	3,419.3	7,515.4
7	Aug. 17, 1952	7,054 ±5	3,356 ±5	.....
6	....do	7,100 ±5	3,078 ±5	7,506 ±2
	Aug. 10, 1953	7,338.2	3,093.7	.....
5	....do	7,551.0	2,612.7	7,506.7
4	July 8, 1952	7,474.3	1,759.7	7,526.4
	July 31, 1952	7,491.5	1,759.8	.....
	July 29, 1953	7,731.2	1,749.5	7,500.3
	Aug. 7, 1954	7,979.3	1,743.3	7,487.0
3a	Aug. 26, 1953	7,602 ±10	980 ±5	7,456 ±2
	July 29, 1953	7,782.6	980.1	7,449.9
	Aug. 7, 1954	7,993.8	961.9	7,439.4
3	Aug. 8, 1952	7,600 ±5	583 ±5	7,432 ±2
2	....do	7,597 ±5	356 ±10	7,423 ±2
1	....do	7,589 ±5	262 ±15	7,409 ±2
5–4	....do	8,640 ±20	2,600 ±10	7,473 ±5
3	....do	8,660 ±20	1,780 ±10	7,459 ±5
2	....do	8,760 ±10	530 ±10	7,396 ±2
1	....do	8,770 ±10	280 ±10	7,360 ±2
6–8	July 25, 1953	11,189.8	2,035.0	7,281.6
	Aug. 31, 1953	11,211.4	2,039.6	7,281.2
	Mar. 5, 1954	11,381.6	2,070.0	7,279.0
6–7	Aug. 26, 1952	10,064.0	2,996.1	7,354.0
	July 28, 1953	10,235.0	3,013.9	7,341.1
	Aug. 31, 1953	10,257.1	3,017.8	7,339.8
	Aug. 5, 1954	10,437.1	3,039.4	7,335.3
6	Aug. 26, 1952	9,661.8	2,268.5	7,372.8
	July 28, 1953	9,858.8	2,272.0	7,354.4
	Aug. 5, 1954	10,076.5	.....	7,342.6
4	Aug. 26, 1952	9,903.8	1,841.7	7,339.0
	July 28, 1953	10,088.9	1,844.3	7,329.5
	Aug. 31, 1953	10,109.9	1,845.1	7,328.6
	Aug. 5, 1954	10,304.3	1,862.4	7,324.8
3	Aug. 26, 1952	9,958.7	966.5	7,331.8
	July 28, 1953	10,119.6	974.6	7,321.4
	Aug. 31, 1953	10,137.9	960.2	7,322.9
	Aug. 5, 1954	10,284.5	953.9	7,326.0
2b	July 5, 1953	9,612.9	434.5	7,327.3
	Aug. 31, 1953	9,615.8	431.9	7,320.6
	Aug. 5, 1954	9,708.1	416.1	7,327.8
2	Aug. 26, 1952	9,968.0	458.8	7,320.8
	July 28, 1953	10,059.3	438.6	7,308.0
	Aug. 31, 1953	10,077.0	440.1	7,303.4
	Aug. 5, 1954	10,167.7	423.0	7,309.5
2a	July 7, 1953	10,535.0	398.5	7,289.8
	Aug. 31, 1953	10,551.9	397.0	7,284.0
	Aug. 5, 1954	10,632.0	384.5	7,290.6
1	Aug. 26, 1952	9,983.4	253.1	7,304.0
	July 28, 1953	10,061.8	239.6	7,291.5
	July 28, 1953	10,074.4	231.3	7,288.5
	Aug. 5, 1954	10,134.1	215.1	7,295.9
15–2	July 25, 1953	12,881.1	2,787.0	7,194.2
	Aug. 5, 1954	13,028.5	2,862.3	7,190.2
1	July 25, 1953	13,247.4	1,055.2	7,211.8
	Aug. 5, 1954	13,314.1	1,076.5	7,210.5
14–5	July 9, 1953	17,085.7	5,853.6	6,847.6
	July 14, 1954	17,204.2	5,900.3	6,835.8
4	July 9, 1953	20,187.8	7,463.0	6,626.0
	Aug. 28, 1955	20,192.9	7,456.0	6,617.3
	July 14, 1954	20,274.5	7,494.8	6,613.5
	July 24, 1954	20,276.2	7,514.4	6,613.4
3	July 9, 1953	18,711.3	6,686.6	6,753.0
	July 14, 1954	18,819.2	6,726.4	6,741.0
2	July 9, 1953	19,453.1	5,452.0	.....
	July 14, 1954	19,544.2	5,488.2	6,710.0
1	July 9, 1953	19,619.8	5,151.4	6,711.8
	July 14, 1954	19,697.7	5,183.2	6,694.1
12–5	July 5, 1953	25,591.4	8,838.8	6,104.6
	Aug. 26, 1953	25,595.6	8,839.9	6,094.6
	July 24, 1954	25,627.0	8,847.8	6,085.0
	Aug. 12, 1954	25,631.6	8,848.2	6,084.2
4	July 5, 1953	26,089.3	8,925.7	6,044.6
	Aug. 26, 1953	26,090.7	8,927.9	6,037.7
	July 11, 1954	26,113.2	8,937.4	6,024.7
	July 24, 1954	26,114.4	8,937.5	6,024.8
	Aug. 12, 1954	26,119.0	8,939.6	6,023.8
3	July 5, 1953	26,530.8	8,983.9	5,972.3
	Aug. 26, 1953	26,530.8	8,984.4	5,960.9
	July 11, 1954	26,545.3	8,990.8	.....
	July 24, 1954	26,545.3	8,991.0	5,952.9
	Aug. 12, 1954	26,551.6	8,989.7	5,951.6
2	July 5, 1953	26,792.8	9,032.8	5,925.7
	Aug. 26, 1953	26,790.2	9,025.9	5,912.7
	July 11, 1954	26,786.0	9,031.0	5,908.2
	July 24, 1954	26,786.6	9,031.2	5,908.2
	Aug. 12, 1954	26,789.5	9,031.1	5,907.8

The data obtained from inclonometer surveys of the boreholes are presented in table 11.

TABLE 11.—*Inclination data for boreholes*

Borehole	Date of survey	Depth below top of pipe (feet)	Inclination from vertical	Direction
1	Aug. 6, 1952	25	1°55′	S. 86° E.
		50	0°50′	S. 85° E.
		75	0°30′	S. 90° E.
		100	1°45′	N. 14° E.
		125	1°20′	N. 17° W.
		151	1°05′	N. 15° E.
		[1] 151.8		
1	Aug. 5, 1954	0	2°05′	S. 76° E.
		25	1°20′	S. 90° E.
		50	0°50′	S. 60° E.
		75	0°45′	N. 05° E.
		100	1°40′	N. 10° W.
		125	[1] 1°35′	[3] N. 50° W.
		132	0°35′	N. 25° W.
		138	(4)	
2	Aug. 4, 1954	5	0°05′	N. 60° W.
		50	0°45′	S. 75° E.
		100	0°30′	S. 75° E.
	Aug. 5, 1954	150	0°20′	S. 90° E.
		200	0°30′	N. 70° E.
		238	0°10′	S. 65° E.
		[1] 238.5		

[1] Bottom of hole.
[2] ±10′
[3] ±10°
[4] The change of length of borehole 1 was due to the removal of sections from the top as ablation progressed.

REFERENCES CITED

Ahlmann, H. W., 1940, The relative influence of precipitation and temperature on glacier regime: Geog. Annaler, v. 22, p. 188–205.

——— 1948, Glaciological research on the North Atlantic coasts: Royal Geog. Soc., Res. ser. 1, 83 p.

Allen, C. R., and Smith, G. I., 1953, Seismic and gravity investigations on the Malaspina Glacier, Alaska: Amer. Geophys. Union Trans., v. 34, p. 755–760.

Bader, Henri, 1951, Introduction to ice petrofabrics: Jour. Geology, v. 59, p. 519–536.

Battle, W. R. B., 1951, Glacier movement in northeast Greenland: Jour. Glaciology, v. 1, p. 559–563.

Bjerrum, Niels, 1952, Structure and properties of ice: Science, v. 115, p. 385–390.

Bruce, R. J. M., and Bull, Colin, 1955, Geophysical work in north Greenland: Nature, v. 175, p. 892–893.

Carol, Hans, 1947, The formation of roches moutonnées: Jour. Glaciology, v. 1, p. 57–59.

Chamberlin, R. T., 1928, Instrumental work on the nature of glacier motion: Jour. Geology, v. 36, p. 1–30.

Chamberlin, T. C., and Salisbury, R. D., 1909, Geology: v. 1, New York, Henry Holt and Co., 684 p.

Cottrell, A. H., 1953, Dislocations and plastic flow in crystals, Oxford, Oxford Univ. Pres, 223 p.

Demorest, Max, 1938, Ice flowage as revealed by glacial striae: Jour. Geology, v. 46, p. 700–725.

Demorest, Max, 1942, Glacier regimens and ice movement within glaciers: Am. Jour. Sci., v. 240, p. 31–66.

——— 1953, Processes of ice deformation within glaciers: Jour. Glaciology, v. 2, p. 201–203.

Drygalski, E. V., and Machatschek, Fritz, 1942, Gletscherkunde (Glaciology): Enzyklopädie der Erdkunde, Vienna, Franz Deuticke, 261 p.

Dushman, Saul, Dunbar, L. W., and Huthsteiner, H., 1944, Creep of metals: Jour. Applied Physics, v. 15, p. 108–124.

Eyring, Henry, Glasstone, Samuel, and Laidler, K. J., 1941, The theory of rate processes, New York, McGraw-Hill Book Co., 611 p.

Field, W. O., and Heusser, C. J., 1954, Glacier and botanical studies in the Canadian Rockies, 1953: Canadian Alpine Jour., v. 37, p. 128–140.

Finsterwalder, Richard, 1951, The glaciers of Jostedalsbreen: Jour. Glaciology, v. 1, p. 557–558.

Gerrard, J. A. F., Perutz, M. F., and Roch, André, 1952, Measurement of the velocity distribution along a vertical line through a glacier: Royal Soc. London Proc., ser. A, v. 213, p. 546–558.

Glen, J. W., 1955, The creep of polycrystalline ice: Royal Soc. London Proc., ser. A., v. 228, p. 519–538.

——— 1956, Measurement of the deformation of ice in a tunnel at the foot of an ice fall: Jour. Glaciology, v. 2, p. 735–745.

Goranson, R. W., 1940, Flow in stressed solids, an interpretation: Geol. Soc. America Bull., v. 51, p. 1023–1034.

Griggs, D. T., and Coles, N. E., 1954, Creep of single crystals of ice: U.S. Army, Corps of Engineers, Snow, Ice and Permafrost Research Establishment, Rept. 11, 24 p.

Haefeli, R., 1948, Schnee, Lawinen, Firn und Gletscher (Snow, avalanches, firn and glaciers) *in* Bendel, L., Ingenieur-Geologie, Vienna, Springer-Verlag, Band 2, p. 663–735.

——— 1951, Some observations on glacier flow: Jour. Glaciology, v. 1, p. 496–500.

Haefeli, R., and Brentani, F., 1955–56, Observations in a cold ice cap: Jour. Glaciology, v. 2, p. 571–581, 623–630.

Hess, Hans, 1904, Die Gletscher (Glaciers): Braunschweig, F. Vieweg, 426 p.

——— 1933, Das Eis der Erde (The ice of the earth): Handbuch der Geophysik, Band 7, Abt. 1, p. 1–121.

——— 1937, Über den Zustand des Eises im Gletscher (On the state of the ice in glaciers): Zeitschr. f. Gletscherk., Band 25, p. 1–16.

Hill, R., 1950, The mathematical theory of plasticity, Oxford, Clarendon Press, 350 p.

Hoel, P. G., 1947, Introduction to mathematical statistics, New York, John Wiley and Sons, 258 p.

Hopkins, W., 1862, On the theory of the motion of glaciers: Philos. Trans., v. 152, part 2, p. 677–745.

Hubbert, M. K., 1951, Mechanical basis for certain familiar geologic structures: Geol. Soc. America Bull., v. 62, p. 355–372.

Ivanov, K. E., and Lavrov, V. V., 1950, Ob odnoi osobennocti mekhanizma plasticheskoi deformatsii l'da (A peculiarity of the mechanism of plastic deformation of ice): Zhurnal Tecknichoi Fiziki, v. 20, p. 230–331 (*see also* U.S. Army, Corps of Engineers, Snow, Ice and Permafrost Research Establishment Trans. 10).

Jellinek, H. H. G., and Brill, R., 1956, Viscoelastic properties of ice: Jour. App. Physics, v. 27, p. 1198–1209.

Kalesnik, S. V., 1939, Obshchaia Gliatsciologiia izdatel'stvo (General glaciology), Leningrad, Gos. Utsch.-Pedag. Isd., 327 p.

Klebelsberg, R. V., 1948, Handbuch der Gletscherkunde und Glazialgeologie (Handbook of glaciology and glacial geology), Vienna, Springer-Verlag, Band 1, 403 p.

Lagally, M., 1929, Versuch einer Theorie der Spaltenbildung

in Gletschern (A trial theory of crevasse formation in glaciers): Zeitschr. f. Gletscherk., Band 17, p. 285–301.

Landauer, J. K., 1955, Stress-strain relations in snow under uniaxial compression: U.S. Army, Corps of Engineers, Snow, Ice and Permafrost Research Establishment Rept. 12, 9 p.

——— 1957, Some preliminary observations on the plasticity of Greenland glaciers: U.S. Army, Corps of Engineers, Snow, Ice and Permafrost Research Establishment Rept. 33, 6 p.

Matthes, F. E., 1900, Glacial sculpture of the Bighorn Mountains, Wyo.: U.S. Geol. Survey, 21st Ann. Rept., part 2, p. 167–190.

——— 1942, Glaciers: Chap. V, p. 149–219, in Meinzer, O. E. (ed.), Hydrology, New York, McGraw Hill Book Co., 712 p.

McCall, J. G., 1952, The internal structure of a cirque glacier: Jour. Glaciology, v. 2, p. 122–131.

Meier, M. F., 1951a, Glaciers of the Gannett-Fremont Peak area, Wyo.: Am. Alpine Jour., v. 8, p. 109–113.

———1956, Preliminary study of crevasse formation: U.S. Army, Corps of Engineers, Snow, Ice and Permafrost Research Establishment Rept. 38, 61 p.

Meier, M. F., Rigsby, G. P., and Sharp, R. P., 1954, Preliminary data from Saskatchewan Glacier, Alberta, Canada: Arctic, v. 7, p. 3–26.

Merrill, W. M., 1956, Structure of the ice cliff, in Goldthwait, R. P., Study of ice cliff in Nunatarssuaq Greenland: U.S. Army, Corps of Engineers, Snow, Ice and Permafrost Research Establishment Rept. 39, 150 p.

Nadai, A., 1950, Theory of flow and fracture of solids, New York, McGraw-Hill Book Co., V. 1, 572 p.

Nielsen, L. E., 1955, Regimen and flow in equilibrium glaciers: Geol. Soc. America Bull., v. 66, p. 1–8.

Nye, J. F., 1951, The flow of glaciers and ice-sheets as a problem in plasticity: Roy. Soc. London Proc., ser. A, v. 207, p. 554–572.

——— 1952a, The mechanics of glacier flow: Jour. Glaciology, v. 2, p. 82–93.

——— 1952b, A comparison between the theoretical and the measured long profile of the Unteraar Glacier: Jour. Glaciology, v. 2, p. 103–107.

——— 1952c, A method of calculating the thicknesses of the ice-sheets: Nature, v. 169, p. 529–553.

——— 1953, The flow law of ice from measurements in glacier tunnels, laboratory experiments and the Jungfraufirn borehole experiment: Roy. Soc. London Proc. ser. A, v. 219, p. 477–489.

——— 1955, Comments on Dr. Loewe's letter and notes on crevasses: Jour. Glaciology, v. 2, p. 512–514.

——— 1957, The distribution of stress and velocity in glaciers and ice-sheets: Royal Soc. London Proc., ser. A, v. 39, p. 113–133.

Orowan, E., 1949, The flow of ice and other solids: Jour. Glaciology, v. 1, p. 231–236.

Orvig, S., 1953, On the variation of shear stress on the bed of an ice cap: Jour. Glaciology, v. 2, p. 242–247.

Perutz, M. F., 1954, Glaciers: Royal Inst. Great Britain, v. 35, p. 571–582.

Perutz, M. F., and Seligman, Gerald, 1939, A crystallographic investigation of glacier structure and the mechanism of glacier flow: Royal Soc. London Proc., ser. A, v. 172, p. 335–360.

Prandtl, L., and Tietjens, O. G., 1934, Fundamentals of hydro- and aero-mechanics, New York, McGraw-Hill Book Co., 265 p.

Reid, H. F., 1896, The mechanics of glaciers: Jour. Geology, v. 4, p. 912–928.

——— 1901, De la progression des glaciers, leur stratification et leur veines bleues: 8th Inter. Geol. Cong., Compt Rendu, pt. 2, p. 749–755.

Rigsby, G. P., 1951, Crystal fabric studies on Emmons Glacier, Mount Rainier, Wash.: Jour. Geology, v. 59, p. 590–598.

——— 1957, Effect of hydrostatic pressure on velocity of shear deformation of single crystals of ice: U.S. Army, Corps of Engineers, Snow, Ice and Permafrost Research Establishment Report 32, 7 p.

Robertson, E. C., 1955, Experimental study of the strength of rocks: Geol. Soc. America Bull., v. 66, p. 1275–1314.

Schwarzacher, W., and Untersteiner, Norbert, 1953, Zum problem der Bänderung des Gletschereises (On the problem of the banding of glacier ice): Sitz. d. Osterr. Akad. Wiss., Wien, Math.-naturwiss., Abt. IIa, Band 162, p. 111–145.

Servi, I. S., and Grant, N. J., 1951, Creep and stress rupture behavior of aluminum as a function of purity: Jour. Metals, v. 3, p. 909–916.

Sharp, R. P., 1948, The constitution of valley glaciers: Jour. Glaciology, v. 1, p. 182–189.

——— 1953, Deformation of borehole in Malaspina Glacier, Alaska: Geol. Soc. America Bull., v. 64, p. 97–100.

——— 1954, Glacier flow, a review: Geol. Soc. America Bull., v. 65, p. 821–838.

Shumskii, P. A., 1947, Energiia oledeneniia i zhizn lednikov (Energy of glacierization and the life of glaciers): Moscow, Geografgiz, Translated by William Mandel, The Stefansson Library, New York, 1950, 60 p.

Steinemann, Samuel, 1954, Results of preliminary experiments on the plasticity of ice crystals: Jour. Glaciology, v. 2, p. 404–413.

Turner, F. J., 1948, Mineralogical and structural evolution of the metamorphic rocks: Geol. Soc. America Memoir 30, 342 p.

Untersteiner, Norbert, 1954, Über die Feinbänderung und Bewegung des Gletschereises (On the fine-banding and movement of glacier ice): Archiv für Met., Geophysik u. Bioklima., ser. A, Band 7, p. 231–242.

——— 1955, Some observations on the banding of glacier ice: Jour. Glaciology, v. 2, p. 502–506.

Weertman, J., 1957, Steady-state creep through dislocation climb: Jour. App. Physics, v. 28, p. 362–364.

White, S. E., 1956, Motion in the ice cliff, in Goldthwait, R. P., Study of ice cliff in Nunatarssuaq Greenland: U.S. Army, Corps of Engineers, Snow, Ice and Permafrost Research Establishment Rept. 39, 150 p.

INDEX

Page

A

Ablation, definition ... iv
measurements ... 8
rate ... 8, 10, 19, 26, 62
surface ... 2
total ... 10
velocity ... 26
yearly values ... 8, 10, 11
Absolute vertical component ... 22, 23
Accumulation ... 5
velocity ... 24
Accuracy, attitudes of structural features ... 50
englacial velocity measurements ... 30
of streamline constructions ... 48
strain-rate measurements ... 33, 35, 36
velocity measurements ... 64–66
Activity of glacier ... 5
Altitude of area ... 2, 15
Andrade's law ... 44, 45
Approximation of plane strain ... 33
Arolla tunnel ... 42, 44
Austerdalsbre tunnel ... 42, 44

B

Banded structure ... 52, 59
Blätterung ... 54
Blue bands ... 52
Boreholes, configuration ... 30
inclination data ... 66, 67
sites ... 30, 31
stress and strain-rate data ... 41
Brittle crust ... 31

C

Cartesian coordinates ... 32
Castleguard sector, ablation in ... 10
altitude ... 8
crevasses in ... 56
cross sections ... 10, 21, 46
definition of ... 4, 5
distribution of velocity components ... 22, 23
flow into ... 46
structures ... 50
location ... 4, 5
mechanical properties of ice ... 33
structural features ... 50, 57, 58
surfaceward flow ... 24
velocity components ... 20, 21, 26
Classification of glaciers ... 5
Columbia Icefield ... 2, 4, 52
Component of, absolute vertical ... 22, 23
laminar flow ... 24
strain rate ... 32
surface rise ... 24
velocity ... 2, 19, 20, 21, 32, 33, 64
Configuration of, bedrock ... 28
borehole ... 30
channel ... 2
surface ... 6, 19
Coordinate systems ... 2, 11, 13, 19, 22, 24, 32
Cracks ... 4, 50, 54, 57, 60, 61, 64

Page

Crevasses, chevron ... 56
en echelon ... 56, 62
longitudinal ... 56
splaying ... 56, 61, 62
transverse ... 56, 62
Criteria for distinguishing foliation from stratification ... 54
Crystal-fabric studies ... 5

D

Density of ice ... 5
Deviator of stress ... 38
Drilling with hotpoints, results ... 31
Druckschichtung ... 54

E

Energy of glacierization ... 5
Eulerian method of hydrodynamics ... 25
Extending flow ... iv, 36

F

Faults ... 50, 57
Feinbänderung ... 52, 59, 60
Firn limit ... iv, 2, 5, 6, 8, 21, 22, 25, 36, 50, 52, 62
Flow centerline ... iv, 6, 11, 27, 28, 35, 36, 41, 45, 48, 49, 59
Flow law ... ix, 2, 37, 41, 44, 45, 50, 64
Fold axes ... 50, 57
Foliation ... iv, 27, 50, 52, 59, 60

G

Gerrard, quoted ... 1
Glen's flow law for ice ... 14, 41, 44, 64
Grain-boundary creep ... 60, 64
Greenland icecap ... 60

H

Haarisse ... 54, 56
Hintereisferner ... 5
Horizontal downglacier component of velocity ... 2, 21
ice surface, assumption ... 35
transverse component of velocity ... 2, 21

I

Instantaneous ice surface ... 2
velocities, substitution of average ... 35

J

Jungfraufirn ... 28, 41, 42, 44

L

Laminar flow, analysis ... 41, 42
component ... 24
deformation in ... 38, 40, 41
Lateral moraines ... 6
Longitudinal bands ... 52
extension ... 41, 42
orientation of foliation ... 54; pl. 2A
profile ... 2, 49, 50, 64
hypothesis ... 50
significance ... 49

Page

M

Malaspina Glacier ... 28, 42, 44
Mass-budget data ... 46
Medial moraine ... 2, 10
  velocity pattern ... 27
Meteorological observations ... 18
Mohr's circle constructions ... 32, 33, 36, 61

N

Nye, equations quoted ... 39, 41, 42

O

Objective of study ... 1
Octahedral shear stress ... iv, 38, 42, 44
  strain rate ... iv, 38, 42, 44
Orientation maximum, characteristics ... 59
Outcrop pattern ... 51, 52, 54, 57
Outlet glacier ... 5

P

Parallelism between streamlines and bedrock ... 49
Pasterze Glacier ... 59, 60
Pattern of crevasses ... 54
  stratification ... pl. 7
Pfiugfurcheneis ... 54
Physical setting of glacier ... 2
Plane of symmetry ... 6
Principal strain rates ... iv, 38
  stresses ... iv, 38

R

Ratio of downglacier velocity to centerline velocity ... 26
Relation between air temperature and velocity ... 17
  deviation of velocity and temperature ... 19
  dispersion and wavelength of velocity variations ... 19
Rhone Glacier ... 5
Roads, accessibility ... 2
Rotation rate ... 35

S

Scherflächen ... 54
Secondary flow structures ... 50
Sedimentary layers ... 50, 52
Seismic explorations ... 6
Shape of glacier ... 1, 2, 5, 6
Shear stress on bed ... 49
Skauthöe tunnel ... 42, 44

Page

Sources of error in measurements of velocity ... 65
Strain rate ... 28, 32–45
  basic equations ... 32, 38, 39, 41, 42
  components ... 28, 32, 33, 35, 37, 41, 42
  function of shear stress. *See* Flow law.
  relation to structures ... 57, 58, 59
  tensor ... 32, 33, 37, 57
  trajectories ... 32, 34, 36, 61
Stratification ... 50, 52, 57, 64
Streamline distribution ... 46, 48, 49, 64
  parallelism with bed ... 49, 64
Structural features ... 2, 50–62
Surface deformation ... 32–37
  lowering, rate ... 26
Surfaceward flow ... 2, 24–26, 46

T

Tectonic blue bands ... 52
Tectonic features, origin ... 59, 60, 61, 64
Temporary snowline ... 8, 12
Thermal characteristics ... 5
Thinning data ... 6, 8
Topography, bedrock ... 6, 9
Transit stations, locations ... 10, 13
  nomenclature ... 10, 12, 13
Transition from convergent to divergent flow ... 22, 23
Transverse component of flow ... 21
  profile ... 25, 41, 42, 45

V

Velocity, at bed ... 46, 50
  at depth ... 2, 45, 46
  components. *See* Components, velocity.
  data, accuracy ... 64–66
  deviation of ... 16, 17
  dispersion of ... 16, 17
  distribution ... 19–28, 31, 45, 48
  englacial ... 28, 31, 32
  instantaneous ... 35
  stakes ... 8, 10, 11, 13, 66
    coordinates of ... 66
    dates of survey ... 14
  standard deviation of ... 16
  stations ... 8, 10, 11, 13, 66
  time-dispersion of ... 16–18
  time variation ... 11, 12, 16, 17
  variations, short-interval ... 16, 17, 18
  vector, direction ... 27
  yearly changes ... 14, 16, 66
Vertical profiles ... 31, 37, 38, 45, 46

U.S. GOVERNMENT PRINTING OFFICE: 1960 O - 509755